PRECLINICAL INVESTIGATIONS TO OPTIMIZE SURGICAL RESTORATION OF SYMMETRICAL VOCAL FOLD VIBRATION

by

Azure Celeste Wilson

Bachelor of Science, Florida Atlantic University, 2008

Master of Science, Florida Atlantic University, 2013

Submitted to the Graduate Faculty of the

School of Health and Rehabilitation Sciences in partial fulfillment

of the requirements for the degree of

Doctor of Philosophy

University of Pittsburgh

2024

UNIVERSITY OF PITTSBURGH

SCHOOL OF HEALTH AND REHABILITATION SCIENCES

This dissertation was presented

by

Azure Celeste Wilson

to the following committee members in partial fulfillment of the Doctorate of Philosophy in

Communication Sciences and Disorders:

Lea Sayce, DPhil, Research Assistant Professor, Communication Science & Disorders

Leah Helou, PhD, CCC-SLP, Assistant Professor, Communication Science & Disorders

Preeti Sivasankar, PhD, CCC-SLP, Professor and Department Head, Department of Speech, Language, and Hearing Sciences, Purdue University

Bernard Rousseau, PhD, MMHC, CCC-SLP, ASHA Fellow, Dean, Doisy College of Health Sciences, Saint Louis University

Dissertation Director: Cecelia Yates, PhD, Associate Professor, Health Promotion & Development

PRECLINICAL INVESTIGATIONS TO OPTIMIZE SURGICAL RESTORATION OF SYMMETRICAL VOCAL FOLD VIBRATION

Azure Celeste Wilson, PhD

University of Pittsburgh, 2024

Unilateral vocal fold paralysis is an ongoing challenge in laryngology due to the impact on phonation from the gap between vocal folds. Medialization laryngoplasty is the gold standard treatment, known for its long-term effectiveness and customization. However, achieving optimal glottal closure often relies on subjective judgment, leading to variable outcomes, longer operative times, and increased costs.

To address these issues, my research introduces a preclinical approach to optimize surgical planning for medialization laryngoplasty. The first aim investigates the biomechanical properties of vocal folds using bioreactors and magnetic microactuators. Clinical observations indicate a direct link between abnormal mechanical signal transduction and voice disorders, emphasizing the need to study vocal fold biomechanics. This research expands on bioreactor use, incorporating magnetic microactuators to adjust frequencies for kinetic stress, aiming to understand tissue responses and explore interventions for enhancing vocal function.

Aim 2 focuses on validating surgical and experimental methods for studying medialization laryngoplasty in an animal model. Type I thyroplasty, the primary surgical intervention, aims to medialize the affected fold. However, challenges like under/over-medialization and implant variability persist, necessitating further research for improved outcomes. Opportunities for refinement include developing customizable implants, novel animal models, and advancements in imaging techniques.

In Aim 3, novel surgical techniques were tested to create a reproducible method for simulating unilateral vocal fold paralysis, aiding in the translation to computational models. A custom laser-cut silicone laryngoplasty implant was developed, offering simplicity, reproducibility, and cost-effectiveness. This innovation has the potential to streamline implant customization and reduce fabrication time and costs. Additionally, *ex vivo* magnetic resonance imaging of vocal folds in simulated paralysis informed three-dimensional finite-element models of laryngeal tissue displacement. These studies demonstrated the feasibility of estimating vocal fold vibration modes and frequencies through computational models based on subject-specific imaging.

Together, these surgical and computational methods establish an experimental phonation paradigm, laying the groundwork for future investigations into the surgical restoration of symmetric vibration through combined experimental and computational approaches.

Table of Contents

List of Tables

List of Figures

1.0 Introduction: Background and context of the research problem

Voice problems due to impaired vocal fold (VF) function affect approximately one-third of individuals in their lifetime, costing the US healthcare system nearly $300,000,000 annually (S. M. Cohen et al., 2012). Such problems have far-reaching effects on an individual's participation in society, including negative self-image, reduced work performance, and limitations to social functioning (Verdolini & Ramig, 2001). Speech-language pathologists (SLPs) are often involved in the treatment of individuals with voice disorders, while in cases of severe loss of voice quality, or dysphonia, a laryngologist may recommend a combination of behavioral interventions and surgical treatment. Given the prevalence and costly impact of voice problems caused by impaired VF function, it is important to understand the fundamental concepts related to their treatment, including relevant anatomy, physiology, and biomechanics of the VF, prevalent disorders such as unilateral vocal fold paralysis (UVFP), and common surgical interventions like medialization laryngoplasty. This chapter introduces foundational concepts in preclinical laryngology research, emerging topics to address current gaps in the field, and the research questions and hypotheses used to guide the investigations in this dissertation. In this chapter, sections marked with an asterisk (*) denote material that has been adapted from Wilson et al. (2021) and (2023).

1.1 Surgical restoration of symmetrical vocal fold vibration

1.1.1 VF anatomy, physiology, and biomechanics

The VF, a layered mucosal tissue consisting of a luminal stratified squamous epithelium, three lamina propria layers, and a basal ligament (vocalis muscle), are housed within the soft tissue and cartilage structure of the larynx (Klepacek et al., 2016; Titze et al., 1988). The thyroid, cricoid, and arytenoid cartilages (see Figure 1) are the primary cartilaginous structures that give shape to the larynx, with the thyroid cartilage being the most externally recognizable. The cricoid cartilage, which is inferior to the thyroid cartilage at the level of the C6 vertebra, is the sole complete cartilaginous ring of the airway, forming a stable base for the larynx by attaching to the thyroid cartilage and the first tracheal ring. The paired arytenoid cartilages articulate with the posterior portion of the cricoid cartilage and are attached to the VF, with the distal end of the VF attached to the thyroid cartilage.

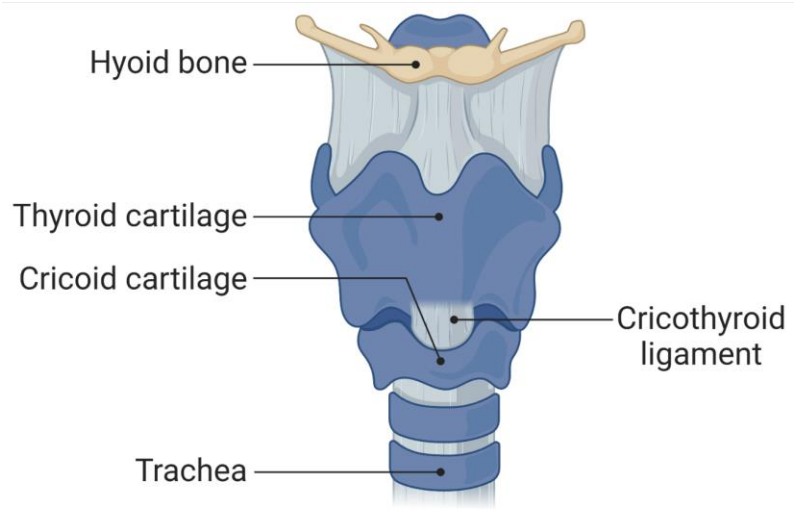

Figure 1 Illustration of the anterior view of the larynx

The intrinsic and extrinsic muscles of the larynx work in harmony to facilitate optimal opening of the glottis for speech, swallowing, respiration, and airway protection. During passive respiration, the VF assume a paramedian position, with the rima glottidis (the opening formed by the separation of the medial edges of the VF) wide enough to allow unobstructed gas exchange. The larynx serves as the primary conduit between oronasal structures and thoracic organs, primarily the stomach via the esophagus, and the lungs via the trachea.

During speech production, the intrinsic muscles of the larynx coordinate as interdependent pairs to control the opening and closing of the rima glottidis or adjust the length of the vocal folds. This dynamic interaction generates adduction tension, which, combined with the myoelastic tension of the adducted vocal folds, produces oscillations that manifest as sound waves. These sound waves undergo further refinement by articulators and resonators, such as the teeth, tongue, and oral and nasal cavities, resulting in speech sounds. The Bernoulli principle is instrumental in this process. As airflow passes through the glottis during exhalation, it accelerates, causing a decrease in pressure between the vocal folds. This pressure reduction creates a force that draws the vocal folds together, facilitating adduction and contributing to sound wave production. Furthermore, research in glottal flow dynamics has revealed that the interaction between the glottal source and the vocal tract filter is nonlinear, giving rise to phenomena such as bifurcations, chaos, and turbulence (Titze et al., 1988). These complex mechanisms further influence the acoustic characteristics of speech, including its timbre, pitch, and intensity.

The interarytenoid muscles, including the transverse and oblique arytenoid muscles, play a crucial role in adduction. When activated, these muscles increase tension between the arytenoid cartilages, aiding in the approximation of the vocal folds. Specifically, the lateral cricoarytenoid (LCA) muscles, the principal adductors of the vocal folds, work in conjunction with the

interarytenoid muscles. The LCA muscles rotate the arytenoid cartilages to bring the vocal processes toward the midline, facilitating the approximation of the vocal folds. In contrast, the posterior cricoarytenoid (PCA) muscles, the sole abductors of the vocal folds, pull the muscular process of the arytenoid cartilage posteriorly and rotate the arytenoid cartilages distally to separate the vocal folds. Together, the coordinated activation of the LCA, PCA, and interarytenoid muscles control the width of the opening of the rima glottidis, crucial for phonatory function. Additionally, phonatory pitch modulation is supported by the cricothyroid muscles and the thyroarytenoid muscles. The cricothyroid muscles elongate and tighten the vocal folds by drawing the thyroid cartilage towards the cricoid cartilage, while the thyroarytenoid muscles act as tuning slides to fine-tune pitch by adjusting the position of the arytenoid cartilages anteriorly or posteriorly.

1.1.2 Unilateral vocal fold paralysis

UVFP is a condition characterized by asymmetry in frequency or amplitude between the left and right VF. This potentially debilitating impairment frequently causes a gap leading to dysphonia and/or dysphagia (C.-C. Wang et al., 2008). SLPs often participate in multidisciplinary teams involved in the treatment of patients with glottic insufficiency. Therefore, it is increasingly important for SLPs to understand the current evidence-based practice and future trends associated with interventions in the treatment of UVFP. This introductory review of UVFP is intended to provide a background on clinical indications for treatment, expected outcomes, and emerging research areas.

1.1.2.1 Etiology and pathophysiology of UVFP

UVFP is typically caused by injury of the recurrent laryngeal nerve or vagus nerve that innervates the larynx, resulting in impaired adduction, one-sided vocal fold immobility, and a widened glottal gap (Havas et al., 1999). Iatrogenic causes, such as thyroidectomy or anterior cervical disk spinal fusion, account for about half of all cases, but UVFP may also occur idiopathically (Rosenthal et al., 2007; Sulica, 2008). UVFP can cause life-altering symptoms for patients, with dysphonia present in 53%-100% of cases, dyspnea in 60%-75% of cases, and dysphagia and potential aspiration risk in approximately 60% of cases (Brunner et al., 2011; Francis et al., 2014, 2016; Leder et al., 2012).

1.1.2.2 Diagnosis and treatment of UVFP

In clinical practice, diagnosis of UVFP is typically diagnosed through subjective clinical judgement of a laryngologist or SLP using laryngoscopic examination, which is preferred for practicality, cost-efficiency, and patient comfort (Stanisz et al., 2021). Physicians may also recommend complementary tests such as laryngeal electromyography or computed tomography (CT) to determine prognosis and plan an appropriate course of treatment for cases of UVFP with idiopathic etiology (Kelchner et al., 1999; Munin et al., 2003; Sanuki et al., 2014).

A multidisciplinary healthcare team including an SLP, a laryngologist, and other healthcare professionals, is most effective in managing UVFP. Treatment planning takes into account symptom severity and patient factors such as age and overall health. Voice therapy is typically the primary intervention for patients with mild to moderate symptoms, which focuses on strengthening the muscles of the airway and producing less effortful speech while optimizing the quality and efficiency of phonation. If voice therapy alone is not recommended, the healthcare team may consider a surgical option such as medialization laryngoplasty.

1.1.3 Medialization laryngoplasty

*Medialization laryngoplasty (ML) is a surgical procedure that adds bulk to VF tissue using an implant or injectable filler to indirectly press the fold toward the midline and facilitate closure during phonation. This method, first described by Isshiki in 1975, quickly became the gold standard as a permanent correction for impaired vocal fold closure (Isshiki et al., 1975). Medialization laryngoplasty maintains the integrity of the VF vibratory margin and preserves the biomechanical properties of the glottis to reduce dysphonia (Bless & Welham, 2010). ML indications, operative procedure, materials, and outcomes for implants and injectable fillers are discussed below.

1.1.3.1 Indications for ML

*ML is primarily used to treat glottic insufficiency caused by UVFP (Daniero et al., 2014). However, in recent years, indications for ML have expanded to include treatment of a variety of conditions associated with incomplete glottic closure, such as vocal fold paresis (Farzal et al., 2019; M. Dominguez et al., 2019), atrophy (Farzal et al., 2019; M. Dominguez et al., 2019), presbylaryngitis (Allensworth et al., 2019), scar (Farzal et al., 2019; Salmerón-González et al., 2020), sulcus vocalis (Yılmaz, 2012), and cordectomy (Mastronikolis et al., 2013) ML has also been used to alleviate symptoms in patients experiencing odynophonia (Kupfer et al., 2015) and puberphonia (Van Den Broek et al., 2016). The broad applications for ML establish its place as an integral tool in laryngologists' treatment toolbox for the management of these voice disorders.

1.1.4 Type I thyroplasty

*Medialization laryngoplasty with a durable implant is known as type I thyroplasty. The laryngologist makes an incision over the thyroid cartilage on the side of the affected fold to expose the lateral thyroid lamina. The surgeon then outlines and cuts a window through the cartilage at the level of the vocal folds. The implant material is positioned through the window into the paraglottic space to compress the tissue and medialize the fold, then sutured to prevent migration. The size of the implant is determined based on the desired outcomes and the surgeon's experience.

1.1.4.1 Type I thyroplasty anesthetic considerations

*Ideally, type I thyroplasty should be performed in an operating room with local anesthesia or local anesthesia combined with conscious sedation. Minimal sedation is preferable to general anesthesia as it reduces the procedure's cost and time spent in the operating room and recovery (Kanazawa et al., 2014). Additionally, an awake technique allows intraoperative perceptual assessment of voice quality without endoscopic visualization of functional vocal fold medialization (Abdelmalak et al., 2009; Rosen et al., 2009).

*However, not all patients can tolerate this anesthetic approach due to patient anxiety, vasovagal response, intolerance to sedatives, anatomic variants, or severe comorbidities (Sproson et al., 2010; Waring et al., 2003). In such cases, type I thyroplasty may be performed under general anesthesia using a laryngeal mask airway, a supraglottic airway device with a silicone or PVC ring that inflates to form a low-pressure seal over the laryngeal inlet (Grundler & Stacey, 1999). The laryngeal mask airway allows the passage of a flexible laryngoscope for intraoperative airway monitoring and confirmation of adequate and appropriate vocal fold medialization (Carrau et al., 1998).

*Another option is a sequential anesthetic protocol to transition from general anesthesia to sedation/analgesia. This minimizes patient discomfort for the initial incision and implant placement while still allowing for patient phonation and intraoperative perceptual voice assessment before completion of the procedure (Saadeh et al., 2017). Subjective voice measures for patients who underwent type I thyroplasty surgery using the laryngeal mask airway or sequential anesthetic approach indicate similar voice outcomes to those under local anesthesia (Buckmire et al., 2011; Kanazawa et al., 2014; Mathison et al., 2009). Therefore, the choice of technique requires an evaluation of the relative risks and advantages for each patient.

1.1.4.2 Type I thyroplasty materials

*Early type I thyroplasty surgeries used a portion of the thyroid cartilage from the contralateral lamina as the implant material (Isshiki et al., 1975). However, this implant material degrades over time and is not ideal for long-term symptom relief. Recent innovations in materials science have led to the use of nonnative, inert materials such as silicone or Gore-Tex® ribbon, a microporous membrane made of expanded polytetrafluoroethylene (McLaughlin et al., 2007) (Crolley & Gibbins, 2017; Montgomery et al., 2000). A 2010 survey indicates that Silastic® and Gore-Tex® implants are widely used (Young et al., 2010). Ultimately, selection of implant material depends on surgeon preference, training, and availability of materials.

*Silicone and silicone-rubber materials, such as Silastic®, have been approved for multiple indications in other tissue systems, notably as breast implants, and rigorous safety research indicates that this material is clinically suitable for implantation (McLaughlin et al., 2007). Silicone-elastomers used in type I thyroplasty demonstrate long-term stability (Benninger et al., 2015; Kwak et al., 2016). Silastic® implants may be pre-formed and pre-sized, such as Montgomery® and Netterville Phonoform® implants (Montgomery et al., 2000; Netterville et al.,

1993), or hand-carved by the surgeon on-site. Pre-formed implants are available in various sizes but are not tailored to the laryngeal geometry of each patient. Hand-carving allows for patient-specific customization, but it is technically challenging, time-consuming, and requires extensive experience on the part of the surgeon (Suehiro et al., 2009). Some surgeons prefer to start with a preformed implant and iteratively insert, test, remove, and adjust the implant until the desired outcome is achieved (Saadeh et al., 2017; Zimmermann et al., 2019).

*In contrast to the fixed shape of Silastic®, Gore-Tex® is a 0.6 mm thick cylindrical braid of expanded polytetrafluoroethylene (ePTFE). The braid forms a mesh onto which the cellular matrix attaches, and the tissue infiltrates after implantation. ePTFE has been used for decades in vascular and cardiac prosthetics (Zdrahala, 1996). Reports of the use of ePTFE in laryngeal implantation suggest that it is well tolerated in most patients (Zeitels et al., 2003). The Gore-Tex® type I thyroplasty technique involves the insertion of the flexible ribbon through a window created in the thyroid cartilage and placement of the material into the paraglottic space. The surgeon stacks the ribbon in an anti-parallel fashion with as many or as few layers needed until appropriate medialization is achieved (McCulloch & Hoffman, 1998). One of the advantages of Gore-tex® as an implant material is that it can be inserted quickly and repositioned in situ during the procedure. However, due to the flexible tubular shape of ePTFE, compression of the space between the layers of the implant may occur over time. The surgeon must account for this compression during medialization, as under-correction compromises effective glottal closure (Iwahashi et al., 2015).

1.1.4.3 Type I thyroplasty outcomes

*Type I thyroplasty has been shown to provide lasting improvements in auditory-perceptual ratings of voice quality post-operatively (Hassan et al., 2014; Malik et al., 2014; Van Ardenne et al., 2011). Similar improvements in voice-related quality of life have been reported

postoperatively using the Voice Handicap Index-10 (Malik et al., 2014; Van Ardenne et al., 2011). Instrumental voice measures have also been shown to improve and remain stable over time. For example, a meta-analysis reported an average increase of 8.9 seconds in maximum phonation time post-operatively (Granato et al., 2019), while others have reported improvements in fundamental frequency, jitter, and shimmer in long-term follow-up (Cantillo-Baños et al., 2013; Kodama et al., 2017; Tsai et al., 2017).

*Although type I thyroplasty is currently the accepted gold standard for the treatment of glottic insufficiency, it is not without risks and limitations. Combined across studies, reported rates of revision for implant procedures range from 4.5% to 16% (J. T. Cohen et al., 2004; Maragos, 2001; Netterville et al., 1993; Parker et al., 2015; Woo et al., 2001) which come with increased risks associated with multiple anesthetic events. Some other complications of type I thyroplasty have been reported in the literature, including hematoma, infection, and implant extrusion (Bray et al., 2008), though these complications are rare. A fibrous capsule or fibrosis around the implant is often observed in implant revisions (Ustundag et al., 2005). The effect of the fibrous capsule on the viscoelastic properties of the vocal folds and potential for reversibility are unknown (Dion et al., 2018). Despite these limitations, the preponderance of evidence suggests type I thyroplasty is safe and effective. Improvements in the understanding of patient-specific factors that influence voice outcomes and advanced biomaterial engineering may provide opportunities to address current limitations.

1.1.5 Vocal fold injection augmentation

*Compared to type I thyroplasty, vocal fold injection augmentation (VFIA) can be performed in-office with improved recovery time, reduced cost, and peri-operative perceptual

voice assessment. For medically vulnerable and elderly patients, office-based VFIA is often used to mitigate the known risks of general anesthesia and provide short term symptomatic relief of dysphonia, dyspnea, dysphagia, odynophonia, cough, and other symptoms associated with glottal insufficiency. Clinically, there appears to be no difference in short-term voice outcomes between injections performed in the office and those performed in the operating room (Ballard et al., 2018).

*The in-office procedure begins with the patient seated in a chair and receiving local anesthesia. Laryngologists often employ a trans-oral needle approach for injection as it offers direct visualization of the needle entering the VF from inside the airway lumen. However, an external trans-cricothyroid membrane, trans-thyrohyoid, or trans-thyroid cartilage approach may be selected based on surgeon preference, patient anatomy, and patient comfort (Rosen et al., 2009; Verma & Dailey, 2014). Once the needle is appropriately positioned and visualized endoscopically, an injectable material is inserted via a syringe into the posterior third of the VF in the TA muscle or paraglottic space. The volume of material injected is determined by visual confirmation of satisfactory VF medialization and subjective voice assessment (Dion & Nielsen, 2019).

*The viability of in-office injections has increased with innovation in micro-fabrication methods and the development of distal chip flexible endoscopes with a digital chip camera at the scope tip. These endoscopes have lower image quality than direct laryngeal imaging with a rigid endoscope but offer a trans-nasal approach with superior maneuverability, allowing for a more dynamic and complete view of the pharynx and larynx during the injection procedure. Compared to fiber-optic endoscopes previously used during in-office laryngoscopy procedures, “chip tip” scopes capture laryngeal images with higher quality and greater reliability (Plaat et al., 2014). The image quality and increased functionality afforded by this technology allow for improved intra-

procedural monitoring of vocal fold medialization and likely contribute to positive outcomes noted in these in-office injection procedures (Rosen et al., 2009).

1.1.5.1 VFIA materials

*Laryngologists may use VFIA as a short-term solution for symptomatic relief during the 'wait and watch' period while determining whether spontaneous recovery will occur in the weeks or months following nerve injury. Short-term trials of injectable materials in the initial 6-12 months following symptom onset allow for the potential of spontaneous recovery while providing non-permanent symptomatic relief. The resurgence of office-based procedures and research into bio-engineered materials has increased the number of options for injectable fillers in the surgeon's arsenal. Four injectable materials from this broad field of options are frequently used clinically based on resorption rate: carboxymethylcellulose, calcium hydroxyapatite, hyaluronic acid, and autologous fat.

*The first, carboxymethylcellulose, is a water-soluble cellulose derivative combined with sterile water, phosphate buffer, and glycerin to form an aqueous solution sometimes referred to as "voice gel" (Renú Gel, RegenScientific, East Troy, WI; Prolaryn Gel™, Merz North America, Raleigh, NC). A study of CMC vocal fold injection in canines revealed an inflammatory reaction coupled with the rapid dispersion of the material in approximately four weeks (Zeitels et al., 2019). However, those complications were not mirrored in human trials; there was no inflammatory response noted in humans, and the material lasted in the VF for two to three months (J. T. Cohen & Benyamini, 2020; T.-K. Kwon et al., 2005; Mallur et al., 2012), putting it at the shorter end of the spectrum of treatment duration.

*Synthetic calcium hydroxyapatite (CaHa) is a mineral component of bones comprised of phosphate and calcium. Microspherules of CaHa have been used in a commercial preparation by

suspension in an aqueous solution containing carboxymethylcellulose (CaHA-CMC). This material has been widely examined within the last decade, with successful reports of complete glottic closure during phonation and return of voice following injection (Carroll & Rosen, 2011; Koçdor, 2014; Mohammed et al., 2016; Verma & Dailey, 2014). CaHA-CMC has been shown to last up to a year for 67%-70.1% of patients (Rosen et al., 2009; Zeleník et al., 2017).

*Hyaluronic acid is a polysaccharide that occurs naturally in the extracellular matrix of tissues, including the VF (Hahn et al., 2006), and is well tolerated by patients. The viscoelasticity of commercially available hyaluronic acid-based derivatives (Restylane®, Medicis Aesthetics, Scottsdale, AZ, USA, and Juvederm®, Allergan, Irvine, CA, USA) is designed to mimic the viscoelasticity of the vocal folds and improve tissue vibratory properties by closely matching the native properties of the vocal folds using cross-linking, binding molecules with chemical bridges (Y. S. Kim et al., 2015). Hyaluronic acid has a variable resorption period, though one study reported patients began to notice a deterioration of voice quality at an average of 10.6 months post-injection (Bertroche et al., 2019).

*Autologous fat has long been a standby in the VFIA lineup. It is comprised of a filtered bolus of fat procured from the patient's abdomen or hip. Autologous materials are considered extremely safe, as there is a low risk of implant rejection or the initiation of a host inflammatory response (Ricci Maccarini et al., 2018). While autologous fat is inexpensive, biocompatible, and readily available, it requires an extra surgical procedure to harvest the fat and additional steps to filter and prepare the fat for re-injection. These steps increase the time burden of the procedure. Autologous fat injection has been reported to improve the auditory-perceptual assessment of voice quality for as long as a year in up to 83% of patients (Fang et al., 2010; Zeleník et al., 2017).

1.1.5.2 VFIA outcomes

*VFIA has excellent short-term outcomes, comparable to those observed in type I thyroplasty. Since injection materials are considered temporary, repeat injections or subsequent type I thyroplasty may be necessary for individuals whose glottic insufficiency cannot be managed by injection alone. A retrospective chart review of 250 patients at a single institution reported that 71.4% of patients who had previously received VFIA elected to have type I thyroplasty after one year due to failure to achieve sufficient glottic competency and expected voice outcomes (Alghonaim et al., 2013). However, it has been reported that patients who receive VFIA during the 'wait and watch' period to allow for spontaneous recovery are less likely to require type I thyroplasty (Friedman et al., 2010; Prendes et al., 2012). VFIA during this interim period may provide the central nervous system with access to immediate sensory feedback to allow for the functional reorganization of the cortical structures associated with laryngeal function (Galgano et al., 2009). Other factors such as age (Choi et al., 2012; Lin et al., 2020), gender (Lin et al., 2020), degree of posterior glottal gap, and history of radiation (J. Chang et al., 2014) have also been reported to impact treatment outcomes.

*Several studies have reported complications of VFIA, including poor placement, overcorrection, and under-correction (Jamal et al., 2014; T. Kwon et al., 2010; Shen et al., 2013; Verma & Dailey, 2014). These complications may be due to challenges in obtaining adequate laryngeal exposure during the procedure, as inadequate visualization or confirmation of placement of the material increases the risk of material extrusion or placement superficially into the superior lamina propria, impairing mucosal wave and phonation (Mathison et al., 2009).

1.2 Emerging topics in surgical restoration of symmetrical VF vibration

*Both type I thyroplasty and VFIA offer relief from functional deficiency and quality of life impairment experienced by individuals with UVFP, but there are opportunities for improvement. Even implant materials that are considered well-tolerated can cause immunologic reactions (Cashman et al., 2002; Chhetri et al., 2004; Hizal et al., 2014; Ustundag et al., 2005). Clinician reliability for laryngoscopic assessment of glottic closure is low (Rosow & Sulica, 2010). Most ML procedures adjust asymmetry on the medial-lateral position of the vocal process but do not correct asymmetries in vertical height, which are correlated with a poorer subjective report of voice (E. Wong et al., 2020). These challenges have driven research towards developing a model for the remediation of glottic insufficiency that ensures valid, reproducible, and clinically viable results. This section details some emerging topics in the field that have yet to be fully explored, as well as the research approach described in this document that has the potential to provide insight into those areas. Specifically, I will address biomechanical properties of laryngeal tissues in phonatory stress models, novel techniques for preclinical investigations of medialization laryngoplasty for UVFP, and incorporation of advanced imaging techniques into computational models.

1.3 Overview of Aim 1

1.3.1 Biomechanical properties of laryngeal tissues in phonatory stress models

Changes in tissue structure or cellular mechanics are responsible for most laryngeal disorders. Biomechanical stress on the VF due to phonotrauma has been shown to contribute to the development of voice disorders through changes in tissue structure and cellular mechanics (Kimball, Sayce, Powell, et al., 2021; Novaleski et al., 2016; Rousseau et al., 2017; Yamashita et al., 2010). This supports clinical observations that suggest a direct role for abnormal transduction of mechanical signals in the etiology or clinical presentation of voice disorders. For example, variations in extracellular matrix structure due to vocal fold scar may impair tissue compliance and lead to dysphonia (Yamashita et al., 2010). Decreased vocal demands or injury may lead to atrophy and diminished voice quality (Johns et al., 2011). On the other hand, increased or heavy voice use can result in epithelial thinning (Kimball, Sayce, Powell, et al., 2021), leading to laryngeal lesions. Therefore, investigating the intrinsic biomechanical properties of the VF is crucial to understand the underlying mechanisms of healthy phonation and the development of voice disorders. The following section describes the potential for the study of laryngeal biomechanics using bioreactors and bioactive materials known as magnetic microactuators.

1.3.2 Bioreactors

Some research laboratories seek to better understand how VF biomechanics contribute to healthy phonation, adding to known VF physiology as described in section 1.1.1. Biomimetic bioreactors have been employed to study vocal fold biology and physiology. A list of these devices

and the force type demonstrated are described in Table 1. These bioreactors include sound transducers, linear actuators, rheometers, and pneumatic actuators (Branski et al., 2007; Farran et al., 2013; D. Kim et al., 2016; Kirsch et al., 2019; Klemuk et al., 2008; Latifi et al., 2016; Titze et al., 2004, 2012; Tong et al., 2013).

Bioreactors provide certain advantages over standard cell culture. These devices allow direct stress to be applied to tissues in a controlled environment. These experimental conditions can effectively model shear stress in the superficial lamina propria and epithelial layers of the human larynx. Although these bioreactors have provided insight into the response of VF fibroblasts or mesenchymal stem cells in vitro, they have not yet fully characterized the interplay of mechanisms to describe the biological effect of stress on the VF epithelial layer, the voice organ's primary barrier against trauma and irritants. Furthermore, direct translation of findings from previously used bioreactor devices cannot be applied to human clinical studies, and the need to translate results from animal models to human patients is a critical biomedical challenge.

Table 1 Bioreactor devices used to study VF biomechanics

Method and approach	Scale of application	Force type	Use in VF studies
Atomic force microscopy (AFM) A silicon cantilever with a microfabricated tip is drawn across or tapped on the surface of the object under study.	Whole cell, cell-cell, cell-matrix	T, S	(Sivasankar & Ivanisevic, 2007) 2007
Cyclic tensile strain transducer Cells cultured on a flexible membrane are subjected to biaxial strain via vacuum control	Whole cell, cell-cell, cell-matrix	T	(Branski et al., 2007)
Engineered substrates Synthetic matrices to reproduce the complexity of the native cell microenvironment	Whole cell, cell-cell, cell-matrix	T, C	(Kimball, Sayce, Xu, et al., 2021)
Rheometers Cells are placed on a plate with a second plate rotating plate placed on top	Whole cell, cell-cell,	S, T	(Klemuk et al., 2008)

Table 1 (continued)			
Speaker-based bioreactors Speakers mounted to vibration chambers supply aerodynamic oscillation to cells grown on a flexible membrane.	Whole cell, cell-cell, cell-matrix	T	(Farran et al., 2013; Kirsch et al., 2019; Tong et al., 2014)
Substrate force transducers Cells cultured on a flexible membrane are mounted on planar or apical-basal linear actuators	Whole cell, cell-cell, cell-matrix	T, I, S	(Gaston et al., 2012; Y.-M. Kim et al., 2013; Wolchok et al., 2009)
Tensile loading Cells on flexible substrates are attached to beams that act as force transducers	Whole cell, cell-cell, cell-matrix	T, C	(Bartlett et al., 2015; Titze et al., 2004)
Force posts and beam-based polymer transducers Cells lie on top of a field of microposts. Cellular adhesion and migration causes deflection which can be used to calculate traction and adhesion forces	Whole cell, cell-cell, cell-matrix	T, S	N/A
Magnetic tweezers (MT) Ligand-coated magnetic beads bind to cells, and magnets are used to apply pulling or twisting force	Cell-cell, cell-matrix	T	N/A
Microelectrical mechanical system (MEMS) Embedded sensors and actuators apply controlled forces to cells (e.g., magnetic microactuators)	Whole cell, cell-cell, cell-matrix	T, C, S	N/A
Micropipette aspiration (MA) Cells are drawn slowly into the tip of a micropipette to study extracellular pressure on individual cells	Whole cell	T, C, S	N/A
Optical tweezers (OT) Dielectric beads are attached to cell membranes or molecules and a single beam optical laser trap pulls on particles	Whole cell, cell-cell, cell-matrix	T	N/A
T = tension; C = compression; S = shear			

1.3.3 Magnetic microactuators

The development of bioactive materials with tunable material properties has made it possible to apply precise physiological loads for *in vitro* or in situ observation and manipulation

of tissue structure and cellular mechanics. Magnetic microactuators have been well established as a method for precise application of biomimetic forces and in some tissues have contributed to the stimulation of regenerative biological mechanisms (Cezar et al., 2016; Chouhan et al., 2019; J. Kim et al., 2011; Sniadecki et al., 2007; Tomás et al., 2019; Yuan et al., 2018; Zhao et al., 2011). Magnetic microactuators allow the direct study of cellular response to realistic physiological loads and therefore are potentially an ideal tool to replicate the biomechanical environment of the larynx.

1.3.4 Aim 1 research question and hypothesis

As a tissue with the unique ability to meet the considerable biomechanical demands of everyday communication, the VF are a prime target for the cutting-edge diagnostic and therapeutic applications of bioreactors coupled with magnetic microactuators. Though microactuators have been used to study biomechanics in other tissues, so far there is limited application to the VF. Therefore, my primary objective was to determine whether the methods and approaches used in previous studies with other tissues were translatable to the VF.

My **research question** was: **What is the bio-tolerability of bioreactors and magnetic microactuators on VF biomechanics, as measured by microscopic examination and biochemical analyses *in vitro*?** Successful research in other fields has established microactuators as a highly tunable method for the application of exogenous forces and have advanced to the point that they have been shown to stimulate regenerative cellular mechanisms. Therefore, my **hypothesis** was: **bioreactors and magnetic microactuators can be feasible and safe for basic science research on laryngeal disorders as demonstrated by healthy cellular growth and proliferation.**

1.4 Overview of Aim 2

1.4.1 Novel techniques for preclinical investigations of medialization laryngoplasty for UVFP

*Surgical intervention is necessary for more than half of patients diagnosed with UVFP, with a primary goal of medializing the affected vocal fold to correct the glottal insufficiency (Francis et al., 2016). Type I thyroplasty, a technique where medialization is achieved by surgical insertion of a bio-tolerable implant (e.g., Silastic) or a stacked Gore-Tex ribbon through a window in the thyroid cartilage, is not without limitations, including: under/over medialization, size and shape variability when hand-carving implants, Gore-tex compression over time, and inflammatory reactions. Inadequate medialization is reported relatively frequently, with 4.5%-16% of type I thyroplasty procedures requiring surgical revision (J. T. Cohen et al., 2004; Maragos, 2001; Netterville et al., 1993; Parker et al., 2015; Woo et al., 2001). Overall, there is a need for continued research in the field of UVFP to improve outcomes and develop more effective and personalized treatment options for patients. The following sections describe specific areas in which there are opportunities to refine UVFP research, including customizable implants, novel animal models to simulate UVFP, and advancements in imaging techniques.

1.4.2 Optimization of implant materials for research in medialization laryngoplasty

*Optimization of laryngeal implant materials is crucial to the success of research in ML. The preclinical stage of research to develop a type I thyroplasty planning tool requires a method of producing implants of a precise size and shape made from medical-grade, bio-tolerable

materials. The choice of material can affect the mechanical properties, biocompatibility, and customizability of the implant. Implants that have been hand-carved from Silastic blocks are common in clinical settings but would not provide the reliability required for standardization of the procedure. The implants are sized on the millimeter scale, and small deviations could hinder the reliability and validity of future investigations. Commercially available laryngeal implants come in fixed sizes and shapes, limiting the ability to customize implants based on subject-specific laryngeal geometry. Some implant materials have been associated with complications such as inflammation, infection, extrusion, and implant migration (Cashman et al., 2002; Hizal et al., 2014; Orestes et al., 2014; Ustundag et al., 2005).

*Furthermore, the selection of laryngoplasty implant material can significantly impact the accuracy of imaging modalities such as CT and magnetic resonance imaging (MRI) for preoperative planning and postoperative evaluation. For example, Huang et al. (2015) evaluated artifact reduction methods for CT imaging and found that these methods underestimated the implant size and introduced new artifacts in imaging planes beyond the metal implant, highlighting the impact of implant material on imaging accuracy. Additionally, Duttenhoefer et al. (2015) investigated artifacts produced by implants in magnetic resonance imaging (MRI) and assessed the accuracy of pre-implant planning and post-implantation assessment, emphasizing the influence of implant material on imaging accuracy. Additionally, Bowen et al. (2022) found moderate agreement between MRI and histology estimates of residual injection laryngoplasty material, indicating the importance of accurate imaging for postoperative evaluation. Therefore, thoughtful design and production of an appropriate implant material is necessary for better reliability and reproducibility of research in the field of laryngology.

1.4.3 Development of novel animal models of UVFP

*Previous efforts to investigate type I thyroplasty methods are largely limited to studies in cadaver larynges assessing changes in biomechanics following implantation, or to histological analyses of larynges post-implantation. However, some animal studies that study type I thyroplasty modify glottal configuration using methods such as nerve cuffing/resection, direct manipulation of laryngeal tissue and cartilage, and electrical stimulation (Chhetri & Blumin, 2012; Döllinger et al., 2018; Sayce et al., 2020). These methods are effective for representing specific glottal configurations in basic science investigations but do not simulate UVFP glottal configuration across multiple timepoints during anatomical imaging.

1.4.4 Advanced laryngeal imaging

*Accurate and detailed diagnostic information is the cornerstone of individualized treatment for UVFP and has been expedited by recently developed laryngeal imaging techniques. Improved camera sensitivity and frame rate have added diagnostic value to laryngeal videoendoscopy with the benefit of live playback and quantitative measurements. Advances in micro-computed tomography and magnetic resonance imaging allow high-resolution 3D imaging of laryngeal tissue microstructure (Elders et al., 2019; Gignac & Kley, 2014). Incorporating advanced imaging techniques into computational models can further enhance our understanding of the changes in physical properties following medialization laryngoplasty, ultimately improving treatment outcomes for patients with UVFP.

1.4.5 Aim 2 research question and hypothesis

*Given the current challenges to selecting an ideal implant size and shape for type I thyroplasty durable implants, more research is needed to improve outcomes and develop more effective and personalized treatment options. Accurate and detailed diagnostic information is crucial for individualized treatment, and advanced imaging techniques can enhance our understanding of the changes in physical properties following medialization laryngoplasty to inform *in silico* studies. Therefore, my overall objective was to refine preclinical research methods in this area, including optimization of implant design and production, development of novel animal models to simulate UVFP, and integration of advancements in imaging techniques.

My **research question** was: **How can holistic optimization of experimental conditions, including implant design, animal models, and advanced imaging, contribute to the successful replication of clinically representative conditions of UVFP in a rabbit model, resulting in improved simulation accuracy and greater reliability of UVFP research outcomes?** My **hypothesis** was: **The integration of findings from the three project arms—implant design, anatomical simulation, and advanced imaging—will collectively optimize experimental conditions for UVFP research in a rabbit model.** Research in this area is ongoing, with studies investigating the effects of implant size and shape, as well as the use of animal models for surgical simulation and the development of a surgical planning tool for UVFP (S. Chang et al., 2013, 2016; Geng et al., 2021; Li et al., 2020; Movahhedi et al., 2021; Zhang et al., 2020).

1.5 Overview of Aim 3

1.5.1 Validating subject-specific predictive computational models

*The mechanisms that govern the relationship between VF biomechanics and aerodynamics have been investigated through a variety of experimental and numerical investigations. Computational mechanics offer unique advantages such as the ability to predict VF vibratory patterns through mathematical modeling and computer simulations. These models typically involve equations to represent the varying physical properties of the phonatory system, with some using fluid-structure interaction (FSI) simulations to capture the interaction between the VF and the air passing through the glottis. Previously studied computational mechanics models include lumped-mass, two-dimensional, and three-dimensional finite-element models, with varying levels of detail yielded by simulation type and corresponding effects on required computing power (S. Chang et al., 2013, 2016; Li et al., 2020; Luo et al., 2009; Movahhedi et al., 2021; Sadeghi et al., 2019; Xue et al., 2014; Yang et al., 2017; Zhang et al., 2020). Recent advances in computational power and medical imaging technologies, such as CT and MRI, have enabled the incorporation of patient-specific laryngeal geometries into finite-element models, allowing for individualized simulations. These technologies hold great promise for *in silico* research to develop more effective and personalized treatments for UVFP.

1.5.2 Aim 3 research question and hypothesis

Previously, *in silico* models simulating VF vibration with finite-element modeling have primarily assigned assumed stiffness properties across phonatory eigenmodes. This assumption

was applied even in simulations of asymmetric vibration in which different stiffness properties were assigned to each VF (Zhang et al., 2013). Additionally, the models did not include equations to account for changes in cartilage displacement angle. However, advanced imaging makes it possible to segment and reconstruct laryngeal structures from MRI or CT scans. The objective of this project was to obtain quantitative information on soft tissue and cartilage physical properties from 3D image data to inform the ideal size, shape, and placement of VF implants and compare expected results to actual results.

My **research question** was: **Can a computational model informed by pre-operative MRI data accurately identify optimal implant placement for type I thyroplasty?** Previous studies have explored the use of computational laryngeal models to optimize surgical techniques for medialization in type I thyroplasty based on implant size and shape. Fluid-Structure Interaction (FSI) models have demonstrated the ability to accurately predict the mechanical behavior of the larynx and the effects of surgical intervention on vocal fold biomechanics (Sadeghi et al., 2019; Zhang et al., 2020). By incorporating 3D imaging data into the modeling process, the accuracy of these predictions can be further improved, providing valuable information for surgical planning and optimization. Therefore, my **hypothesis** was: **The integration of findings from the three project arms—implant design, anatomical simulation, and advanced imaging—will collectively optimize experimental conditions for UVFP research in a rabbit model.**

1.6 Overview of the study design

The following illustrates the overall study design encompassing all three aims (Figure 2).

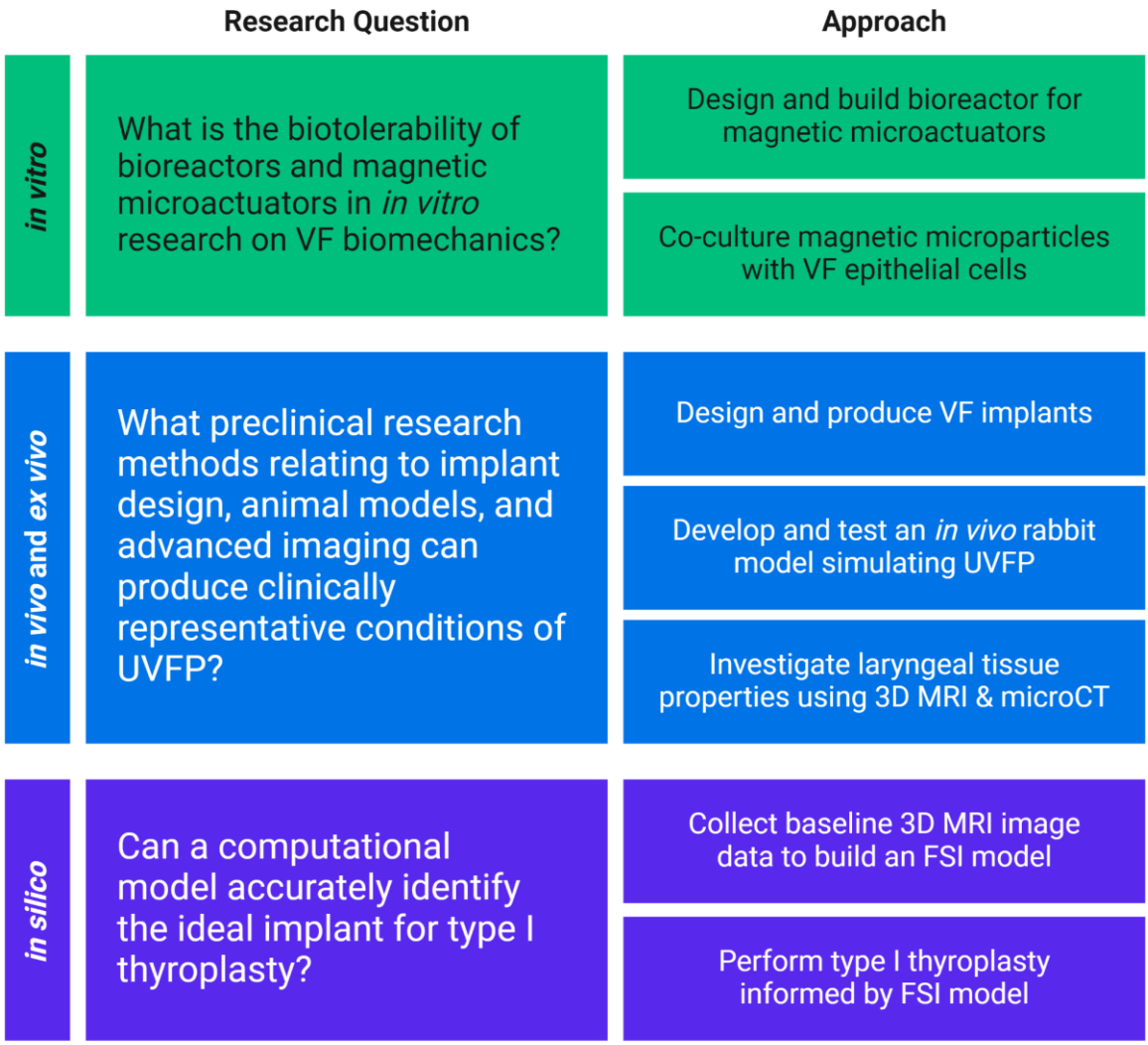

Figure 2 Flow chart of the overall study design

1.7 Significance and contribution of the study

Voice and swallowing disorders have a profound impact on an individual's quality of life, and can lead to social isolation, depression, and decreased work productivity. Through the advancement of technology and research, our understanding of the underlying mechanisms of

laryngeal disorders and in developing new treatments has increased, leading to improved outcomes for patients with laryngeal disorders, including those with vocal fold paralysis and glottal insufficiency.

The present study contributes to the field of laryngology by examining the feasibility and safety of bioreactors and bioactive materials in preclinical research on laryngeal disorders, as well as exploring the potential of computational models to optimize the design and placement of implants for type I thyroplasty. By providing a more comprehensive understanding of the biomechanics and interactions between laryngeal tissues and airflow during phonation, this research has the potential to improve the development of new treatment approaches, such as biocompatible materials and tissue engineering techniques. Furthermore, the use of advanced imaging and mathematical modeling to optimize surgical techniques could lead to more precise and effective treatments for patients with glottal insufficiency, reducing the need for revision surgeries and improving patient outcomes. Overall, this study has the potential to impact the field of laryngology by advancing the understanding and treatment of laryngeal disorders.

2.0 Aim 1: What is the bio-tolerability of bioreactors and magnetic microactuators on vocal fold (VF) biomechanics, as measured by microscopic examination and biochemical analyses *in vitro*?

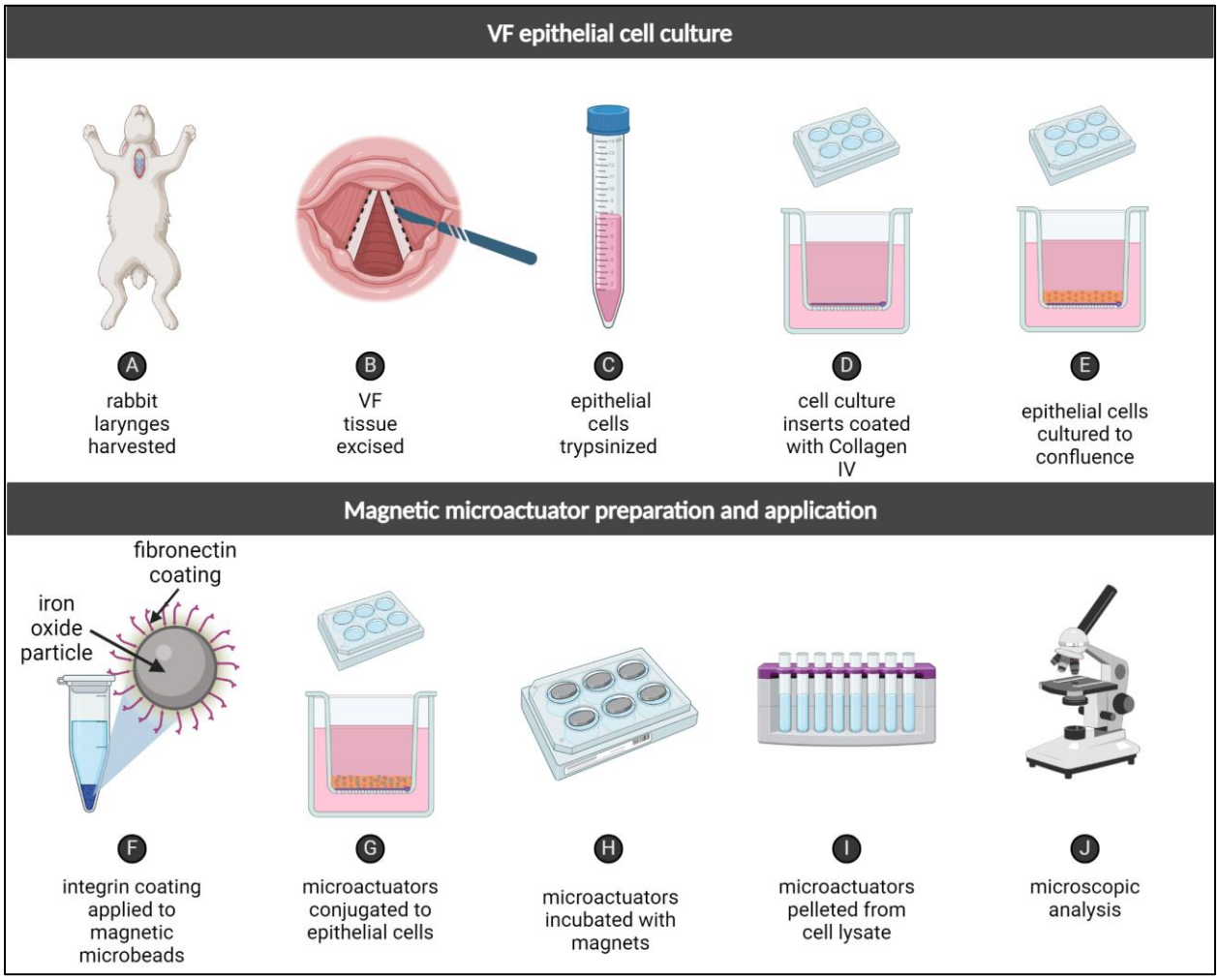

Figure 3 Graphical abstract of the Aim 1 study design

2.1 Project summary

The nature of communication disorders related to voice may present a profound barrier to individuals' participation in day-to-day activities. Loss of voice may deter individuals from engaging in activities that typically involve spoken communication, such as running errands, attending social gatherings, and making phone calls. Though behavioral voice treatments offer relief to many people with voice disorders, others experience symptoms that can't be resolved with voice therapy alone. Medical intervention for the treatment of voice disorders continues to improve as research into the biomechanics of the vocal folds progresses apace with biomedical research findings at large. One such area of research with relevance to voice disorders is biomedical engineering.

Biomedical engineering has opened new avenues for the development of bioreactors and magnetic microactuators to study the biomechanics of VF *in vitro*. Bioreactors and magnetic microactuators mimic biomechanical processes under research conditions to throw light on the effect of physical forces on tissues and cells. Such devices may have the potential for clinical implementation, yet the bio-tolerability of the devices for *in vivo* applications is not well established. My **research question** for this aim was: **What is the bio-tolerability of bioreactors and magnetic microactuators on VF biomechanics, as measured by microscopic examination and biochemical analyses *in vitro*?** Any investigation into the application of bioengineering devices for clinical implementation begins with a clear picture of their safety and efficacy. I investigated the following **hypothesis**: **bioreactors and magnetic microactuators would be feasible and safe for basic science research on laryngeal disorders as demonstrated by healthy cellular growth and proliferation.** The constituent parts of the research approach, depicted in Figure 3, toward investigating this hypothesis were: the co-culture of magnetic

microparticles with VF epithelial cells and the design and production of a bioreactor for use with magnetic microactuators.

2.2 Methods

This study presents a combined system of a bioreactor and magnetic microparticle culture designed to enable precise real-time measurement of VF epithelium cellular activity following oscillatory applied shear and tensile force as an approximation of physiological conditions during phonation. Magnetic microbeads were coated with bovine fibronectin, an ECM component that binds to receptors on the cell surface. A bioreactor device suspended a magnetic field over the culture plate and induced torque on the microparticles. The microparticles, bound to the cell surface receptors through the fibronectin coating (Elosegui-Artola et al., 2018), transduce force to the cytoskeleton, thus eliciting a mechanobiological cellular response (Bonde et al., 2008). Contactless interaction with a permanent magnetic field allows the application of force through sealed interfaces, limiting the potential for contamination and reducing threats to internal validity such as changes in humidity or temperature.

The research design for the bioreactor production was descriptive with a focus on the system's potential to replicate physiologically relevant parameters such as applied force type, applied force magnitude, vibration frequency, and vibration amplitude. The research design for the magnetic microparticle co-culture was primarily qualitative, with cell viability determined by microscopic observation of epithelial cell growth and proliferation at multiple timepoints compared to controls. The methods were integrated and described by identifying areas of

agreement or disagreement between test cells and controls to determine the validity and reliability of the findings.

2.2.1 Cell culture

VF epithelial cells were cultured consistent with methods previously published by our laboratory, identifying normative development of a multilayered epithelium (Kimball, Sayce, Xu, et al., 2021; Mizuta et al., 2017). New Zealand white rabbits weighing between 2.5 kg - 4.0 kg were sedated with 20 mg/kg ketamine hydrochloride and 0.125 mg/kg dexmedetomidine via intramuscular injection in the hindquarter. A stable plane of anesthesia was confirmed by the absence of pain responses and involuntary reflexes. The neck and chest were shaved, and the rabbit was arranged in a supine position. A skin incision was made from the sternal notch to the submentum, and the fascia and muscle were dissected at the midline to expose the larynx and trachea. Animals were euthanized by an overdose of sodium pentobarbital (390 mg/ml) via an intravenous 25-gauge catheter in the marginal ear vein. Death was confirmed by cessation of breathing and heartbeat, in addition to the absence of responses to painful stimuli. Following death, the larynx was immediately harvested superior to the epiglottis and inferior to the second tracheal ring and hemisected to be prepared for cell culture.

2.2.1.1 Materials preparation

The growth of rabbit VF epithelial cells in physiological conditions to be used for experimental purposes requires the preparation of specialized materials. When considering the cell culture plate coating, the ideal substrate functions as an extracellular matrix similar to the VF basement membrane in situ. The VF basement membrane does not typically contain Collagen I, a

commonly used substrate in primary culture (Garrett et al., 2000). Previous studies have demonstrated a single-protein collagen IV substrate may emulate the multilayered VF epithelial layer most closely (Bartlett et al., 2015, 2019; Kimball, Sayce, Powell, et al., 2021). A physiologically relevant *in vitro* model of VF epithelium requires a representation of the basement membrane in direct contact with the epithelium. These conditions are necessary to grow eukaryotic cells with similar morphology, proliferation, and cell fate to VF epithelia (Kimball, Sayce, Xu, et al., 2021). Rabbit VF epithelial tissue harvest also demands a careful process of dissociating the epithelium from the underlying matrix, the lamina propria. These methods are described below.

2mL of 37.5 µg/mL collagen solution (Advanced Biomatrix PureCol-S) diluted in PBS was added to each well to coat the plates (not in direct contact with the cells) with ultra-pure collagen. The plates were incubated at 37°C for 2.5 hours, and the remaining liquid was aspirated with a sterile pipette. The plates were rinsed with PBS, re-sterilized under UV light for 30 minutes, and stored at 4°C for up to 3 weeks before use.

Collagen IV (Corning Collagen IV, mouse) was diluted in 0.05M HCl per manufacturer protocol and added to cell culture inserts at a concentration of 0.5µg/cm^2. Inserts were left to dry overnight in a dark biosafety cabinet with the fan on. In the morning, each insert was rinsed with PBS, wrapped in parafilm, and stored at 4°C for up to 3 weeks before use.

For passage 0 (P0) and passage 1 (P1) of the epithelial cells, cells were co-cultured with feeder cells (3T3-Swiss Albino, ATCC CCL®-92TM, ATCC, Manassas, VA) onto the collagen IV coated plates. Passage 2 (P2) epithelial cells were seeded onto protein-coated cell culture inserts (Millipore, PET 1µm) without feeder cells. For P0 and P1, feeder cells were treated with 10 µg/mL mitomycin-C (Sigma-Aldrich) at 37°C for 3 hours before seeding to halt proliferation and were

seeded together with the epithelial cells on a collagen I-coated 6-well plate at a density of 2.0 x 104 cells/cm^2.

Excised VF were stored in a culture medium composed of DMEM/F12 (1:1 with 1-glutamine, 15mM HEPES, 1 mM $CaCl^2$, GIBCO, Grand Island, NY), 10% fetal bovine serum (FBS, HyClone, South Logan, UT), penicillin (100U/mL), streptomycin (100µg/mL, HyClone, South Logan, UT), epidermal growth factor (10µg/mL, Peprotech, Rocky Hill, NJ), insulin (5 µg/mL, Sigma-Aldrich), adenine (24µg/mL, Sigma-Aldrich), hydrocortisone (0.4µg/mL, Sigma-Aldrich), cholera toxin (0.1 nM, Sigma-Aldrich), and triiodo-L-thyronine (2nM, Sigma-Aldrich; (Mizuta et al., 2017). The vocal folds were treated with 66U/mL Dispase II (Roche Life Science, Indianapolis, IN) in the culture medium at 37°C for 4 hours to separate the epithelial layer from the lamina propria.

The epithelial layer of each VF was removed under microscopy and the cells were dissociated in a solution of 0.05% trypsin/0.02% EDTA (Sigma-Aldrich, St. Louis, MO) at 37°C. The culture medium was added after 20 minutes to stop cellular dissociation, and the cells were suspended by needle aspiration followed by gentle pipetting. The suspension of dissociated cells was centrifuged at 500g for 5 minutes, supernatant aspirated, and the obtained pellet was re-suspended in the culture medium. Cells from each fold were seeded into wells on a 6-well plate and co-cultured with mitomycin C-treated (Fisher BioReagents, NJ, USA, BP25312) feeder cells at a seeding density of 2.0 x 104 cells/cm^2.

2.2.1.2 Epithelial cell passaging

When the VF epithelial cells reached local confluence (occurring on or about P0, day 7), they were counted via hemocytometry and passaged into P1 at a seeding density of 2.2 x 104 cells/cm^2, co-cultured with mitomycin-C treated feeder cells at a seeding density of 2 x 104

cells/cm^2. P1 was cultured on prepared pure collagen-coated 6-well plates. When P1 cells reached 70-80% confluence (occurring on or about P1 day 4), the cells were counted and seeded at P2 onto prepared collagen IV-coated cell culture inserts.

2.2.2 Magnetic microactuator bioreactor

The methods described herein are preparatory steps in the design and use of a magnetic microactuator device intended to fine-tune physical and chemical properties for the *in vitro* study of VF biology, physiology, and biomechanics. Iron oxide beads 2.8 microns in size are coated in ligands that bind to targeted cell proteins on the surface of the vocal fold epithelial cell membrane. The application of an external magnet creates mechanical tension on the beads to engage the mechanosensitive signaling pathway (J. H.-C. Wang & Thampatty, 2006).

2.2.2.1 Device design

I collaborated with Dr. Kosaku Kurata at Kyushu University to adapt an open-source cell stretching device (Kurata et al., 2019) to serve as a novel magnetic microactuator loading device. The original device was designed to be easy to reproduce and modify. It was constructed with laser-cut acrylic sheets and applied stretching shear force by deforming a silicone culture dish. An electric motor served as a uniaxial reciprocating actuator, controlled by a touch-screen single-board computer. The device reliably produced between 0.5% and 5% uniaxial stretch to the silicone cell culture dish at 0.1-2 Hz. Though highly configurable, the original device was not suited for testing forces relevant to the VF. I sought to adapt the device to program and simulate phonatory tensile and shear force at frequencies and amplitude similar to what VF epithelial cells experience during typical vocal function.

2.2.2.2 Magnetic microactuator preparation and conjugation to VF epithelial cells

40μL of iron oxide particles with a 2.8μm diameter in suspension (ThermoFisher, NJ, USA, 14203) were thrice washed and resuspended at a concentration of 4.4 x 104 in a solution of 1mL 0.1M Na-phosphate pH 7.4 containing 100 μg bovine fibronectin (Sigma Aldrich, TX, USA, F1141-5MG). The particles in the fibronectin solution were incubated for 24 hours at 37°C. The microactuator solution was combined with epithelial cells at 70-80% confluence and incubated for 20 minutes at 37°C to conjugate the fibronectin-coated microactuators to the cells at the adhesion complexes. ½"-diameter neodymium magnets were fixed to the lid of each cell culture well. The distance from the pole face of the magnet to the apical surface of the cells was 6mm, exerting a force of ~40pN. The cells were incubated for 24 hours at 37°C to allow proliferation. Cell count was determined via hemocytometry.

2.2.2.3 Preparation of magnetic microactuator-treated cell lysates

Cells were washed in ice-cold PBS, and ice-cold lysis buffer (150μL 150mM NaCl; 500μL 0.1% Triton X-100; 250μL 50mM Tris-HCl) was added. Cells were incubated on ice for 10 minutes. The lysate was collected using a cell scraper and the magnetic microactuators were pelleted using a magnetic separation stand. The supernatant was collected and frozen at -80°C until biochemical analysis.

2.2.3 Ethical considerations

This study was approved by the University of Pittsburgh Institutional Animal Care and Use Committee (IACUC #18114069). All procedures were conducted within the University of Pittsburgh Department of Laboratory Animal Research, an AAALAC-accredited facility, in

compliance with the Guide for the Care and Use of Laboratory Animals (*Guide for the Care and Use of Laboratory Animals*, 2011) and the Animal Welfare Act (United States Department of Agriculture, 2019).

2.3 Results

The adapted bioreactor comprises a laser-cut acrylic base for attaching a cell culture dish and a loading unit housing a stepping motor driver circuit and connectors, constructed from 5-mm and 1.5-mm plates. Figure 4 illustrates the entire cell extension system with the base, loading unit, and single-board computer with a touch screen for device settings selection.

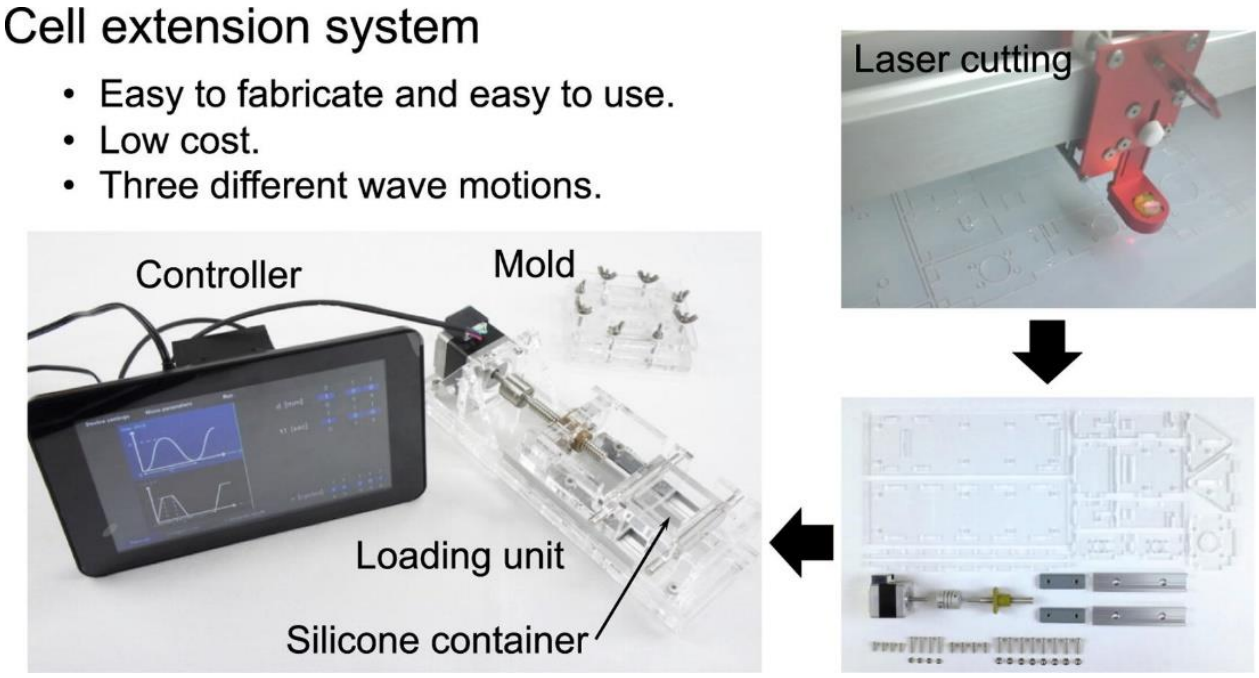

Figure 4 Open-source cell extension system

(Kurata, 2019)

I created a 3D computer model adaptation of the original device (Figure 5) tailored for use in a magnetic microparticle system to study physiologically relevant loads in VF epithelial cell

culture. In this modified design, recesses were incorporated into the underside of the loading unit to house 1.5-inch diameter neodymium magnets and guide rails along which the loading unit could reciprocate. While a minor adjustment, suspending magnets over the culture dish was crucial for applying tensile and shear force to the microactuators.

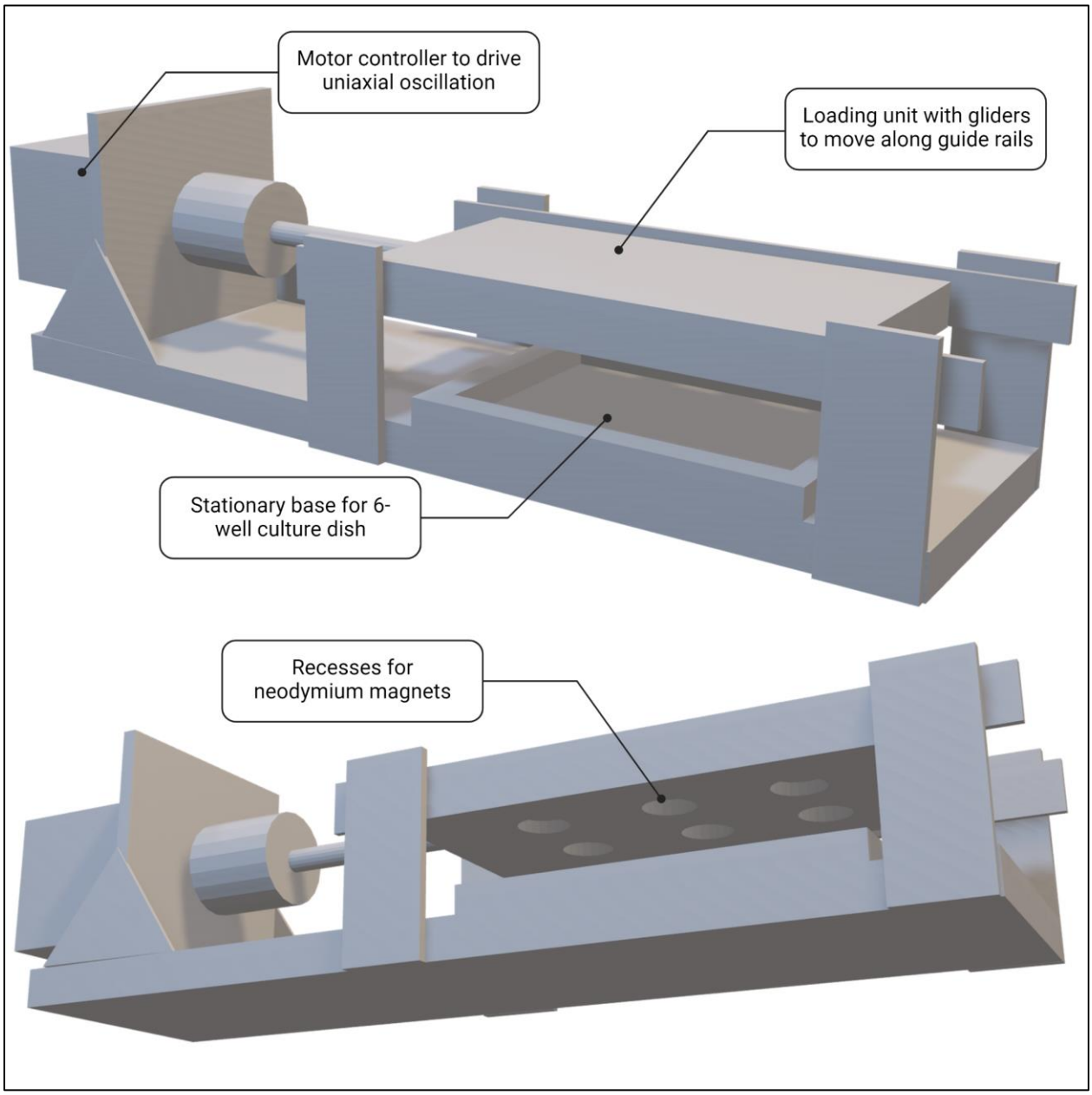

Figure 5 3D illustration of the adapted cell-extension system

A prototype of the device used was produced to validate the experimental approach, but testing revealed its inability to replicate phonatory physical stress due to limitations in the hardware. The rotary motor oscillated only up to 50 Hz and for a brief duration to overheating. Therefore, the design also needed to be modified to allow optimization of the oscillatory parameters to approximate applied stress from phonation. The activator needed to be capable of reproducing established physiological relevant parameters of 1000-micrometer displacement amplitude and up to 200 Hz frequency (Cochereau et al., 2020; Gracioso Martins et al., 2022). The maximum force generation required for the actuator was calculated with the following formula:

$$Fmax = m \times A \times \omega$$

where m is the mass, A is the amplitude, and ω is the angular frequency. Given the system as designed, the variables were as follows:

$$Fmax = 0.03 \times 0.001 \times (2\pi \times 200)^2$$

The maximum force needed would therefore be 47.3 N, provided by a 50.8mm linear voice coil actuator with an integrated Hall effect sensor to validate frequency and amplitude (Moticont, Van Nuys, CA #LVCM-051-054-02).

As previously discussed, ensuring the compatibility of microactuators with VF epithelial cells in cell culture necessitated viability testing. Following established guidelines for iron oxide particle administration to minimize alterations to cell-cell interactions (Millon-Frémillon et al., 2017), test cultures containing microactuators were incubated for 24 hours with magnets exerting a constant force, measured by magnetometer to be approximately 40pN. Subjective observation of the proliferation and morphology of VF epithelial cells treated with microactuator-induced force showed comparability to untreated cells after 24 hours of cell culture as depicted in Figure 6.

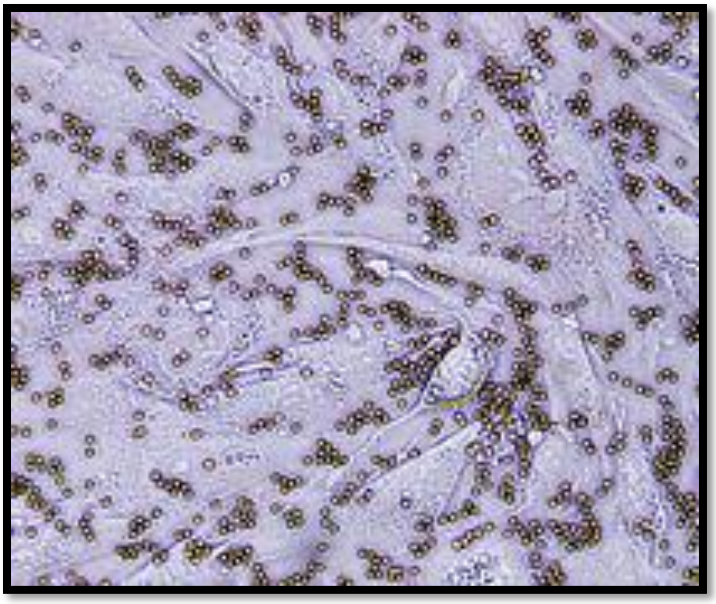

Figure 6 VF epithelial cells treated with magnetic microactuators

2.4 Discussion

In this chapter, I presented a bioreactor design based on an open-source cell extension device, tailored for use in a magnetic microparticle system to investigate physiologically relevant loads in VF epithelial cell culture. Through crucial adaptations, the modified device enables the remote application of magnetic force to microactuators, mimicking some elements of phonatory physical stress with tensile and shear force. The findings suggest that, with hardware and software enhancements, the magnetic microparticle system could prove valuable for studying physiologically relevant loads in VF epithelial cell culture.

Prototype testing demonstrated the inability of the current system to replicate physical stress at a phonatory frequency due to overheating, underscoring the need for further hardware optimization. As a potential solution, I propose the addition of a linear voice coil actuator with an

integrated Hall effect sensor and heat sink, which could offer the required resolution to reproduce established physiologically relevant parameters.

These findings suggest that an optimized *in vitro* system for studying VF epithelia may have implications for understanding phonatory physical stress. The modified bioreactor design offers precise and configurable force application to cells, potentially enhancing our understanding of the mechanisms underlying phonation and VF injury. This knowledge could inform the development of novel treatments for voice disorders and improve surgical techniques for VF restoration, such as type I thyroplasty.

However, despite the achievements in this chapter, there are inherent limitations. The uniaxial stroke mechanism cannot fully replicate the complex multidirectional forces experienced by VF epithelial cells during speech. Additionally, the *in vitro* environment, while useful for controlled experimentation, diverges from the complexities of forces experienced by cells *in vivo*, where factors like inflammation and blood supply play crucial roles in cellular behavior.

Though the application of magnetic microactuators in this study was solely designed for in vitro investigations, there is a potential for a future application as a minimally invasive approach to treating VF disorders. These devices can provide precise mechanical stimulation to the VFs, restoring or enhancing their vibratory function. Designed from non-toxic, durable materials, these microactuators could be implanted using minimally invasive techniques like endoscopic surgery. Controlled externally by a wearable device that generates magnetic fields, the microactuators could dynamically adjust VF tension and position based on real-time feedback from advanced imaging or acoustic monitoring systems.

The primary benefits of this technology include high precision, dynamic adjustment, and reduced recovery times due to the minimally invasive nature of the implantation procedure.

Challenges remain in ensuring long-term biocompatibility, developing a reliable control system, and guaranteeing the durability of the microactuators under the mechanical stresses of vocalization. Future research should focus on optimizing these aspects to ensure safety, efficacy, and practical usability in clinical settings.

Additionally, bioreactors enable the investigation of biochemical pathways by introducing various stimuli and testing their effects on fibrotic responses. One open question relating to this topic is the effect of fibrotic capsule formation around implants, shown in previous studies (Dion et al., 2018; Ustundag et al., 2005). These systems can replicate mechanical forces, fluid flow, and biochemical environments to observe how tissues respond to implants over time. By monitoring cellular and molecular responses in real-time, bioreactors would enable monitoring of fibroblast activity and extracellular matrix (ECM) deposition, key processes in fibrosis.

Bioreactors also may serve as a platform for evaluating different biomaterials and surface modifications, such as anti-inflammatory coatings, to identify methods that reduce fibrosis. Overall, bioreactors facilitate detailed, longitudinal studies that can lead to the development of strategies to prevent or mitigate fibrotic capsule formation, improving the biocompatibility and longevity of implants.

3.0 Aim 2: How can holistic optimization of experimental conditions, including implant design, animal models, and advanced imaging, contribute to the successful replication of clinically representative conditions of UVFP in a rabbit model, resulting in improved simulation accuracy and greater reliability of UVFP research outcomes?

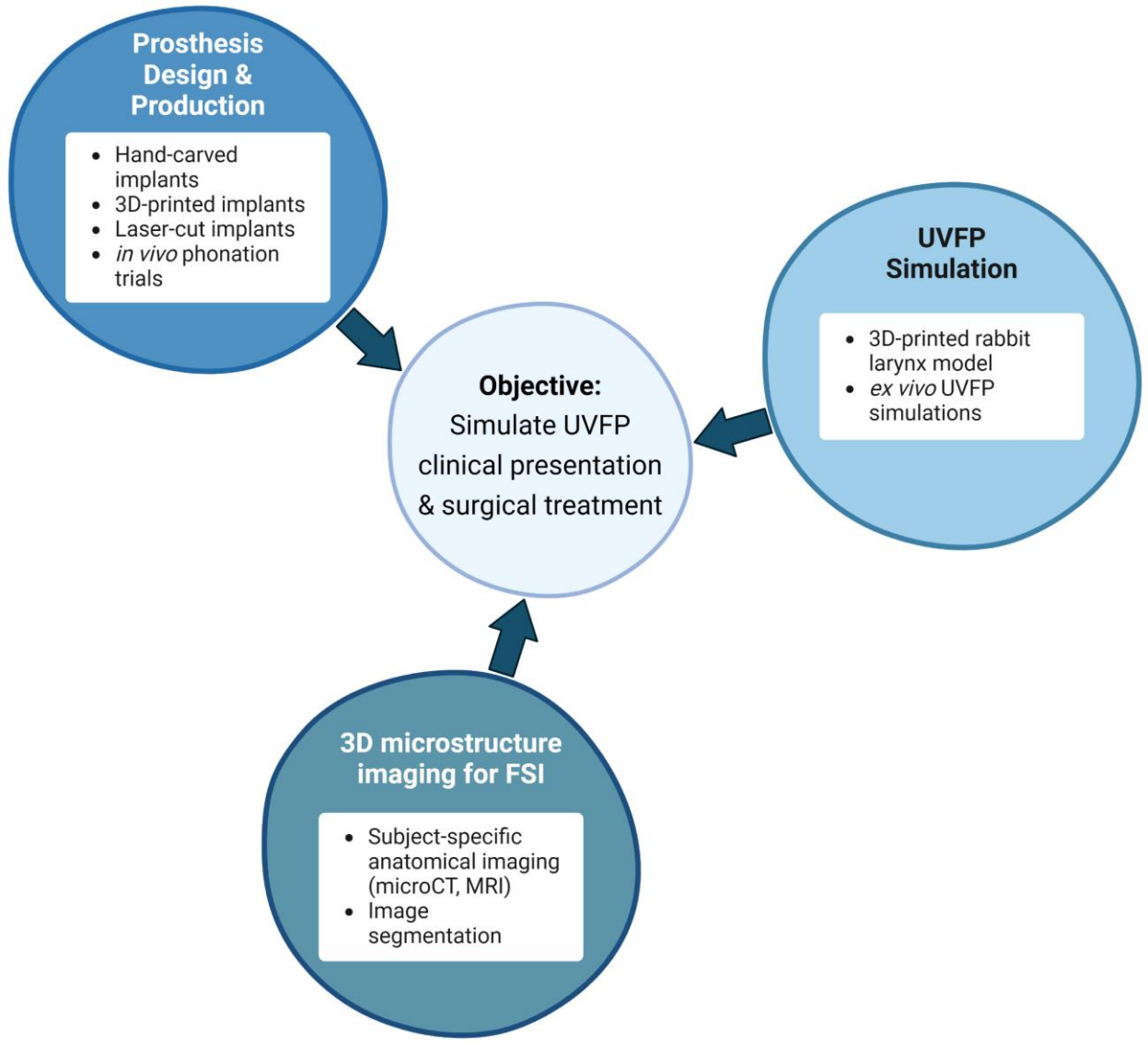

Figure 7 Visual abstract for the Aim 2 study design

Achieving optimal outcomes in the treatment of UVFP necessitates an individualized approach that accounts for the unique laryngeal anatomy and tissue properties of each patient. The current standard practice for type I thyroplasty relies on perioperative manual adjustments guided by subjective assessments of glottal space and voice quality. To enhance this procedure and mitigate the risk of early complications, computational modeling is being employed to pre-plan surgical interventions for UVFP. This innovative approach aims to create personalized implants based on precise anatomical data. The preclinical investigations detailed in this study were designed to provide essential insights into vocal fold tissue properties that are necessary inputs in accurate computational models for surgical planning.

3.1 Project summary

The overarching objective of this research was to recreate the conditions of UVFP and its surgical treatment in a rabbit model. This multifaceted endeavor encompassed three distinct investigative arms, each contributing to the optimization of experimental conditions for UVFP research. These three arms, depicted in Figure 7, comprised prosthesis design and production, UVFP simulation, and 3D microstructure imaging for a finite element model.

In the first arm, I focused on the design and production of various implant types, including hand-carved, 3D-printed, and laser-cut implants. This aspect of the project aimed to fulfill the need for an implant design that could seamlessly integrate into *in vivo* phonation research.

The subsequent arm revolved around the physiological simulation of UVFP, facilitated by a 3D-printed representative rabbit larynx model. This model served as a tool for generating and comparatively evaluating two distinct surgical methods intended to replicate the clinical

presentation of UVFP. The investigations within this arm determined whether these distinct surgical approaches would yield varying outcomes, with one method resulting in laryngeal geometry representative of the condition for *ex vivo* phonation trials.

In the third arm, I explored advanced imaging techniques, employing subject-specific anatomical imaging methods such as microCT and MRI along with segmentation of the images into various cartilaginous and soft tissue components. These techniques facilitated the construction of a highly precise subject-specific finite element model, forming the basis for the research's quantitative analyses. The application of these techniques was intended to enhance the accuracy of research outcomes.

Incorporating these project arms, my **research question** for this aim was: **How can holistic optimization of experimental conditions, including implant design, animal models, and advanced imaging, contribute to the successful replication of clinically representative conditions of UVFP in a rabbit model, resulting in improved simulation accuracy and greater reliability of UVFP research outcomes?** In each arm of this research, attention was given to both descriptive and quantitative analyses, including factors such as glottal area, vibration eigenmodes, and vibratory frequency. The objective was to systematically assess areas of consensus and divergence across these arms, ultimately providing a comprehensive evaluation of the validity and reliability of the research outcomes. Therefore, my **hypothesis** was: **The integration of findings from the three project arms—implant design, anatomical simulation, and advanced imaging—will collectively optimize experimental conditions for UVFP research in a rabbit model.**

3.2 Methods

In this section, I will elaborate on the methods employed to examine the three arms indicated above: VF implant design and production, UVFP simulation, and 3D microstructure imaging for finite element modeling. These three arms combine to explore UVFP comprehensively and enhance our understanding of this condition and its treatment.

3.2.1 Designing and producing VF implants

When approaching the design and production of VF implants, my goal was to develop implants for preclinical research that met essential criteria, including precision, customizability, cost-effectiveness, and adaptability to various experimental needs. These implants were crafted to align with the research requirements, ensuring accuracy and reproducibility in our experiments. The process was largely iterative, spanning hand-carved, 3D-printed, and laser-cut implants. This process was used to identify an implant design that could be feasibly mass-produced with accuracy. The implants were subsequently used in *in vivo* rabbit phonation experiments.

3.2.1.1 Hand-carved implants

In the initial stages of implant design and testing, I prepared a sheet of two-part polydimethylsiloxane elastomer (Sylgard™ 184, Dow Chemical Company), creating a layer approximately 2mm thick (equivalent to about 0.08-inches) with a 5-to-1 ratio of base to curing agent. Once the elastomer had fully cured, approximately 24 hours later, I hand-carved the implants with a scalpel. Two preliminary implant shapes were produced: S1, a rectangular shape,

and S2, a tetrahedral shape with greater depth toward the rear part of the implant, featuring an internal depth of either 1mm (about 0.04-inches) or 2mm (about 0.08-inches). Implants were hand-carved under 4x magnification, using a ruler to ensure precise measurements (see Figure 8).

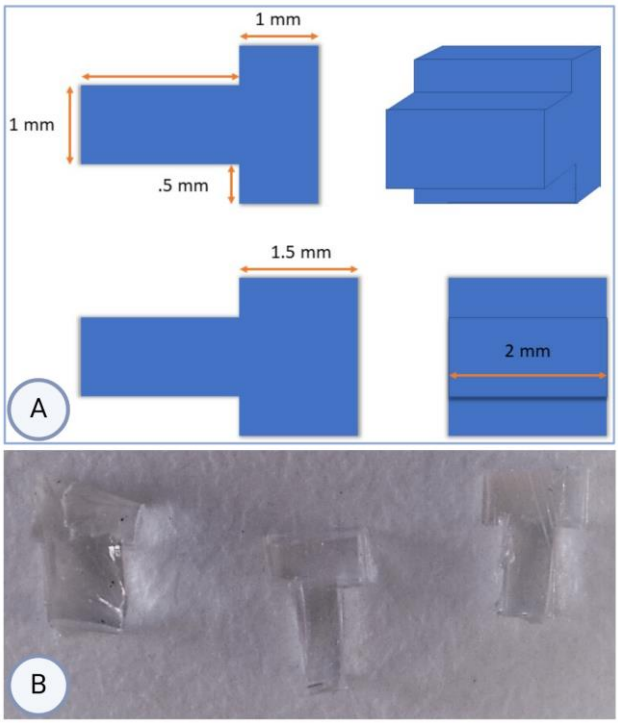

Figure 8 Hand-carved implants.
A) Dimensions to guide hand-carving. B) Initial hand-carving trials of the polydimethylsiloxane elastomer

3.2.1.2 3D-printed implants

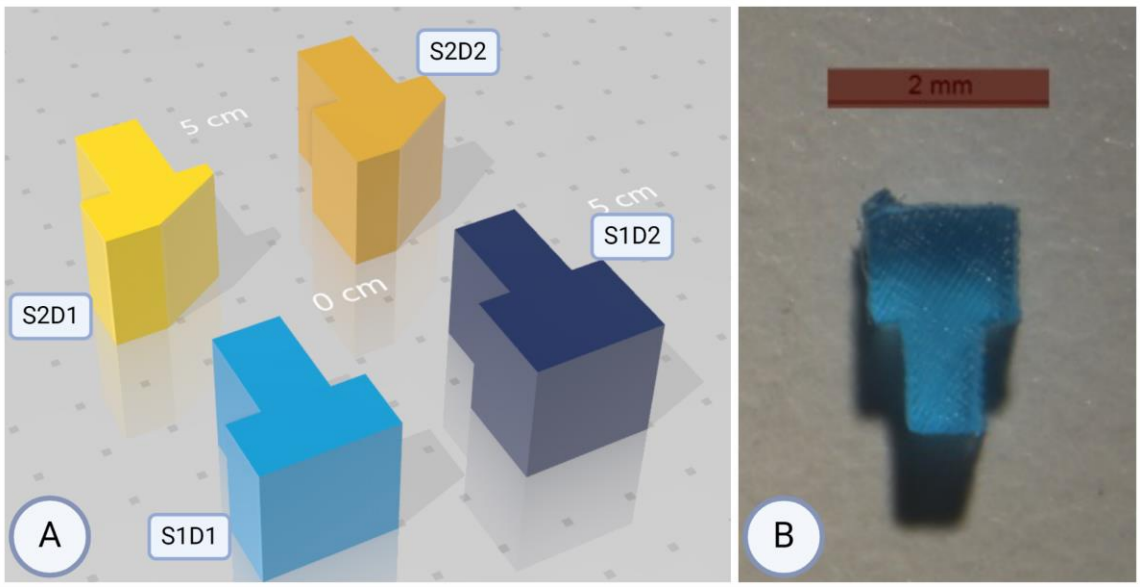

Figure 9 3D-printed implants

A) Dimensions used as inputs for 3D printing. S1 indicates a rectangular implant shape. S2 indicates a divergent angled implant shape. D1 indicates an implant depth of 1.5mm. D2 indicates an implant depth of 2mm. B) Implant 3D printed with 50-micrometer resin filament

The next stage of implant design involved the creation of 3D-printed implants. I used 3D modeling software (Tinkercad, 2019) to develop computer-aided design (CAD) models for four distinct implant variations, comprising two shapes and two sizes (see Figure 9a). The implants were designed with a shelf on the part located distal to VF placement to ensure a secure snug fit within the thyroplasty window. The implant size was scaled to one-quarter of commercially produced human VF implants, according to the approximate size difference between rabbit and human larynges (Bailey et al., 2020; Eckel et al., 1994; Loewen & Walner, 2001). I manufactured

the implants on a Form 3+ Low Force Stereolithography 3D printer (Formlabs, Boston, MA) with 1mm diameter resin filament at 50-micrometer thickness (see Figure 9b)[1].

3.2.1.3 Laser-cut implants

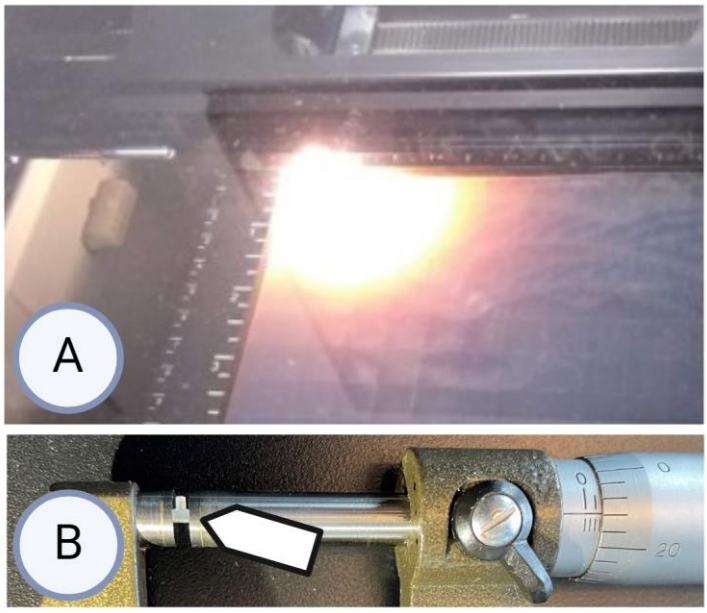

Figure 10 Laser-cut implant
A) A photograph of the laser-cutting machine during the printing process. B) Laser-cut implant measured with calipers.

In further iterations of implant design, I used the same design parameters to produce the implants using a laser printer with a 50W CO2 laser (Epilog Zing 24) at the University of Pittsburgh. Twelve implants of each size and shape (*N*=48) were produced to determine production speed. The precision was set to 500 dpi. Implants were vector-cut from a single sheet of medical-

[1] I would like to acknowledge Aaron Graham and Will Hinson of the Open Lab at the University of Pittsburgh for providing the facilities, materials, and guidance to produce the implants.

grade silicone elastomer (6 x 8 x .080in non-reinforced sheeting, Bentec Medical, Woodland, CA) at 50% power, 40% speed, and 5000 Hz (see Figure 10a).

3.2.2 *in vivo* phonation trials

I tested laser-cut implants during *in vivo* phonation trials to assess the performance and functionality within an active physiological environment. The trials were carried out via standard practice for type I thyroplasty surgery methods, described below. All surgical procedures were performed by me with the assistance of one or more surgical support members[2]. Veterinary staff were on hand if necessary.

3.2.2.1 Surgical anesthesia

I sedated rabbits by intramuscular injection of 20mg/kg ketamine hydrochloride and 0.125mg/kg dexmedetomidine into the latissimus dorsi. Efficacy was determined through the absence of movement, absence of response to stimuli (e.g. ear pinch, toe pinch, skin manipulation), and decrease in respiratory rate. To maintain a stable anesthetic plane, continuous rate infusion was provided per procedures outlined in Sayce et al. (2020). 350μg/kg/min ketamine and 1.65μg/kg/min dexmedetomidine were provided intravenously via 25G catheter to the marginal ear vein beginning 30 minutes after the sedation dose. Heart rate, respiratory rate, temperature, and blood oxygen saturation were recorded at 15-minute intervals for the duration of the procedure.

---

[2] I would like to acknowledge the support of Lea Sayce, Gary Gartling, Zachary Zimmerman, and Alysha Slater for their assistance during surgical procedures.

3.2.2.2 Peri-operative setup

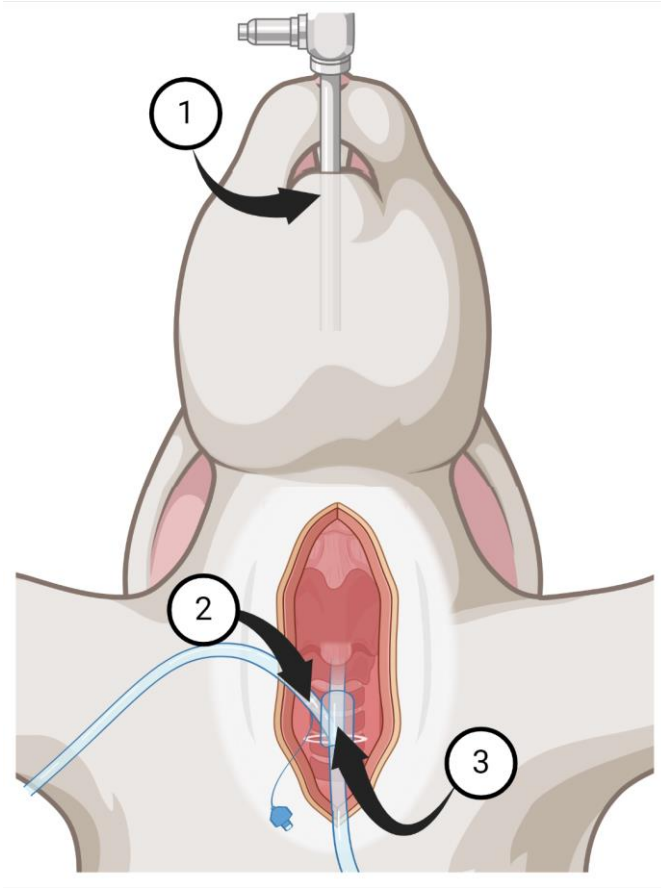

Figure 11 Surgical setup
1) Pediatric laryngoscope placed to visualize VF during implantation. 2) Uncuffed endotracheal tube providing oxygen to lungs. 3) Cuffed endotracheal tube providing humidified airflow to pass through the glottal space.

The surgical setup is illustrated in Figure 11. Once anesthetized, I shaved the neck and chest of the rabbits, and the rabbit was arranged in a supine position on a water-circulating heat mat. Subcutaneous Lidocaine was injected into the skin of the neck to alleviate local pain, followed by a pinching test from the suprasternal notch to the hyoid bone to gauge any pain responses. I palpated the soft tissue to feel for the larynx, then made an incision into the epidermis from the superior portion of the thyroid cartilage to the fourth tracheal ring. Subsequent dissection of the skin, fascia, and muscle layers exposed the larynx to view. I bisected the trachea and placed an

uncuffed endotracheal tube into the arboreal portion to provide direct oxygen to the lungs. I positioned a cuffed endotracheal tube in the upper portion of the trachea and provided humidified airflow at 37°C to the subglottis. I inserted a pediatric laryngoscope via the mouth to suspend the larynx and visualize the vocal folds. A combination of humidified airflow and VF medialization via suture approximation as described below was used to achieve phonation.

3.2.2.3 Phonation setup

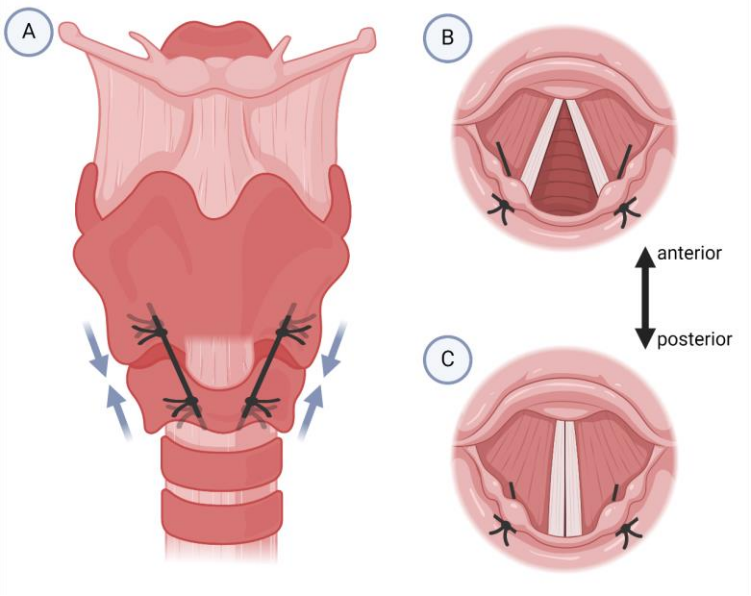

Figure 12 Illustration of cricothyroid approximation for the phonation procedure
A) Anterior view of the larynx with sutures secured at the level of the anteriolateral thyroid cartilage and cricoid cartilage. B) Visualization of suture placement in axial view for lateral and C) medialization positions.

Five New Zealand white rabbits weighing between 2.5kg and 4.0 kg were used to verify successful implantation. A method for Isshiki-type type IV thyroplasty (see Fig 12), inducing bilateral vocal fold approximation by cricothyroid suture, has previously been described by our lab (Novaleski et al., 2016). Briefly, I passed a size 5 tapered polyglactin 910 braided suture (Ethicon) through the mediolateral cricoid cartilage and secured it in position, then passed the

suture through the ipsilateral thyroid cartilage. Tension was applied to bring the two cartilages together to simulate cricothyroid adduction and medialize the vocal folds; physically lengthening the vocal fold to increase tension and achieve vibration more readily. The suture was secured to maintain the relative position of the VF.

3.2.2.4 Implantation and high-speed video capture

Implant shapes and sizes, specifically, S1D1 (n = 1), S1D2 (n = 1), S2D1 (n = 2), and S2D2 (n = 1) were selected using simple random sampling (see Figure 9 caption for specifications). I outlined a 1mm x 2mm thyroplasty window approximately 2mm posterior to the anterior laryngeal midline and just above the inferior tubercule. I incised the cartilage according to the outline (see Figure 13), and the resected fragment was carefully separated from the internal perichondrium. I placed the implant within the thyroplasty window and placed a resorbable hemostat to help maintain the implant position. I opened airflow through the cuffed endotracheal tube and the forced humidified air elicited phonation. High-speed video of phonation events was captured using a KayPENTAX FastCam MC2.1 system coupled to a 0° rigid endoscope at 8,000 frames per second.

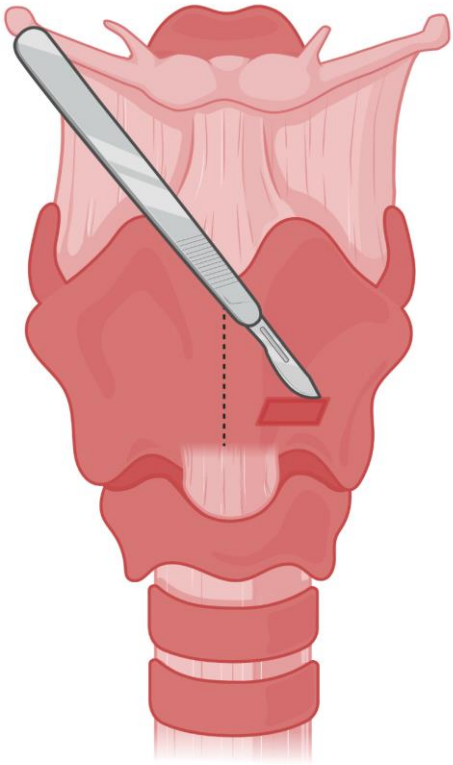

Figure 13 Illustration of thyroplasty window incision

Once I verified successful implantation and phonation via laryngoscopic observation, animals received an overdose of intravenous Sodium pentobarbital. Death was confirmed by cessation of breathing and heartbeat, absence of vital signs, and absence of stimuli to pain response. Larynges were harvested with incisions made at the level of the thyrohyoid membrane and the third tracheal ring.

3.2.3 Capturing and processing 3D microstructure images for finite element modeling

This section outlines the adaptation of a previously published 3D-printed laryngeal model to represent the anatomical features of the rabbit larynx. Additionally, it details the procedures for

obtaining and processing MRI and micro-CT images to develop customized computational models of excised larynges.

3.2.4 3D-printed rabbit larynx model

I adapted a previously published 3D-printed laryngeal model to mimic the anatomy of the rabbit larynx, aiming to enhance my proficiency in laryngological operative skills and novel surgical procedures (Lee et al., 2021). I obtained the STL files for the original model from https://wikifactory.com/@3dlaryngology/3d-larynx-surgery-trainer and scaled them to 31% of the original size using print preparation software. The cartilaginous framework was then 3D printed using a Form 3+ Low Force Stereolithography 3D printer (Formlabs, Boston, MA) with 1mm diameter resin filament at a 50-micrometer thickness[3]. Additionally, a soft tissue mold was scaled, 3D-printed, and injection-filled with a room-temperature vulcanized silicone sealant (J-B WELD, Marietta, GA) and allowed to cure overnight. The resulting silicone soft-tissue model was inserted into the cartilaginous framework.

[3] I would like to acknowledge T. Kevin Hitchens, Director of the Advanced Imaging Center at the University of Pittsburgh, for providing the facilities, materials, and time to produce the model.

3.2.5 Subject-specific anatomical imaging

Figure 14 Bruker AV3HD 11.7 tesla/89 mm vertical-bore micro-imaging system

MRI images of excised larynges were obtained using a Bruker AV3HD 11.7 tesla/89 mm vertical-bore micro-imaging system (see Figure 14) equipped with a 40-millimeter set capable of 1500 mT/m and ParaVision 6.0.1 software (Bruker Biospin). Three-dimensional T2-weighted images were collected at an isotropic resolution of 60-micrometer using a fast spin echo sequence with the following parameters: TR/TE 1000/28 ms, 256 x 384 x 286 matrix, 16 x 16mm field-of-view, and a RARE factor of 8 (Li et al., 2021)[4].

[4] I would like to acknowledge T. Kevin Hitchens and Lesley Foley, of the Advanced Imaging Center at McGowan Institute of Regenerative Medicine at the University of Pittsburgh, for providing the facilities, time, and expertise to acquire MRI data.

Micro-CT images of the larynx were captured on a Scanco µCT50 at 10µ voxel resolution at a density of 90Kvp[i]. Iodine staining was used to increase contrast between tissue and implants[5].

3.2.6 Digital image segmentation for finite-element modeling

MRI scans were imported to ITK-SNAP to manually segment the images. The following structural components were identified and segmented for model reconstruction: thyroid cartilage, arytenoid cartilages, cricoid cartilage, and soft tissue. Two distinct layers were segmented within the vocal folds due to known differences in tissue properties (Hirano, 1974): the pliable VF cover, composed of the epithelium and superficial lamina propria, and the much stiffer VF body, composed of the deep lamina propria and thyroarytenoid muscles (S. Chang et al., 2016; Chen et al., 2020; Li et al., 2020) (see Figure 15).

[5] I would like to acknowledge Kostas Verdelis and Lyuda Lukashova of the microcomputed Tomography Core at the Center for Craniofacial Regeneration at the University of Pittsburgh, for providing the facilities, time, and expertise to acquire microCT data.

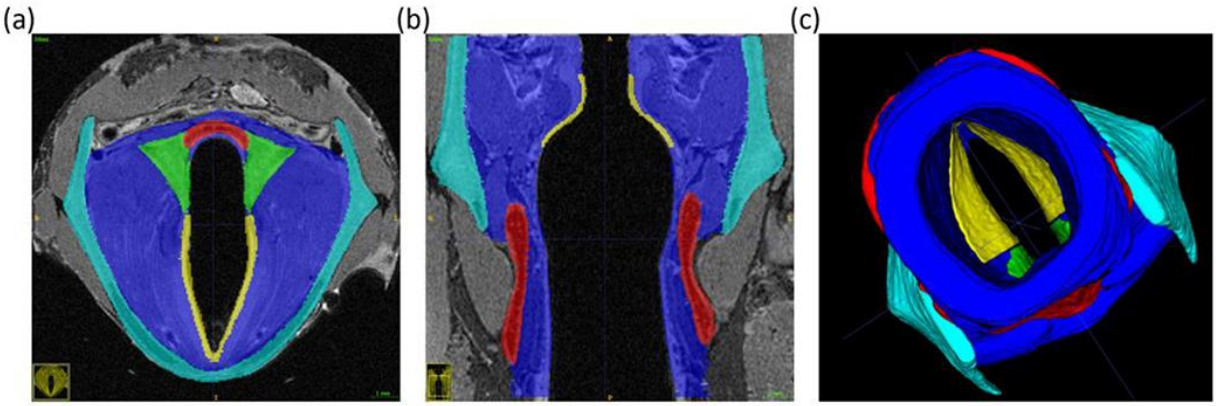

Figure 15 MRI image segmentation for a representative sample

Green = arytenoids; red = cricoid; cyan = thyroid; blue = VF body; yellow = VF cover. (a) axial view; (b) coronal view; (c) superior-inferior view of trachea (Li et al., 2021).

3.2.7 *ex vivo* UVFP simulation experiment

Six New Zealand white breeder rabbits were included in *ex vivo* MRI studies, $n = 3$ for the cricothyroid approximation and $n = 3$ for the transmuscular suture approximation method.

3.2.7.1 Cricothyroid approximation

I performed cricothyroid approximation in the style of traditional type IV thyroplasty as described in section 3.2.1. with the following modification: the suture applying tension to the left VF was removed to allow for the vocal fold to return to a resting position and simulate the inability of the paretic fold to medialize.

3.2.7.2 Transmuscular suture approximation

I adapted the method for transmuscular suture approximation from a cadaveric model (Owusu-Ayim et al., 2020). A 17mm 0.5c taper suture was passed through one side of the

cricothyroid muscle into the subglottal space. I then passed the suture through the contralateral posterior end of the thyroarytenoid muscle at the location of the vocal process into the supraglottal space. The suture was passed back through the ipsilateral thyroid ala. I tightened the distal end of the thread to draw the VF toward the midline and secured the suture line to the second and third tracheal ring. This method allows both unilateral and bilateral approximation of the vocal folds without unnecessary orthogonal stress on the larynx as a whole or tearing of the laryngeal cartilage. A depiction of the anterior and supraglottic views of suture placement is shown in Figure 16.

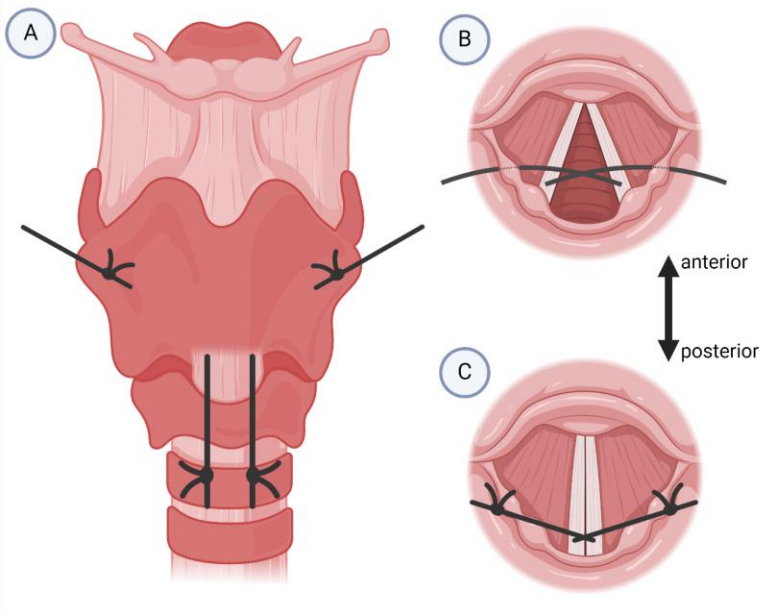

Figure 16 Illustration of transmuscular suture approximation

3.3 Results

3.3.1 Implant design

The following section provides an overview of the outcomes of the various implant designs in the context of vocal fold medialization, ranging from hand-carved and 3D-printed implants to laser-cut alternatives. Through *in vivo* trials, the efficacy and fidelity of each approach are evaluated, shedding light on their potential applications in laryngeal research and treatment.

3.3.1.1 Hand carved implants

I crafted hand-carved implants in two shapes, rectangular and divergent, each with depths of 1.5mm and 2mm. While these implants were cost-effective, highly customizable, and appropriately sized, their fidelity to the original design was poor. As shown in Figure 8b, all dimensions demonstrated marked inconsistency between trials. This inconsistency hindered accurate replication of the required shapes for the laryngeal model, particularly at the scale of a rabbit.

3.3.1.2 3D-printed implants

The 3D-printed implants exhibited a clear enhancement in fidelity to the design specifications concerning physical dimensions. As shown in Figure 9b, the implant produced was consistent with the dimensions of the specified implants, demonstrating a slight reduction in scale. However, the resin filament utilized for printing exhibited stiffness that could potentially harm the delicate tissue of the vocal fold mucosal layer, particularly at the edges of the implants. At the time

of writing, no commercially available 3D printer enables the cost-effective production of high-resolution Silastic® objects.

3.3.1.3 Laser-cut implants

Forty-eight implants were laser-cut from Silastic® sheeting in less than one minute. Assessment of size and shape using calipers demonstrated reliability to the CAD model (see Figure 10b). The approximate cost per implant was $0.30. Effective VF medialization was confirmed *in vivo* using laryngoscopic evaluation and *ex vivo* using MRI (see Figure 17).

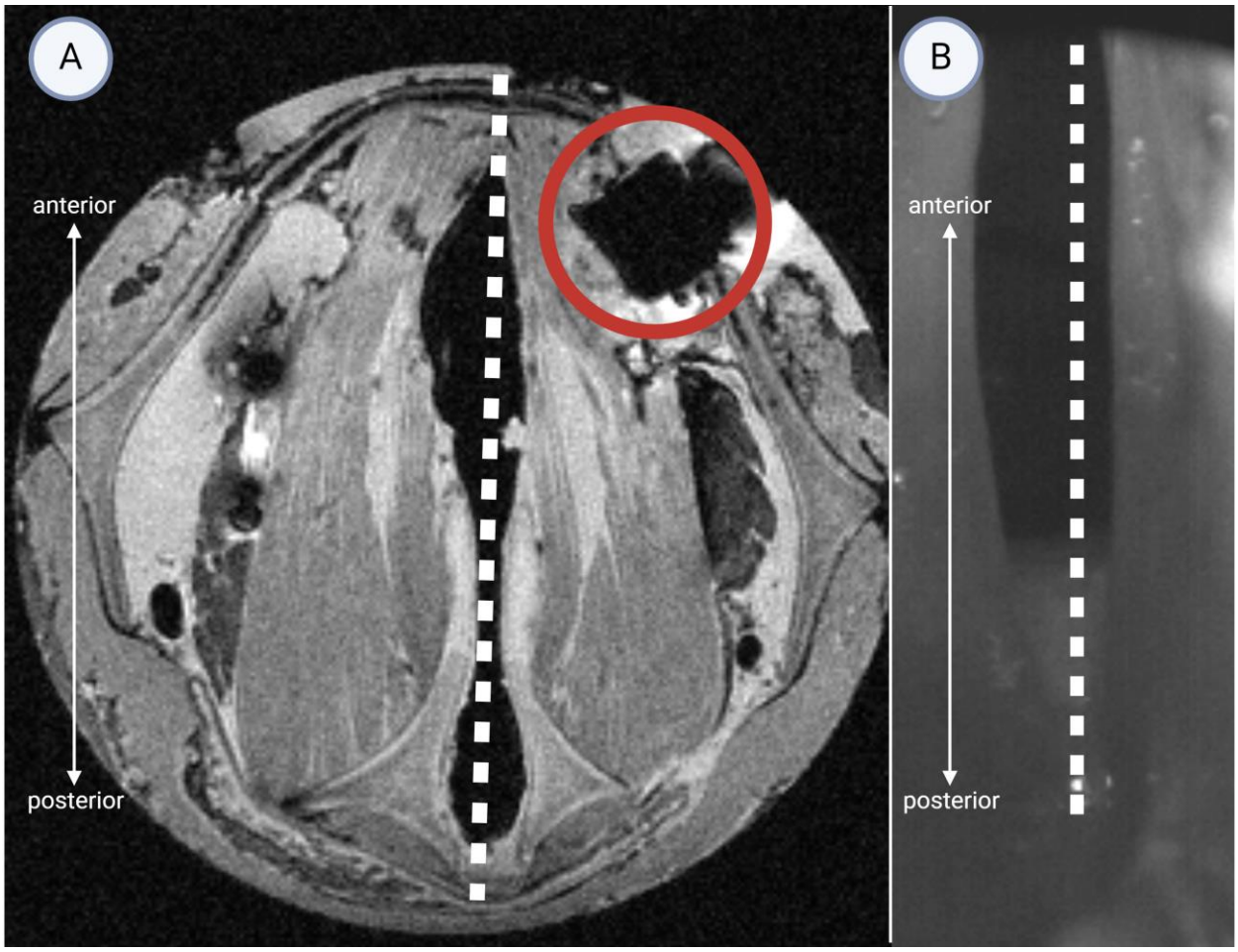

Figure 17 High-speed video and MRI images of implanted VF

3.3.2 *in vivo* phonation trials

MRI images were segmented according to VF body and cover as described in section 3.2.6 before and after the unilateral right-sided insertion of the implant[6]. A comparison of the VF edge in the rest condition, highlighted in blue, with the VF edge in the implanted condition, highlighted in red, demonstrates successful implant-induced medialization in the right VF (see Figure 28).

To quantify VF medialization, we compared VFs in rest and implanted conditions at the narrowest plane in the larynx. We defined the following parameters to evaluate the VF adduction qualitatively; detailed results are listed in Table 2. In the sample shown in Figure 11, the overall VF adduction ratio from the implant is 39%, indicating substantial medialization of the VF toward the midline. Medialization was observed across all samples, with variations observed in medialization between subjects consistent with differences in laryngeal anatomy.

Table 2 Quantitative parameters to evaluate vocal fold adduction

A_0 = glottal area at rest condition; A = glottal area in implanted condition; D_0 = initial distance between VF medial surface and midline; D = distance from midline after implant insertion; Max(D_0-D) = maximum displacement; Max((D_0-D)/D_0) = maximum relative displacement

Sample	Implant Side	A_0 (mm^2)	A (mm^2)	(A_0-A)/A_0	Max(D_0-D) (mm)	Max((D_0-D)/D_0)
1	Right	1.99	1.73	13%	0.23	37%
2	Left	3.15	2.90	8%	0.31	32%
3	Right	4.51	2.76	39%	0.48	47%
4	Right	1.93	2.5	-	0.15	30%
5	Left	3.76	3.35	11%	0.25	25%

[6] I would like to acknowledge the support of Amit Avhad, Alice Ding, and Zheng Li from Vanderbilt University for their assistance with MRI image segmentation.

3.3.3 3D microstructure imaging and segmentation

This section describes what was found regarding the utility of physical laryngeal models, advanced imaging techniques, and digital segmentation for computational modeling to enhance our understanding of laryngeal structures and their behavior.

3.3.4 3D-printed larynx model

The scale reduction of the 3D human laryngeal model to the relative size of the rabbit larynx yielded a physical model conducive to the evaluation of various surgical techniques before application in animal studies. The model was used to fine-tune operative techniques for *in vivo* and *ex vivo* experimental animal procedures, thereby reducing overall animal use. The injection mold process and completed 3D-printed laryngeal cartilage are depicted in Figure 18.

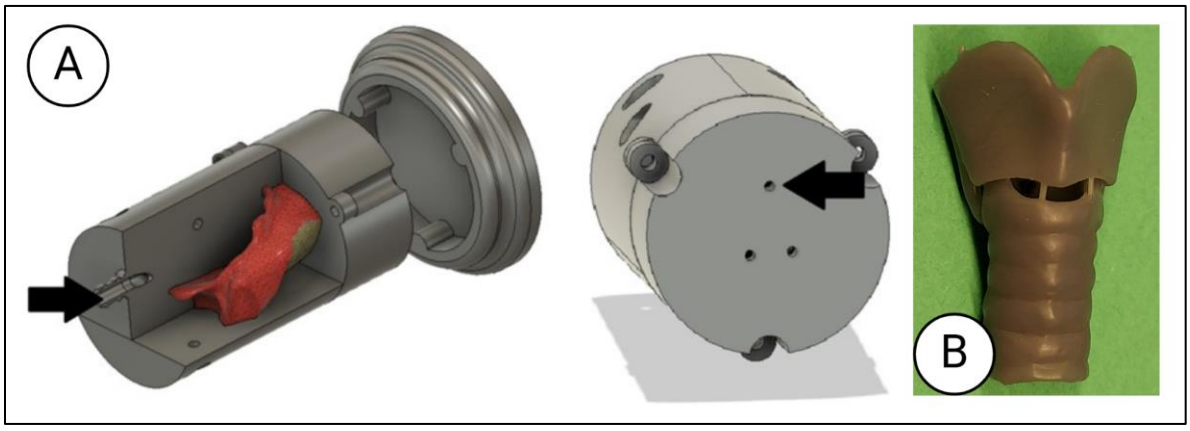

Figure 18 3D printed laryngeal model scaled for rabbits

(a) Soft tissue injection mold, as depicted in Lee et al. (2021). b) 3D printed scaled laryngeal cartilage.

3.3.5 Application of subject-specific anatomical imaging and digital image segmentation to finite-element modeling

microCT is a highly advanced imaging technique predominantly used in research settings to obtain detailed images of hard tissue structures such as bones and teeth. The technology operates similarly to traditional CT scans but at a much higher resolution, suitable for small objects and subtle features, making it invaluable in fields like material science, developmental biology, and biomedical research.

The primary strength of microCT lies in its capacity to render highly detailed and precise images of hard tissues. This is due to the technology's high resolution and the ability to capture fine structural details without physically sectioning the specimen. However, microCT has limitations when it comes to imaging soft tissues, which are less dense and do not absorb X-rays as effectively as hard tissues. To overcome this limitation, specimens are often stained with iodine-based contrast agents before scanning. Iodine effectively binds to the soft tissues, enhancing their contrast and making them more visible in the scans. This step is crucial for studies that require detailed visualization of both hard and soft tissue structures, such as in developmental studies of organisms or disease models.

Despite its effectiveness in research, there are significant challenges in translating microCT's use to clinical trials and regular medical practice. One major challenge is the requirement for iodine staining, which is impractical and invasive for living subjects. Furthermore, the high doses of radiation associated with microCT make it unsuitable for routine use on humans where radiation exposure needs to be minimized. These limitations restrict its application primarily to *ex vivo* studies and non-living specimens.

As expected, the micro-CT images acquired exhibited exceptional clarity and detail, (see Figure 19) however, they proved unsuitable for our research aims and clinical application. The choice of MRI for research involving digital image segmentation and finite-element modeling aligns with the goals of minimizing invasiveness and maximizing applicability to living subjects. MRI's ability to offer detailed visualization of soft tissues without radiation exposure or the need for invasive preparations makes it an ideal tool for studies aimed at understanding complex biological structures and their functions, predicting the outcomes of medical procedures, and developing therapeutic strategies. Thus, while microCT provides superior resolution for hard tissues, MRI's versatility and safety profile make it more suitable for a broader range of research applications, particularly those involving live subjects or clinical trials.

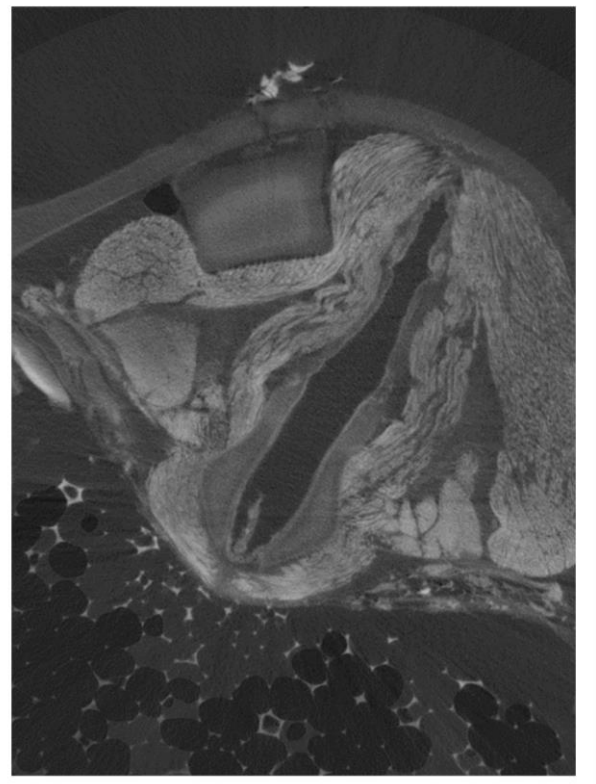

Figure 19 Representative image of laryngeal image acquisition using microCT

Laryngeal reconstruction was performed digitally using MRI images taken from removed larynges. Here's a simplified breakdown of the process and some complex terms:

Surface Meshes: These are networks of interconnected points that outline the shape of the larynx. These meshes were smoothed to eliminate any irregularities and ensure accuracy in the model.

COMSOL Multiphysics: This is a software used for simulating various physical processes and phenomena. In this context, it was used to convert the smoothed surface meshes of the larynx into solid three-dimensional bodies.

Unstructured Volume Meshes: These are 3D meshes that fill the inside of the larynx model. Unlike structured meshes, which have a regular pattern, unstructured meshes have a flexible arrangement that can more accurately conform to complex shapes.

Minimum Distance Criterion: This method was used to identify and differentiate various structural components within the larynx mesh. It involves calculating the shortest distance between points to determine where one component ends and another begins.

Mesh Refinement for the Vocal Fold Cover: The mesh in the area representing the vocal folds was made denser. This means that the mesh in this area was packed with more points to increase the model's accuracy, particularly for simulating movements and vibrations of the vocal folds.

Mesh-Independence Study: This is a verification process where different meshes of varying densities are used to calculate the eigenfrequency of the vocal folds. Eigenfrequency refers to the natural vibration frequency of the vocal folds under certain conditions. The purpose of this study is to ensure that the simulation results are not affected by the mesh size or density but are instead true representations of the physical properties being studied.

Through these advanced techniques, the reconstructed larynx model allows for detailed study and simulation of its structure and function, providing valuable insights into its biomechanical behavior under various conditions (see Figure 20).

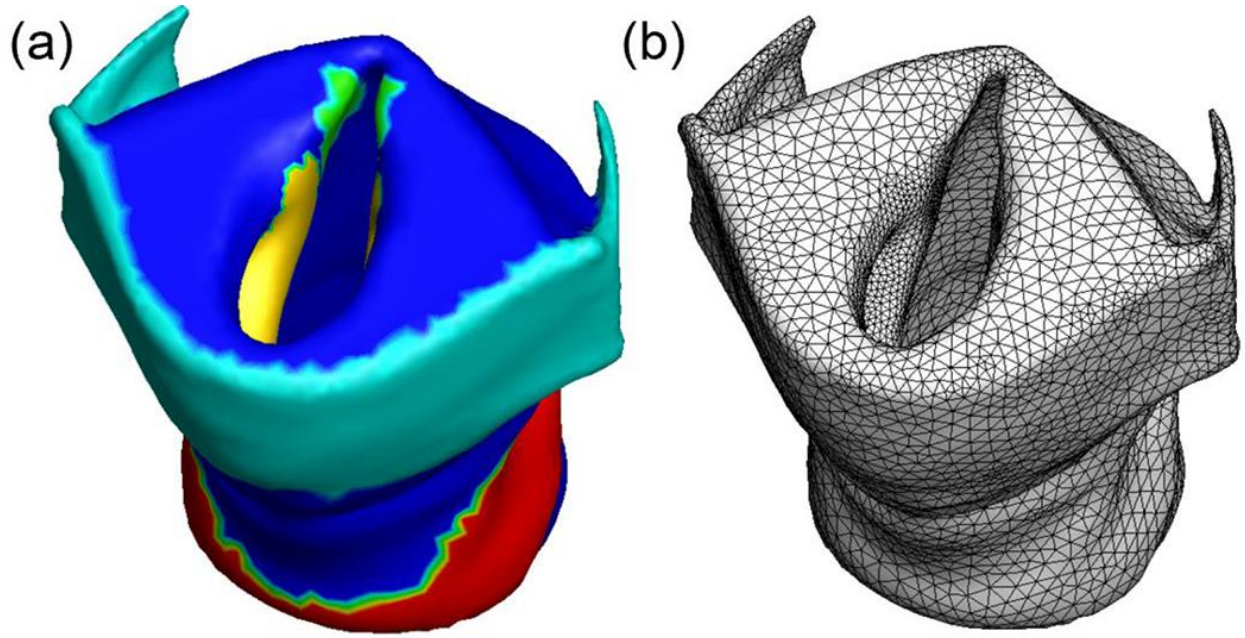

Figure 20 Model reconstruction of sample 1

(a) reconstuction of 3D MRI images following laryngeal cartilage and soft tissue segmentation Green = arytenoids; red = cricoid; cyan = thyroid; blue = VF body; yellow = VF cover. (a) axial view; (b) coronal view; (c) superior-inferior view of trachea; (b) mesh reconstruction using the finite-element model (Li et al., 2021).

3.3.6 *ex vivo* UVFP simulation

The following results detail the outcomes of employing two different surgical methods, cricothyroid approximation and transmuscular suture approximation, in replicating UVFP in a rabbit model, focusing on their impact on the laryngeal configuration and cartilage displacement. Combining the surgical technique with subglottal airflow, both methods were sufficient for

phonation. However, there were notable differences in laryngeal geometry which would impact the potential for simulation of UVFP.

3.3.6.1 Cricothyroid approximation

The cricothyroid approximation method enabled the glottis to remain in a phonatory glottal configuration for MRI before and after phonation tests (see Figure 20). Model reconstruction of unilateral cricothyroid approximation revealed that the VF were in a phonatory glottal configuration with nearly symmetrical medialization. The larynx demonstrated notable thyroid cartilage displacement, with a 40–45-degree difference in the displacement angle (see Figure 21a). Furthermore, tension on the suture damaged the thyroid cartilage by tearing in the direction of tension. The MRI images also revealed considerable separation and detachment of the muscle from the thyroid cartilage in the proximal plane (see Figure 21b).

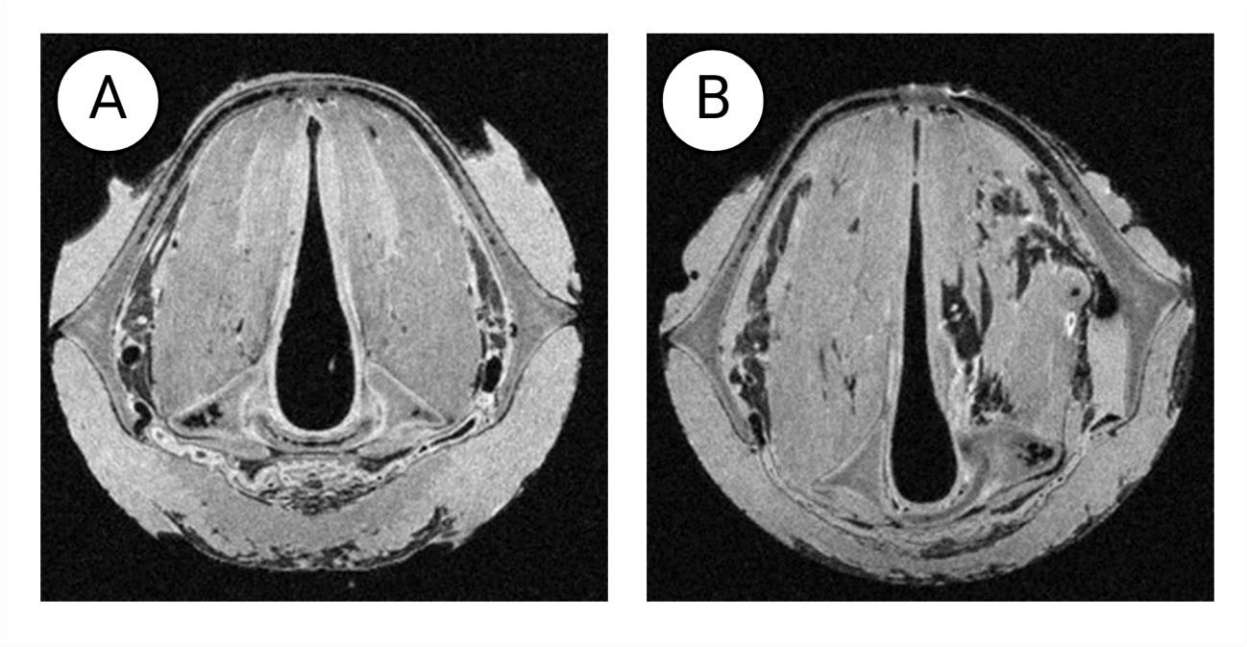

Figure 21 MRI image of the larynx in axial view following cricothyroid approximation

a) resting state; b) bilateral suture placement

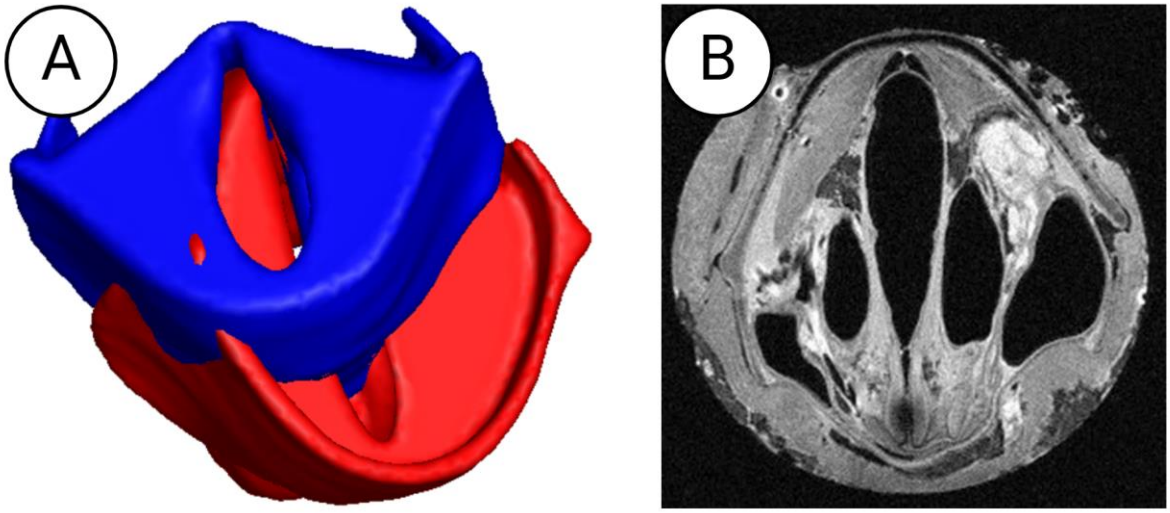

Figure 22 Results from cricothyroid approximation

(a) Computational model superimposing the baseline condition with a unilateral vocal fold paralysis (UVFP) simulation demonstrating a displacement angle of 40-45 degrees; (b) MRI image depicting damaged soft tissue following the procedure.

3.3.6.2 Transmuscular suture approximation

Comparatively, the transmuscular suture approximation also sustained glottal configuration adequate for phonation for MRI before and after phonation tests (see Figure 22). The model reconstruction revealed that the right VF remained in an open glottal configuration, while the contralateral fold demonstrated compensatory medialization consistent with the clinical presentation of UVFP. The larynx also demonstrated a 5-10-degree difference in the angle of displacement with no cartilage damage (see Figure 23).

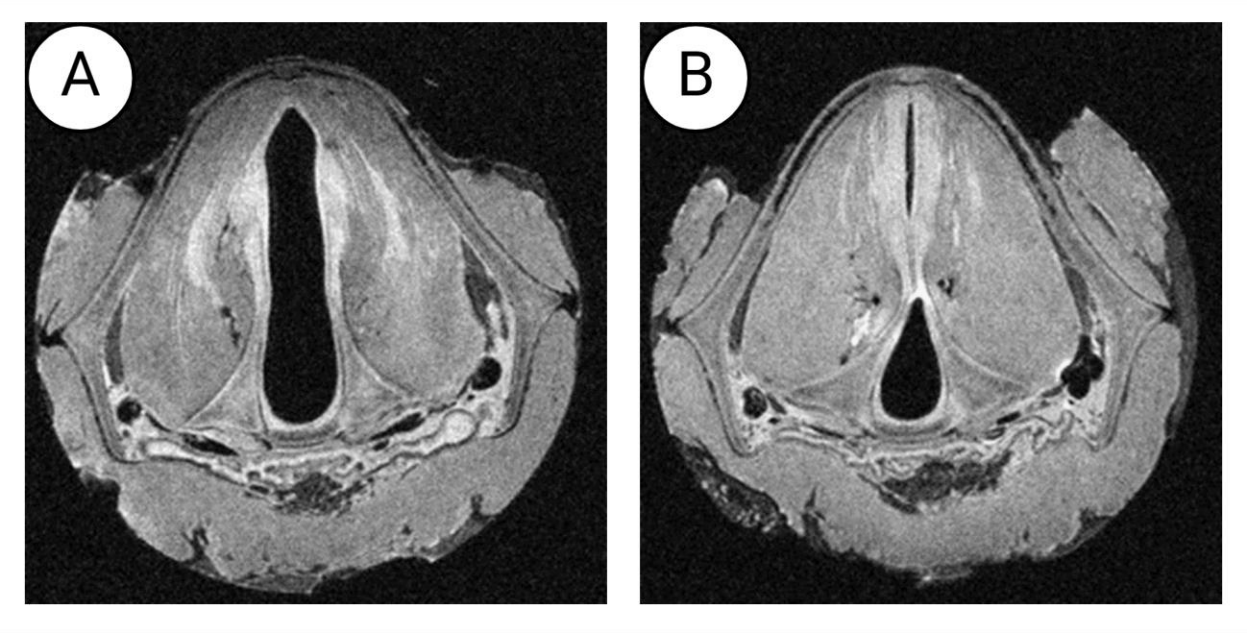

Figure 23 MRI image of the larynx in axial view following transmuscular suture approximation

a) resting state and b) bilateral suture placement

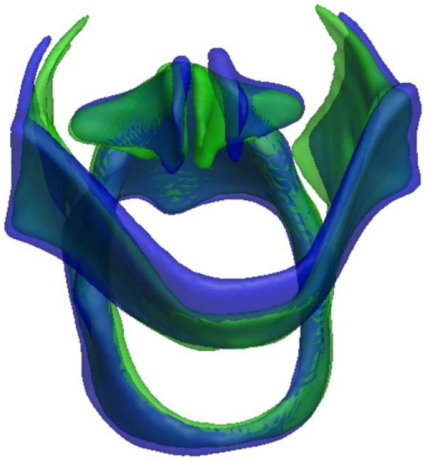

Figure 24 Results from transmuscular suture approximation

Computational model superimposing the baseline condition with a unilateral vocal fold paralysis (UVFP) simulation following transmuscular suture approximation

3.4 Discussion

The first arm of this project aimed to devise an implant design suitable for *in vivo* rabbit experiments. While hand-carved implants offer cost-effectiveness and customization, their fidelity to the intended design was lacking, particularly challenging at the scale of a rabbit's larynx. Conversely, 3D-printed implants exhibited improved fidelity to design specifications but carried a risk of damaging vocal fold mucosal tissue due to resin stiffness. Laser-cut implants, costing approximately $0.30 each, demonstrated consistent size and shape conformity, successfully facilitating VF medialization in both *in vivo* and *ex vivo* trials. MRI-based model reconstructions further underscored the efficacy of laser-cut implants in inducing medialization despite variations reflecting individual laryngeal anatomy. While each implant type presented advantages and challenges, laser-cut implants emerged as a cost-effective solution with dependable size and shape conformity for experimental trials in medialization laryngoplasty.

In the following arm, I explored advanced imaging techniques, employing subject-specific anatomical imaging methods such as micro-CT and MRI along with image segmentation. The integration of subject-specific anatomical imaging, notably MRI, facilitated the computational reconstruction of laryngeal structures, followed by segmentation and mesh refinement vital for computational modeling of VF behavior under specific conditions. The resulting highly precise subject-specific finite element models served as the foundation for quantitative analyses.

The last project arm compared two surgical techniques intended to physiologically simulate the clinical manifestation of UVFP for subsequent *ex vivo* phonation experiments in a rabbit model.

The adaptation of a 3D human laryngeal model to mimic the rabbit larynx size facilitated the refinement of surgical techniques, optimizing procedures for both *in vivo* and *ex vivo* studies while minimizing animal use. The practical application of scaling down a 3D human laryngeal

model to the relative size of a rabbit larynx involves several beneficial aspects, particularly in the realm of medical research and surgical training. First, by creating a scaled-down model of the human larynx that mimics the size and complexity of a rabbit's larynx, surgeons and researchers can practice and refine surgical techniques in a controlled, repeatable environment. This allows for the development and perfection of new surgical approaches without the immediate need for live subjects. Surgeons can perform multiple iterations of surgical procedures to improve their skills and confidence before applying these techniques to live animal models. Both *in vivo* and *ex vivo* experimental studies can benefit from the pre-tested and refined surgical techniques developed using the 3D models. *In vivo* experiments can proceed with greater assurance of successful outcomes, reducing the risk of procedural failure and the need for repeated animal trials. *Ex vivo* studies can also utilize these models for testing the viability of surgical interventions on biological tissues in a lab setting, which may further reduce the need for live animals. Beyond research and surgical refinement, these models serve as excellent educational tools for medical students and trainees. They provide a hands-on learning experience that is crucial for understanding the anatomical complexities and surgical intricacies of the laryngeal area without the immediate use of live models. Overall, the practical application of scaling down the 3D human laryngeal model to the size of a rabbit's larynx offers a comprehensive approach to enhancing surgical techniques, reducing reliance on animal models, and advancing medical education, thereby supporting both ethical research practices and educational advancements in the medical field.

Both cricothyroid approximation and transmuscular suture approximation, coupled with subglottal airflow, enabled phonation; however, they exhibited distinct differences in laryngeal geometry, affecting UVFP simulation potential. While cricothyroid approximation maintained a

phonatory configuration, the result was accompanied by significant thyroid cartilage displacement and muscle detachment observed via MRI. Transmuscular suture approximation sustained glottal configuration with compensatory medialization consistent with UVFP, along with minimal cartilage damage and slight angle displacement differences.

The translatability of findings from *ex vivo* experiments to human clinical practice is a topic of concern. *Ex vivo* experiments provide detailed quantitative information about VF dynamics (Döllinger et al., 2016). However, the use of animal models, such as rabbits, in *ex vivo* experiments presents inherent challenges due to differences in laryngeal anatomy and physiology compared to humans (Döllinger et al., 2016). Rabbit models are commonly employed in the study of phonation and voice disorders due to their similarities with the human larynx in terms of size and histological features (Henrich et al., 2003; Shiba et al., 2015; Thibeault et al., 2002). These combined contributions have added to our understanding of the rabbit larynx through experimental research on its phonatory characteristics. Their work not only emphasizes the suitability of rabbits as models for investigating VF behavior but also provides valuable baseline data for comparisons with other animal models and human subjects. Nevertheless, the anatomical and physiological differences are such that interpretation of these results should be made judiciously. Additionally, *ex vivo* simulations for UVFP may not fully replicate the dynamic physiological environment present in living organisms, where factors such as blood flow, tissue healing, and neural control mechanisms could influence outcomes differently (Erickson & Sivasankar, 2010). For instance, studies on VF injury recovery in a rabbit model have highlighted the challenges in understanding VF scarring and its implications for human clinical practice (Kolosova et al., 2021). Therefore, caution is warranted when drawing comparisons to clinical practice, and further research involving *in vivo*

studies is necessary to validate the observed effects and understand their implications for patient care (Durkes & Sivasankar, 2016).

Furthermore, several technical and methodological limitations impact the reliability and applicability of our research. The small sample size used limits the robustness and generalizability of our findings. Additionally, tissue shrinkage during sample preparations could have affected measurement precision with unknown effects on laryngeal physiology during phonation. The absence of objective acoustic data due to noise conditions in the surgical suite further restricts our ability to evaluate the effectiveness of surgical interventions objectively, preventing a comprehensive assessment of the functional outcomes of the surgical techniques tested in the study.

Moreover, the unreasonably long MRI scan time, lasting over three hours to achieve the necessary resolution, poses practical challenges for scalability and applicability to human patients. While this prolonged scanning duration may be manageable for rabbit models, it may not be feasible or practical for human patients undergoing similar procedures. Despite efforts to optimize scanning protocols, the lengthy duration remains a consideration for translating our findings to human clinical practice, necessitating optimization strategies for reduced scan times without compromising image quality. These limitations underscore the need for continued research efforts to address these challenges and ensure the relevance and validity of our findings for human applications.

The exploration of various implant designs, particularly the validation of laser-cut implants as a cost-effective and reliable solution, offers clinicians a viable option for vocal fold medialization procedures in cases of UVFP. The findings highlight the importance of implant fidelity and conformity in achieving successful outcomes, providing clinicians with valuable

insights into implant selection and design considerations. Additionally, the integration of advanced imaging techniques and subject-specific finite element modeling enhances the precision of pre-operative planning, allowing clinicians to tailor surgical interventions more accurately to individual patient anatomy. Furthermore, the comparison of surgical techniques for simulating UVFP underscores the importance of understanding laryngeal geometry and its impact on treatment outcomes, guiding clinicians in selecting the most appropriate approach based on patient-specific factors. Overall, this research contributes to improving the efficacy and safety of surgical methods for UVFP treatment, ultimately benefiting patient care in clinical practice.

4.0 Can a computational model informed by pre-operative MRI data accurately identify optimal implant placement for type I thyroplasty?

Computational mechanics models, spanning lumped-mass, 2D, and 3D finite-element simulations, have significantly advanced our understanding of VF vibratory patterns and airflow dynamics through the glottis. These models have provided insights into various aspects of phonation, including vibratory characteristics, geometric and material parameters, and acoustic output. While earlier studies using simplified or idealized structural models have successfully simulated generic vibratory characteristics of the VF, recent efforts have focused on employing more realistic laryngeal models based on MRI or CT scans of individual subjects. By incorporating subject-specific anatomical details, these computational models hold promise for evaluating the effects of interventions, such as prosthetics, on VF vibration, thus serving as valuable planning tools for improving surgical outcomes.

Despite recent advancements, several questions and challenges remain unaddressed in previous research. One such challenge is ensuring optimal implant placement and design during surgical procedures for treating UVFP. Current methods rely heavily on anatomical landmarks and experiential judgment, leading to inconsistencies and variations in outcomes. Factors such as peri-operative inflammation and edema further complicate assessment, potentially resulting in suboptimal outcomes and the need for revision surgery. Additionally, previous studies have focused primarily on the development and validation of computational models but have not extensively explored their integration with experimental approaches to validate model performance and assess the effects of implants on VF vibratory characteristics.

The present research study aims to address these gaps by leveraging subject-specific 3D simulations of VF vibration in excised rabbit larynges to propose and evaluate a customized VF implant design for restoring phonation in larynges with impaired glottal closure. Building upon previous research, which has laid the groundwork for computational modeling of VF vibration and experimental validation, this study will integrate computational models with experimental approaches to assess the effects of implants on VF vibratory characteristics. By combining computational simulations with *in vivo* experiments, this study seeks to provide a comprehensive understanding of implant-mediated changes in VF vibration, thus informing more precise and effective treatments for UVFP.

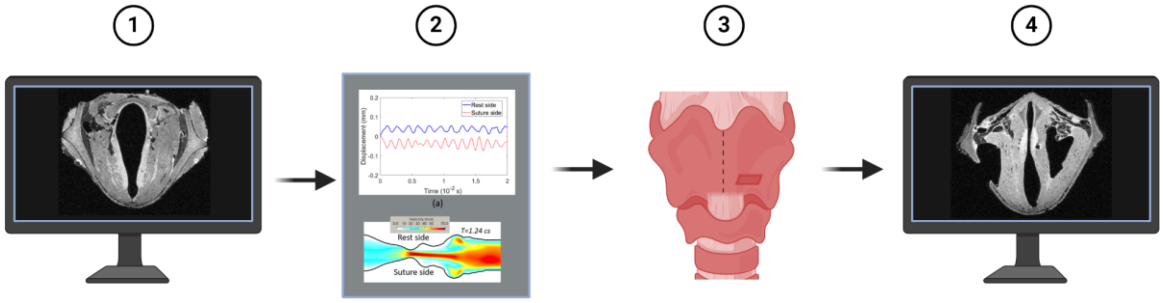

Figure 25 Graphical abstract depicting the research approach for Aim 3

1) Collection and reconstruction of baseline 3D MRI data from excised rabbit larynges to create subject-specific computational 3D models. 2) Glottal flow simulations to optimize the surgical approach for type I thyroplasty. 3) Guided type I thyroplasty based on optimal implant size, shape, and thyroplasty window placement determined by FSI simulation. 4) Collection and reconstruction of post-surgical 3D MRI data to compare simulated outcomes with actual surgical results.

4.1 Project summary

The objective of this project was to ascertain the ability of a computational fluid-structure interaction (FSI) simulation of glottal airflow informed by pre-intervention MRI scans to prescribe the optimal placement and design of VF implants in rabbit larynges. 3D imaging data obtained from excised rabbit larynges were employed in 3D FSI simulations of type I thyroplasty. Vibratory characteristics derived from these simulations were analyzed to inform surgical planning, particularly in predicting the ideal placement of the thyroplasty window and determining the size and shape of the implant. The **research question** for this aim was: **Can a computational model informed by pre-operative MRI data accurately identify optimal implant placement for type I thyroplasty?**

I investigated the following **hypothesis**: **finite-element model simulations of glottal airflow informed by pre-operative MRI data can accurately identify the optimal placement of VF implants in excised rabbit larynges.** Prior research has demonstrated the efficacy of computational mechanics in predicting VF biomechanics and enhancing surgical outcomes in type I thyroplasty (Sadeghi et al., 2019; Zhang et al., 2020). Therefore, the integration of computational modeling in this study was anticipated to yield valuable insights into the optimization of implant design and placement. Building on the research findings from Aim 2, this study adopted an integrated approach to develop and validate a computational model rooted in rabbit phonation. As a result, the study captured the direct impact of the implant on vibration and validated it against high-speed video recordings of the same VF sample.

4.2 Methods

The stages for this study, illustrated in Figure 24, were: 1) baseline 3D MRI image data of excised rabbit larynges were collected and reconstructed as a subject-specific computational 3D model; 2) glottal flow simulations were conducted to determine optimized surgical approach for type I thyroplasty; 3) optimal implant size and shape and thyroplasty window placement as indicated by the FSI simulation were used to guide type I thyroplasty in individual excised larynges in the experimental group, whereas the control group received unguided type I thyroplasty; and 4) post-surgical 3D MRI image data was collected and reconstructed to compare simulated results with actual results. This study was quasi-experimental observational in design with model-assisted thyroplasty as the independent variable and medialization measured by maximum relative displacement as the dependent variable. A *t*-test was performed to determine whether there was a meaningful difference in the relative degree of medialization between the model-assisted and unguided thyroplasty groups.

I personally performed all surgical procedures. 3D MRI images were segmented with my guidance by collaborators at Vanderbilt University, namely, Dr. Zheng Li, Amit Avhad, and Alice Ding. FSI simulation calculations were performed by the aforementioned team. Statistical analyses were performed jointly.

4.2.1 Baseline data collection

Baseline data collection involved the use of eight New Zealand white rabbits, weighing between 2.5kg and 4.0kg, randomly assigned to either a control group (n = 3) or an experimental group (n = 5). Sedation was induced via intramuscular injection of 20mg/kg ketamine

hydrochloride and 0.125mg/kg dexmedetomidine into the latissimus dorsi, confirmed by the absence of pain responses and involuntary reflexes. Following shaving of the neck and chest, the rabbits were positioned supine, and a skin incision was made from the sternum to the submentum to expose the larynx and trachea. The larynx was excised, and the rabbits were euthanized via a 390 mg/ml Sodium pentobarbital injection in the marginal ear vein to induce overdose. Bilateral sutures were placed using the transmuscular suture approximation method described in Chapter 3 to approximate the VF to a phonatory glottal configuration, and the larynges were suspended in a 10-milliliter syringe filled with perfluoropolyether vacuum oil (FOMBLIN Y, Sigma-Aldrich Inc.) (see Figure 25).

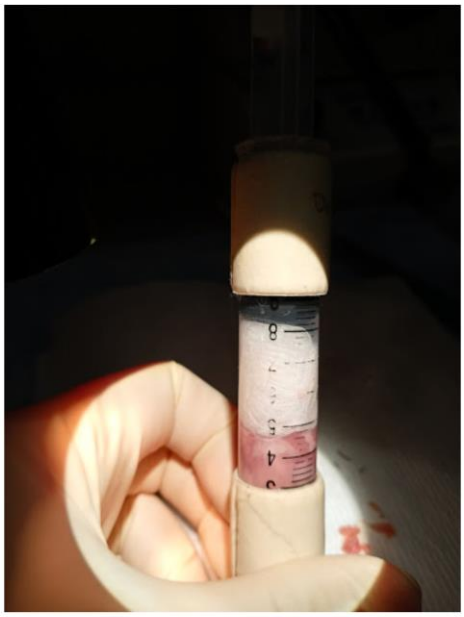

Figure 26 Larynx in 10mm syringe suspended in perfluoropolyether oil

4.2.2 3D model reconstruction

3D MRI imaging was conducted on a Bruker AV3HD 11.7 tesla/89mm vertical-bore microimaging system with an isotropic resolution set to 60μm, capturing two laryngeal configurations: a rest condition, in which both VF were unaltered, and a type I thyroplasty with a unilateral implant.

In the study, the displacement of the thyroid cartilage relative to the cricoid cartilage was quantified and applied to the mesh nodes of the reconstructed larynx model. Here's a clearer explanation of the terms and processes involved:

Thyroid Cartilage Displacement: This term refers to the movement of the thyroid cartilage, which forms the bulk of the front wall of the larynx and protects the vocal cords. Displacement measurements were applied to specific points (nodes) on the digital mesh of the larynx model.

Mesh Nodes: These are key points in a computational model where measurements like displacement are applied. They form the framework of the model, defining its shape and how it behaves under various conditions.

Saint-Venant Kirchhoff Model: This model was used to simulate how the tissues of the larynx deform. It is a mechanical model that describes the behavior of materials (like tissues) under small deformations, assuming that the material's stress (force per area) is proportional to its strain (deformation relative to original size).

Parameters set in the model based on past research included the following:

Subglottal Pressure: The pressure below the vocal folds that influences how they vibrate.

Inlet Pressure: The pressure at the airway entrance.

Exit Pressure: The pressure at the airway exit.

Young’s Modulus for the VF Body and Cover: A measure of the stiffness of the vocal fold body and its outer layer (cover), indicating how much they resist deformation.

Dominant Eigenfrequency: The primary natural frequency at which the vocal folds vibrate, determined to be about 600Hz. This frequency is crucial for understanding how the vocal folds produce sound and how they might be affected by various conditions or treatments.

This approach, using the cricoid cartilage as a reference for thyroid cartilage displacement and employing the Saint-Venant Kirchhoff model, allows for a detailed and realistic simulation of laryngeal mechanics. Calculations derived from prior studies (Avhad et al., 2022; Chen et al., 2020; Li et al., 2021) (Table 3) standardized these parameters to ensure accurate and consistent modeling. Each model-guided sample was independently evaluated for degree of VF edge approximation and maximum relative displacement to determine optimal implant placement.

Table 3 Tissue properties of cartilages, VF body, and cover

	Young’s modulus (kPa)	Poisson's ratio	Density (kg/m^3)
VF body	10	0.4	1000
VF cover	1	0.4	1000
Cartilages	500	0.4	1000

4.2.3 Glottal flow simulation

In this study, the glottal flow area was divided into a specialized mesh using a non-uniform Cartesian grid. Here's an explanation of the process and terms involved:

Non-Uniform Cartesian Grid: This type of grid divides the space into a mesh (network of nodes and elements) where the spacing between grid points varies. In this case, the grid is denser around the vocal folds to capture more detail in areas where complex air flows occur, thereby enhancing the accuracy of simulations.

Rectangular Flow Domain and Subdivision: The area being simulated, shaped like a rectangle, was split into several sections. This subdivision allows for parallel processing, where different parts of the simulation run simultaneously on different processors, thus speeding up the computational process.

Parallel Processing: The simulation leveraged multiple processors to handle the complex calculations simultaneously, enhancing computational speed and enabling more detailed simulations. Stampede2, a supercomputer at the Texas Advanced Computing Center, was used, employing between 65 and 133 processors for each simulation.

Temporal Resolution and FSI Stability: A temporal resolution of $\Delta t = 10^{-4}$ centiseconds was used to ensure stability in Fluid-Structure Interaction (FSI) simulations, which consider both the fluid dynamics (air flow) and structural behavior (movement of VF). Approximately 3000 time-steps were required to fully simulate one vibration cycle of the vocal folds.

Implant Testing: Ten different locations and two depths for implant insertion were tested in each model to find the optimal placement for maximum relative displacement, thereby determining the most effective surgical approach. Maximal displacement values are shown in Table 4.

Table 4 Fluid-structure interaction simulation measurements for the experimental group based on pre-surgical MRI scans

Sample	A_0 (mm^2)	A (mm^2)	$(A_0-A)/A_0$	Max(D_0-D) (mm)	Max $((D_0-D)/D_0)$
6	3.50	2.64	25%	0.35	73%
7	3.61	2.29	37%	0.44	68%
8	3.17	2.30	27%	0.40	80%
9	3.25	2.14	34%	0.41	76%
10	2.34	1.09	53%	0.41	68%
11	2.48	1.31	47%	0.31	68%

4.2.4 Surgical procedures and implant selection

Laser-cut silastic implants were crafted following the methodology outlined in Chapter 3 and adjusted to resemble commercially available Montgomery implants, with the posterior portion deeper than the anterior portion for consistency (see Figure 19). To minimize animal use, implants were positioned bilaterally on both sides of the VF in all but three larynges—control samples 3, 4, and 5. Implant placement was performed by the same surgeon (myself) to ensure uniformity. A thyroplasty window was incised through the thyroid cartilage at the level of the VF. The implant was fitted through the window into the paraglottic space to compress the tissue and medially displace the fold, subsequently securing it with sutures to prevent migration. An absorbable hemostat was applied over the fenestrated area to complete the procedure.

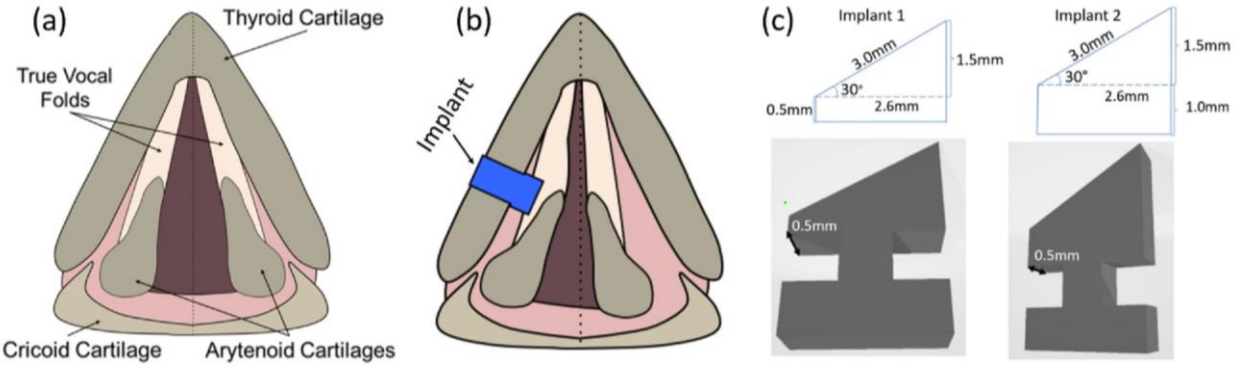

Figure 27 Implant dimensions and placements; from Li et al. (2021)

In the control group, the implants were placed in a thyroplasty window for which placement was determined using anatomical markers. Specifically, a surface depression on the anterior commissure of the thyroid cartilage, Montgomery's aperture, was used as an external landmark for the VF, as the indentation has been used as an accurate predictor of VF position (Epperson et al., 2022). In the experimental group, precise measurements guided by the model simulation were

used to position thyroplasty window placement. Post-operative MRI images were obtained using identical device settings as those used for pre-operative imaging.

To determine the optimal implant placement, post-hoc simulations were conducted on the control group. Simulations were performed using the same methods as described above. The results from the simulations were compared to the actual implant locations used during the surgical procedures. This comparison aimed to assess the accuracy of the initial implant placements and identify any discrepancies.

4.3 Results

The study sample comprised 11 implanted VF from excised larynges, with n = 5 in the control group and n = 6 in the experimental group. All larynges exhibited distinct 3D laryngeal geometries both above and below the glottis, resulting in variability in baseline, FSI modeling, and postoperative measures.

The post-surgical 3D reconstruction models from the control group showed that there was minimal movement of the vocal folds (VF) towards the midline on the side where the implant was placed. Out of the five samples in the control group, only the third sample (sample #3) achieved a medialization greater than 40%, as detailed in Table 5. See Figure 28 for representative model images.

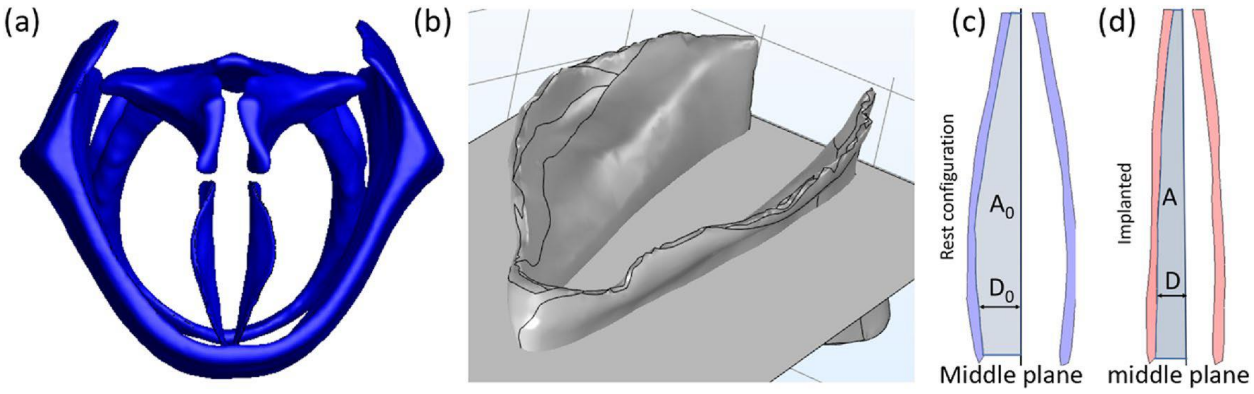

Figure 28 Post-surgical computational reconstruction assessment of VF approximation

(a) representative reconstructed model of laryngeal cartilages and VF cover; (b) plane selected for VF displacement, at which VF are at maximum approximation; (c) VF cover before implant insertion; (d) VF cover after implant insertion (Li et al., 2023)

Additionally, the 3D reconstruction of the post-surgical model for sample #3 indicated that the thyroplasty window (the opening made in the thyroid cartilage during surgery) was not properly aligned with the implant. This misalignment suggested that the implant had moved forward (anterior displacement) after it was initially placed.

Post-hoc simulations were conducted on the control group with predefined implant locations to ascertain optimal location as defined by maximum relative displacement. Sample #3 demonstrated less than 1mm between the actual and simulated implant locations, while control group samples demonstrated distances of 3-4mm.

In the experimental group, post-surgical 3D reconstruction models were used to assess implant placement accuracy by overlaying the actual post-surgical laryngeal model onto the model simulating the suggested implant placement. The reconstructed thyroid cartilage (highlighted in green) showed both sides of the implant inserted close to the suggested model location, with a variability of approximately +/-1.0 mm. Substantial VF medialization was observed for all six

implants at the narrowest section of the VF, indicating successful mid-membranous portion medialization.

Table 6 provides a quantitative evaluation of VF medialization following implantation guided by the model. Implant 2, with greater depth, resulted in increased VF medialization across all samples. Post-hoc comparisons were made between optimal implant placement determined by the computational model and actual type I thyroplasty outcomes, revealing reasonable differences in quantitative outcomes, yet effective medialization was observed in all samples. The six samples in the experimental group (M = 51.5, SD = 8.31) compared to the 5 samples in the control group (M = 34.2, SD = 8.35) demonstrated significantly greater maximal relative displacement $t(-3.4) = 8.6$, $p < 0.01$.

Table 5 Fluid-structure interaction simulation measurements for the experimental and control groups based on post-surgical MRI scans (results from Table 3 are repeated here for ease of reference)

Group	Sample	A_0 (mm^2)	A (mm^2)	$(A_0-A)/A_0$	Max(D_0-D) (mm)	Max $((D_0-D)/D_0)$
Control Group	1	1.99	1.73	13%	0.23	37%
	2	3.15	2.90	8%	0.31	32%
	3	4.51	2.76	39%	0.48	47%
	4	1.93	2.50	-	0.15	30%
	5	3.76	3.35	11%	0.25	25%
Test Group	6	3.50	2.64	25%	0.35	73%
	7	3.61	2.29	37%	0.44	68%
	8	3.17	2.30	27%	0.40	80%
	9	3.25	2.14	34%	0.41	76%
	10	2.34	1.09	53%	0.41	68%
	11	2.48	1.31	47%	0.31	68%

Overall, the control group exhibited minimal VF medialization and larger discrepancies between actual and simulated implant locations, whereas the experimental group demonstrated successful medialization at the narrowest section of the VF, with implants inserted near the

locations suggested by the computational model. Greater implant depth correlated with increased VF medialization across all samples.

4.4 Discussion

Previous research has demonstrated the potential of computational modeling in predicting VF biomechanics and improving surgical outcomes in procedures like type I thyroplasty. This study builds upon these findings by specifically applying computational modeling techniques to guide VF implant surgery in rabbit larynges.

Guided surgery, using computational models to determine optimal implant placement, demonstrated improved surgical outcomes. The simulations of various implant locations and their effects on VF medialization gave me, as the surgeon, guidance on the best implant placement before performing the actual surgery. While there were some differences between the predicted outcomes based on model simulations and the actual surgical results achieved, the study observed effective medialization of the VF in all samples. This represents a meaningful improvement over the control group, where minimal VF medialization was observed, and misalignment of the thyroplasty window was noted.

Several factors contributed to the improved outcomes observed with guided surgery. The analysis and prediction of the most effective implant locations translated to more accurate surgical execution, reducing the likelihood of suboptimal implant positioning and misalignment. The computational models also provided a customized surgical plan for each subject using the unique anatomical characteristics of each rabbit larynx. Computational guidance minimized the subjective element of my individual judgment during implant placement. By relying on objective data and

simulations, the likelihood of human error was reduced, leading to more consistent and reliable outcomes.

These findings align with and expand upon the existing body of research highlighting the significant benefits of subject-specific computational modeling in guiding surgical implantation procedures. The use of subject-specific computational models in our study mirrors the advantages reported in previous research. By utilizing detailed anatomical data from the rabbit larynges, the computational models provided a highly accurate representation of the physiological conditions, an important steppingstone for more personalized treatment planning in laryngoplasty. Such models may prove incredibly valuable in the diagnostic and treatment planning processes, simulating the behavior of soft tissues (Subramaniam et al., 2018), blood flow (Gaidulis & Padala, 2023; Hsia et al., 2020), and interactions between components in complex systems (Henak et al., 2013), such as the larynx . The precise implant placements achieved in our study, especially in sample #3 with less than 1 mm discrepancy between actual and simulated locations, underscore the value of these models in enhancing surgical accuracy.

The limitations of the present study primarily revolve around the reliance on computational modeling and the experimental approach used. The computational models used in this study are based on simplifications and assumptions about tissue behavior. These models may overlook the intricate dynamics of the larynx, particularly the nonlinearities in tissue properties, which could affect the accuracy of predictions. The complexities of the laryngeal structures, including the varying stiffness and elasticity of different tissues, are challenging to replicate accurately in a computational environment.

Additionally, the study predominantly utilized excised larynges, which may not fully replicate the physiological conditions encountered during *in vivo* procedures. The lack of *in vivo*

conditions means that factors such as blood flow, tissue healing responses, and neuromuscular activity are not considered. Consequently, the effectiveness and safety of the surgical techniques guided by computational models need further validation in live animal or human subjects to assess real-world applicability and effectiveness.

Despite attempts to standardize surgical procedures, intrinsic variability exists in each operative instance, influencing implant placement accuracy and surgical outcomes. This variability is exacerbated by the small physical size of the rabbit larynx compared to human larynges, making precise implant placement more challenging. Furthermore, the relatively small sample size limits the generalizability of the findings, emphasizing the need for larger-scale studies to corroborate the effectiveness of computational modeling in guiding VF implant surgery.

Cartilage fragility in the rabbit larynges may also affect outcomes. The fragility can lead to fractures or deformation during surgery, impacting the stability and effectiveness of the implants. To address this within the model, incorporating more detailed biomechanical properties of the cartilage, including its failure thresholds and viscoelastic behavior, could improve the model's accuracy and predictability.

Implant drifting, observed as anterior displacement in the post-surgical analysis, is another limitation. This drifting can occur due to inadequate fixation, movement during healing, or the mechanical properties of the implant materials. Implant drifting impacts results by potentially reducing the effectiveness of VF medialization over time. To address implant drifting, future studies could explore improved fixation techniques, such as the use of bioadhesives or more rigid implant materials and monitor implant stability over longer periods.

Internal validity is threatened by the aforementioned variability in surgical techniques, the small sample size, and the use of excised rather than live tissues. These factors can introduce bias

and reduce the confidence in the causal relationships observed. External validity is threatened by species differences, as findings in rabbit larynges may not directly translate to human anatomy and physiology. The small size and different biomechanical properties of rabbit larynges necessitate cautious interpretation when considering clinical applications in humans.

Translating these findings to human subjects requires caution due to significant species differences. Rabbit larynges differ from human larynges in size, tissue composition, and biomechanical properties. Further research involving human subjects or larger animal models that more closely mimic human laryngeal anatomy is essential to validate the applicability of computational modeling in clinical practice.

The tool described here allowed for the evaluation of VF adduction using a quantitative criterion and demonstrated strong improvement in mid-membranous VF adduction in 3D computational model-guided type I thyroplasty compared to controls without model guidance. Future studies will focus on expanding the model for *in vivo* study to assess its effectiveness on VF adduction and vibration during phonation.

Additionally, long-term follow-up evaluations are necessary to ascertain the durability and stability of VF medialization achieved through computational model-guided surgery. Future research should also consider other factors influencing voice production, such as mucosal wave dynamics, vocal tract resonance, and neuromuscular control, to provide a comprehensive assessment of vocal outcomes. Expanding the sample size and conducting studies on human subjects or larger animal models will enhance the generalizability and clinical relevance of the findings.

Building on the findings of this study, future research directions could explore several avenues to further enhance the application of computational modeling in guiding VF implant

surgery. Incorporating more detailed anatomical and biomechanical data into the computational model through *in vivo* imaging modalities, such as dynamic MRI or high-resolution ultrasound, could lead to more accurate predictions of VF dynamics and implant behavior in real-time during surgery.

Translational research is also needed to validate the efficacy of computational modeling-guided VF implant surgery in clinical settings. Prospective clinical trials involving human subjects could assess factors like long-term implant stability, patient-reported voice outcomes, and complication rates, thereby establishing the real-world effectiveness of this approach.

Furthermore, investigations into novel surgical techniques or materials, informed by computational modeling predictions, could further improve the outcomes of VF implant surgery and advance the field of laryngology. By pursuing these research directions, future studies can continue to push the boundaries of computational modeling in personalized medicine and contribute to improved treatments for VF disorders.

In summary, while the current study demonstrates significant improvements in VF medialization through computational model-guided surgery, addressing the identified limitations and expanding research into these proposed areas will be crucial for translating these findings into clinical practice and ultimately enhancing patient care.

5.0 Conclusion

In this dissertation, I proposed three hypotheses aimed at advancing our understanding and treatment of laryngeal disorders, particularly focusing on VF pathology.

The first hypothesis centered around the feasibility and safety of utilizing bioreactors and magnetic microactuators for basic science research on laryngeal disorders. Through the development of a bioreactor design integrated with magnetic microactuators, the study aimed to mimic physiologically relevant loads experienced by vocal fold epithelial cells. While initial findings were promising, prototype testing revealed limitations in replicating phonatory stress frequencies due to overheating, indicating the need for further hardware optimization. Despite these challenges, the modified bioreactor design showed potential for enhancing our understanding of vocal fold biomechanics and injury mechanisms.

The second hypothesis focused on the integration of findings from various project arms, including implant design, anatomical simulation, and advanced imaging, to optimize experimental conditions for research on UVFP in a rabbit model. The study compared different implant types for inducing vocal fold medialization, ultimately identifying laser-cut implants as a cost-effective solution with consistent size and shape conformity. Advanced imaging techniques, particularly MRI, facilitated precise anatomical reconstructions crucial for computational modeling of vocal fold behavior under specific conditions. The integration of these findings collectively optimized experimental conditions for UVFP research, aligning with the hypothesis.

The third hypothesis delved into comparing surgical techniques for simulating UVFP in a rabbit model and utilizing computational modeling to guide surgical outcomes. The study compared cricothyroid approximation and transmuscular suture approximation techniques, noting

distinct differences in laryngeal geometry and simulation potential. Computational modeling techniques aided in predicting VF biomechanics and guiding surgical outcomes, albeit with some discrepancies between predicted and actual results. Overall, the study observed effective medialization of the VF in all samples, indicating a meaningful improvement over controls and supporting the hypothesis of computational modeling's role in improving surgical techniques for UVFP and related disorders.

The limitations identified in the study have important implications for the validity and generalizability of the findings across all three hypotheses.

Relating to Aim 1, the inability of the uniaxial stroke mechanism to fully replicate the multidirectional forces experienced by VF epithelial cells during speech limits the applicability of the findings to real-world scenarios. Additionally, the controlled *in vitro* environment diverges from the complexities of *in vivo* conditions, potentially influencing cellular behavior differently. The limitations of *in vitro* models are well-recognized, and they are particularly relevant in the context of studying complex biological processes such as wound healing (V. W. Wong et al., 2011) (Wong et al., 2011). These limitations suggest that while the study provides valuable insights into cellular responses under controlled conditions, caution is warranted when extrapolating these findings to physiological contexts.

The refinement of the bioreactor system could be explored to better replicate the complex multidirectional forces experienced by VF epithelial cells during speech. Incorporating advanced imaging techniques, such as real-time microscopy, might provide more realistic insights into cellular responses under physiological conditions. Additionally, integrating factors like inflammation and blood supply into *in vitro* models could help mimic the microenvironment of VF tissue more accurately (Kumai, 2019; Kumai et al., 2010; Svensson et al., 2011). Furthermore,

the use of Förster Resonance Energy Transfer-based Molecular Tension Microscopy would allow for mechanical force measurements at a molecular scale *in situ*, providing a deeper understanding of the mechanical architecture of cells and tissues, and mechanotransduction pathways (Gayrard & Borghi, 2016). Overall, the integration of these advanced techniques and factors into *in vitro* models holds promise in addressing the limitations of current bioreactor systems and providing more physiologically relevant platforms for studying VF epithelial cell responses.

The translatability of the *ex vivo* experiments in rabbit models performed in Aim 2 to human clinical practice is uncertain due to inherent anatomical and physiological differences between species. Moreover, technical and methodological limitations, such as small sample size, tissue shrinkage, and absence of objective acoustic data, raise concerns about the reliability and generalizability of the results. The practical challenges associated with prolonged MRI scan times further hinder the scalability and applicability of the findings to human patients, necessitating optimization strategies. These limitations underscore the need for further research, particularly involving *in vivo* studies, to validate the observed effects and understand their implications for patient care.

In terms of animal models, longitudinal studies with larger sample sizes and follow-up evaluations over time would be beneficial to assess the durability and stability of interventions. Efforts to optimize imaging protocols, reducing scan times while maintaining image quality, could enhance applicability to human patients. Exploring alternative imaging modalities, such as high-resolution ultrasound or optical coherence tomography, could provide real-time imaging capabilities during phonation.

Furthermore, the reliance on computational modeling and excised larynges in Aim 3 presents several limitations. Simplifications and assumptions in computational models may

overlook the complex dynamics of the larynx, while excised larynges may not fully replicate *in vivo* physiological conditions. Variability in surgical procedures and the small sample size further challenge the generalizability of the findings. Moreover, the focus on VF medialization overlooks other factors influencing vocal outcomes, necessitating consideration of additional variables in future studies. Translating findings to human subjects requires caution due to species differences, highlighting the need for further validation in clinical settings.

The refinement of computational models to capture the nonlinear dynamics of VF tissue and account for individual variability is another promising area. Incorporating additional variables like mucosal wave dynamics and neuromuscular control could provide a more comprehensive understanding of VF function. Further validation of computational models through *in vivo* studies in both animal models and human subjects would improve their applicability to clinical practice. Furthermore, investigating additional factors influencing vocal outcomes, such as vocal tract resonance and neuromuscular control, would provide a more holistic understanding of voice production and rehabilitation. Longitudinal studies assessing the impact of interventions on vocal quality, patient-reported outcomes, and quality-of-life measures would offer valuable insights into the effectiveness of treatment strategies.

Overall, while the findings of the combined aims provide valuable insights into laryngeal disorders and potential interventions, addressing these limitations is crucial to ensure the relevance, validity, and generalizability of the findings for clinical practice. Future research endeavors should strive to address these identified gaps through collaborative efforts and innovative methodologies, ultimately advancing the diagnosis, treatment, and management of laryngeal disorders.

5.1 Future healthcare implications

The field of laryngeal surgery, particularly for treating VF disorders, is poised for advancements through the integration of cutting-edge technologies and innovative research. As demonstrated in this dissertation, computational modeling has emerged as a powerful tool in understanding and optimizing the biomechanics of the vocal folds, providing a foundation for enhancing surgical precision and improving patient outcomes. This section explores how the insights and methodologies developed in this research can be applied to revolutionize healthcare, particularly in the realm of laryngeal surgery.

One of the most promising applications of this research lies in enhancing surgical precision through advanced technological integration. By leveraging the detailed anatomical and biomechanical data obtained from computational modeling, surgical robots like the Medici could be programmed to execute highly precise and individualized surgical procedures. These robots could utilize real-time data to adjust their actions dynamically, ensuring optimal implant placement and reducing the risk of human error. This level of precision is particularly crucial for delicate surgeries such as in the VF, where millimeter-level accuracy can significantly impact patient outcomes.

Hologram and laser projection could also be utilized to project detailed images of the surgical target onto the patient's anatomy during the procedure. This technique, based on computational modeling, would provide surgeons with a visual guide that enhances their spatial awareness and accuracy.

The integration of advanced imaging techniques such as dynamic MRI or high-resolution ultrasound into preoperative planning can provide surgeons with a comprehensive view of the patient's unique anatomy. These detailed images can be used to create personalized surgical plans

that consider the specific biomechanics of each patient's larynx. This individualized approach ensures that each surgery is tailored to the patient's needs, leading to better outcomes and reduced recovery times.

Incorporating real-time intraoperative feedback systems, powered by computational models, can further refine surgical techniques. For example, using sensors and imaging tools to provide continuous feedback on tissue response during surgery can help surgeons adjust their techniques at the point of performance. This immediate feedback loop can enhance the precision of implant placement and minimize the likelihood of complications such as implant drifting or tissue damage.

Computational modeling also has potential applications to postoperative monitoring to ensure long-term stability and effectiveness of VF medialization. SLPs developing personalized rehabilitation programs may be able to use advanced computational models to monitor voice and VF function over time and adjust treatments based on real-time data develop personalized rehabilitation programs that monitor vocal fold function over time, leading to improvements in vocal quality and overall patient satisfaction.

Integrating computational modeling and advanced surgical techniques into medical education and training programs can equip future surgeons with the skills and knowledge needed to utilize these technologies effectively. Simulation-based training modules that replicate real-world surgical scenarios can enhance the learning experience and improve surgical outcomes.

The integration of artificial intelligence (AI) into the field of laryngeal surgery and computational modeling presents an exciting frontier in the precision, safety, and effectiveness in treating VF disorders. AI can be employed to simulate and evaluate countless variations in implant placement and shape, optimizing parameters such as size, material, and positioning to tailor

implants to individual patients' unique anatomy. By utilizing machine learning models and predictive analytics, AI can provide surgeons with precise, data-driven insights, improving preoperative planning and real-time decision-making. AI-powered virtual surgery simulations can further refine techniques, enhancing surgical outcomes and reducing complications.

Moreover, AI can significantly improve intraoperative safety by identifying and highlighting safe and danger zones within the surgical field. Real-time image analysis and augmented reality (AR) integration can provide surgeons with critical information, minimizing the risk of accidental damage. In surgical robotics, AI can control robotic movements with extreme precision, continuously learn from each procedure, and offer intelligent assistance, thereby enhancing the consistency and accuracy of implant placements. Additionally, AI can aid in long-term patient monitoring by analyzing postoperative data to predict recovery trajectories and assess vocal quality, ensuring personalized and effective postoperative care. The synergy between AI, computational modeling, and surgical innovation holds the potential to revolutionize VF surgery, offering more effective, personalized, and safer treatments for laryngeal disorders.

Smart materials like shape-memory alloys and polymers or DNA manufactured scaffolds could enable implants to alter their properties in response to environmental stimuli, providing dynamic modifiable structural support for the VF. These materials would enable intraoperative adjustments and non-invasive postoperative modifications, ensuring optimal medialization throughout the healing process. Bio-integration techniques, such as biocompatible coatings and tissue engineering, can enhance tissue integration and promote natural repair, reducing complications and improving long-term outcomes.

The technologies described in this chapter offer exciting opportunities in laryngeal surgical research. This dissertation has demonstrated the potential of emerging technologies to

revolutionize surgical precision and patient outcomes, even if that potential starts with a big idea. Computational modeling based on detailed anatomical and biomechanical data is poised for integration with advanced technologies to pave the way for more effective, personalized, and safer treatments for VF disorders, ultimately transforming patient care and setting new standards in the field of laryngeal surgery.

In conclusion, this dissertation has contributed insights into the realm of laryngeal disorders research, particularly in understanding phonatory physical stress and optimizing experimental conditions for investigating conditions like UVFP. The findings support the feasibility and safety of using bioreactors and magnetic microactuators for basic science research, evidenced by healthy cellular growth and proliferation. Moreover, the integration of findings from the three project arms—implant design, anatomical simulation, and advanced imaging—has collectively enhanced experimental conditions for UVFP research in a rabbit model. By bridging theoretical insights with practical applications, this research sets the stage for advancements in the diagnosis, treatment, and management of laryngeal disorders, ultimately benefiting patients and clinicians alike.

Appendix A List of Abbreviations

Table 6 Abbreviations

The following table lists abbreviations and acronyms used in this document and the page on which the term is first used or defined.

Abbreviation	Meaning	Page
VF	vocal fold	1
SLP	speech-language pathologist	1
UVFP	unilateral vocal fold paralysis	1
LCA	lateral cricoarytenoid	3
PCA	posterior cricoarytenoid	3
CT	computed tomography	5
ML	medialization laryngoplasty	5
ePTFE	expanded polytetrafluoroethylene	9
VFIA	vocal fold injection augmentation	10
MRI	magnetic resonance imaging	21
FSI	fluid-structure interaction	24
ECM	extracellular matrix	41
CAD	computer-aided design	47
AI	artificial intelligence	94

Bibliography

Abdelmalak, B., Gutenberg, L., Lorenz, R. R., Smith, M., Farag, E., & Doyle, D. J. (2009). Dexmedetomidine supplemented with local anesthesia for awake laryngoplasty. *Journal of Clinical Anesthesia*, *21*(6), 442–443. https://doi.org/10.1016/j.jclinane.2008.11.009

Alghonaim, Y., Roskies, M., Kost, K., & Young, J. (2013). Evaluating the timing of injection laryngoplasty for vocal fold paralysis in an attempt to avoid future type 1 thyroplasty. *Journal of Otolaryngology - Head & Neck Surgery*, *42*(1), 24. https://doi.org/10.1186/1916-0216-42-24

Allensworth, J. J., O'Dell, K., Ziegler, A., Bryans, L., Flint, P., & Schindler, J. (2019). Treatment Outcomes of Bilateral Medialization Thyroplasty for Presbylaryngis. *Journal of Voice*, *33*(1), 40–44. https://doi.org/10.1016/j.jvoice.2017.10.014

Avhad, A., Li, Z., Wilson, A., Sayce, L., Chang, S., Rousseau, B., & Luo, H. (2022). Subject-Specific Computational Fluid-Structure Interaction Modeling of Rabbit Vocal Fold Vibration. *Fluids*, *7*(3), 97. https://doi.org/10.3390/fluids7030097

Bailey, T. W., dos Santos, A. P., do Nascimento, N. C., Xie, S., Thimmapuram, J., Sivasankar, M. P., & Cox, A. (2020). RNA sequencing identifies transcriptional changes in the rabbit larynx in response to low humidity challenge. *BMC Genomics*, *21*(1), 888. https://doi.org/10.1186/s12864-020-07301-7

Ballard, D. P., Abramowitz, J., Sukato, D. C., Bentsianov, B., & Rosenfeld, R. M. (2018). Systematic Review of Voice Outcomes for Injection Laryngoplasty Performed under Local vs General Anesthesia. *Otolaryngology–Head and Neck Surgery*, *159*(4), 608–614. https://doi.org/10.1177/0194599818780207

Bartlett, R. S., Gaston, J. D., Ye, S., Kendziorski, C., & Thibeault, S. L. (2019). Mechanotransduction of vocal fold fibroblasts and mesenchymal stromal cells in the context of the vocal fold mechanome. *Journal of Biomechanics*, *83*, 227–234. https://doi.org/10.1016/j.jbiomech.2018.11.050

Bartlett, R. S., Gaston, J. D., Yen, T. Y., Ye, S., Kendziorski, C., & Thibeault, S. L. (2015). Biomechanical Screening of Cell Therapies for Vocal Fold Scar. *Tissue Engineering Part A*, *21*(17–18), 2437–2447. https://doi.org/10.1089/ten.tea.2015.0168

Benninger, M. S., Manzoor, N., & Ruda, J. M. (2015). Short- and Long-Term Outcomes After Silastic Medicalization Laryngoplasty: Are Arytenoid Procedures Needed? *Journal of Voice*, *29*(2), 236–240. https://doi.org/10.1016/j.jvoice.2014.07.008

Bertroche, J. T., Radder, M., Kallogjeri, D., Paniello, R. C., & Bradley, J. P. (2019). Patient-defined duration of benefit from juvederm (hyaluronic acid) used in injection laryngoplasty. *The Laryngoscope*, *129*(12), 2744–2747. https://doi.org/10.1002/lary.27842

Bless, D. M., & Welham, N. V. (2010). Characterization of vocal fold scar formation, prophylaxis, and treatment using animal models. *Current Opinion in Otolaryngology & Head and Neck Surgery*, *18*(6), Article 6. https://doi.org/10.1097/MOO.0b013e3283407d87

Bonde, J., Wirthlin, L., B. Kohn, D., & A. Nolta, J. (2008). Human Hematopoietic Cell Culture, Transduction, and Analyses. *Current Protocols in Human Genetics*, *56*(1). https://doi.org/10.1002/0471142905.hg1307s56

Bowen, A. J., San-Marina, S., Hunter, D., Voss, S., Bartemes, K., Macura, S., Meloche, R., Spragg, A. M., Lohse, C., Oldenburg, M. S., & Ekbom, D. C. (2022). MRI imaging versus histologic volumetric estimation of residual injection laryngoplasty material. *Laryngoscope Investigative Otolaryngology*, *7*(2), 454–459. https://doi.org/10.1002/lio2.744

Branski, R. C., Perera, P., Verdolini, K., Rosen, C. A., Hebda, P. A., & Agarwal, S. (2007). Dynamic Biomechanical Strain Inhibits IL-1β–induced Inflammation in Vocal Fold Fibroblasts. *Journal of Voice*, *21*(6), 651–660. https://doi.org/10.1016/j.jvoice.2006.06.005

Bray, D., Young, J. P., & Harries, M. L. (2008). Complications after type one thyroplasty: Is day-case surgery feasible? *The Journal of Laryngology & Otology*, *122*(7), 715–718. https://doi.org/10.1017/S0022215108002144

Brunner, E., Friedrich, G., Kiesler, K., Chibidziura-Priesching, J., & Gugatschka, M. (2011). Subjective Breathing Impairment in Unilateral Vocal Fold Paralysis. *Folia Phoniatrica et Logopaedica*, *63*(3), 142–146. https://doi.org/10.1159/000316320

Buckmire, R. A., Bryson, P. C., & Patel, M. R. (2011). Type I Gore-Tex Laryngoplasty for Glottic Incompetence in Mobile Vocal Folds. *Journal of Voice*, *25*(3), 288–292. https://doi.org/10.1016/j.jvoice.2009.12.003

Cantillo-Baños, E., Jurado-Ramos, A., Gutiérrez-Jódas, J., & Ariza-Vargas, L. (2013). Vocal fold insufficiency: Medialization laryngoplasty vs calcium hydroxylapatite microspheres (Radiesse Voice®). *Acta Oto-Laryngologica*, *133*(3), 270–275. https://doi.org/10.3109/00016489.2012.728717

Carrau, R. L., Herlich, A., & Rosen, C. A. (1998). Visualization of the Glottis Through a Laryngeal Mask During Medialization Laryngoplasty. *The Laryngoscope*, *108*(5), 769–771. https://doi.org/10.1097/00005537-199805000-00026

Carroll, T. L., & Rosen, C. A. (2011). Long-term results of calcium hydroxylapatite for vocal fold augmentation. *The Laryngoscope*, *121*(2), 313–319. https://doi.org/10.1002/lary.21258

Cashman, S., Simpson, C. B., & McGuff, H. S. (2002). Soft Tissue Response of the Rabbit Larynx to Gore-Tex Implants. *Annals of Otology, Rhinology & Laryngology*, *111*(11), 977–982. https://doi.org/10.1177/000348940211101105

Cezar, C. A., Roche, E. T., Vandenburgh, H. H., Duda, G. N., Walsh, C. J., & Mooney, D. J. (2016). Biologic-free mechanically induced muscle regeneration. *Proceedings of the National Academy of Sciences*, *113*(6), 1534–1539. https://doi.org/10.1073/pnas.1517517113

Chang, J., Courey, M. S., Al-Jurf, S. A., Schneider, S. L., & Yung, K. C. (2014). Injection laryngoplasty outcomes in irradiated and nonirradiated unilateral vocal fold paralysis. *The Laryngoscope*, *124*(8), 1895–1899. https://doi.org/10.1002/lary.24622

Chang, S., Novaleski, C. K., Kojima, T., Mizuta, M., Luo, H., & Rousseau, B. (2016). Subject-Specific Computational Modeling of Evoked Rabbit Phonation. *Journal of Biomechanical Engineering*, *138*(1), 011005. https://doi.org/10.1115/1.4032057

Chang, S., Tian, F.-B., Luo, H., Doyle, J. F., & Rousseau, B. (2013). The Role of Finite Displacements in Vocal Fold Modeling. *Journal of Biomechanical Engineering*, *135*(11), 111008. https://doi.org/10.1115/1.4025330

Chen, Y., Li, Z., Chang, S., Rousseau, B., & Luo, H. (2020). A reduced-order flow model for vocal fold vibration: From idealized to subject-specific models. *Journal of Fluids and Structures*, *94*, 102940. https://doi.org/10.1016/j.jfluidstructs.2020.102940

Chhetri, D. K., & Blumin, J. H. (2012). Laryngeal reinnervation for unilateral vocal fold paralysis using ansa cervicalis nerve to recurrent laryngeal nerve anastomosis. *Operative Techniques in Otolaryngology-Head and Neck Surgery*, *23*(3), 173–177. https://doi.org/10.1016/j.otot.2012.06.003

Chhetri, D. K., Jahan-Parwar, B., Bhuta, S. M., Hart, S. D., & Berke, G. S. (2004). Injection Laryngoplasty with Calcium Hydroxylapatite Gel Implant in an in Vivo Canine Model. *Annals of Otology, Rhinology & Laryngology*, *113*(4), 259–264. https://doi.org/10.1177/000348940411300402

Choi, J., Son, Y.-I., So, Y. K., Byun, H., Lee, E.-K., & Yun, Y.-S. (2012). Posterior glottic gap and age as factors predicting voice outcome of injection laryngoplasty in patients with unilateral vocal fold paralysis. *The Journal of Laryngology & Otology*, *126*(3), 260–266. https://doi.org/10.1017/S0022215111002702

Chouhan, D., Mehrotra, S., Majumder, O., & Mandal, B. B. (2019). Magnetic Actuator Device Assisted Modulation of Cellular Behavior and Tuning of Drug Release on Silk Platform. *ACS Biomaterials Science & Engineering*, *5*(1), 92–105. https://doi.org/10.1021/acsbiomaterials.8b00240

Cochereau, T., Bailly, L., Orgéas, L., Henrich Bernardoni, N., Robert, Y., & Terrien, M. (2020). Mechanics of human vocal folds layers during finite strains in tension, compression and shear. *Journal of Biomechanics*, *110*, 109956. https://doi.org/10.1016/j.jbiomech.2020.109956

Cohen, J. T., Bates, D. D., & Postma, G. N. (2004). Revision Gore-Tex Medialization Laryngoplasty. *Otolaryngology–Head and Neck Surgery*, *131*(3), 236–240. https://doi.org/10.1016/j.otohns.2004.03.023

Cohen, J. T., & Benyamini, L. (2020). Voice outcome after vocal fold injection augmentation with carboxymethyl cellulose versus calcium hydroxyapatite. *The Journal of Laryngology & Otology*, *134*(3), 263–269. https://doi.org/10.1017/S0022215120000481

Cohen, S. M., Kim, J., Roy, N., Asche, C., & Courey, M. (2012). Direct health care costs of laryngeal diseases and disorders. *The Laryngoscope*, *122*(7), 1582–1588. https://doi.org/10.1002/lary.23189

Crolley, V. E., & Gibbins, N. (2017). One hundred years of external approach medialisation thyroplasty. *The Journal of Laryngology & Otology*, *131*(3), 202–208. https://doi.org/10.1017/S0022215116010033

Daniero, J. J., Garrett, C. G., & Francis, D. O. (2014). Framework Surgery for Treatment of Unilateral Vocal Fold Paralysis. *Current Otorhinolaryngology Reports*, *2*(2), 119–130. https://doi.org/10.1007/s40136-014-0044-y

Dion, G. R., Benedict, P. A., Coelho, P. G., Amin, M. R., & Branski, R. C. (2018). Impact of medialization laryngoplasty on dynamic nanomechanical vocal fold structure properties. *The Laryngoscope*, *128*(5), 1163–1169. https://doi.org/10.1002/lary.26963

Dion, G. R., & Nielsen, S. W. (2019). In-Office Laryngology Injections. *Otolaryngologic Clinics of North America*, *52*(3), 521–536. https://doi.org/10.1016/j.otc.2019.02.006

Döllinger, M., Berry, D. A., & Kniesburges, S. (2016). Dynamic vocal fold parameters with changing adduction in *ex-vivo* hemilarynx experiments. *The Journal of the Acoustical Society of America*, *139*(5), 2372–2385. https://doi.org/10.1121/1.4947044

Döllinger, M., Kniesburges, S., Berry, D. A., Birk, V., Wendler, O., Dürr, S., Alexiou, C., & Schützenberger, A. (2018). Investigation of phonatory characteristics using *ex vivo* rabbit larynges. *The Journal of the Acoustical Society of America*, *144*(1), 142–152. https://doi.org/10.1121/1.5043384

Durkes, A., & Sivasankar, M. P. (2016). In vivo investigation of acidified pepsin exposure to porcine vocal fold epithelia. *The Laryngoscope*, *126*(1). https://doi.org/10.1002/lary.25478

Duttenhoefer, F., Mertens, M. E., Vizkelety, J., Gremse, F., Stadelmann, V. A., & Sauerbier, S. (2015). Magnetic resonance imaging in zirconia-based dental implantology. *Clinical Oral Implants Research*, *26*(10), 1195–1202. https://doi.org/10.1111/clr.12430

Eckel, H., Sittel, C., Zorowka, P., & Jerke, A. (1994). Dimensions of the laryngeal framework in adults. *Surgical and Radiologic Anatomy*, *16*(1), 31–36. https://doi.org/10.1007/BF01627918

Elders, B. B. L. J., Hermelijn, S. M., Tiddens, H. A. W. M., Pullens, B., Wielopolski, P. A., & Ciet, P. (2019). Magnetic resonance imaging of the larynx in the pediatric population: A systematic review. *Pediatric Pulmonology*, *54*(4), 478–486. https://doi.org/10.1002/ppul.24250

Elosegui-Artola, A., Trepat, X., & Roca-Cusachs, P. (2018). Control of Mechanotransduction by Molecular Clutch Dynamics. *Trends in Cell Biology*, *28*(5), 356–367. https://doi.org/10.1016/j.tcb.2018.01.008

Epperson, M. V., Tang, A. L., Owens, P., Tabangin, M. E., Altaye, M., Khosla, S., & Howell, R. (2022). Montgomery's Aperture: An External Anatomic Landmark for Surgical Identification of the Anterior Commissure. *Journal of Voice*, *36*(1), 123–127. https://doi.org/10.1016/j.jvoice.2020.04.033

Erickson, E., & Sivasankar, M. (2010). Simulated reflux decreases vocal fold epithelial barrier resistance. *The Laryngoscope*, *120*(8), 1569–1575. https://doi.org/10.1002/lary.20983

Fang, T.-J., Li, H.-Y., Gliklich, R. E., Chen, Y.-H., Wang, P.-C., & Chuang, H.-F. (2010). Outcomes of Fat Injection Laryngoplasty in Unilateral Vocal Cord Paralysis. *Archives of Otolaryngology–Head & Neck Surgery*, *136*(5), 457. https://doi.org/10.1001/archoto.2010.42

Farran, A. J. E., Teller, S. S., Jia, F., Clifton, R. J., Duncan, R. L., & Jia, X. (2013). Design and characterization of a dynamic vibrational culture system: Vibrational culture system. *Journal*

of Tissue Engineering and Regenerative Medicine, *7*(3), 213–225. https://doi.org/10.1002/term.514

Farzal, Z., Overton, L. J., Farquhar, D. R., Stephenson, E. D., Shah, R. N., & Buckmire, R. A. (2019). Sex-based outcomes in type I thyroplasty for nonparalytic glottic incompetence. *The Laryngoscope*, *129*(11), 2543–2548. https://doi.org/10.1002/lary.27770

Francis, D. O., McKiever, M. E., Garrett, C. G., Jacobson, B., & Penson, D. F. (2014). Assessment of Patient Experience With Unilateral Vocal Fold Immobility: A Preliminary Study. *Journal of Voice*, *28*(5), 636–643. https://doi.org/10.1016/j.jvoice.2014.01.006

Francis, D. O., Williamson, K., Hovis, K., Gelbard, A., Merati, A. L., Penson, D. F., Netterville, J. L., & Garrett, C. G. (2016). Effect of injection augmentation on need for framework surgery in unilateral vocal fold paralysis: Effect of Injection Augmentation in UVFP. *The Laryngoscope*, *126*(1), 128–134. https://doi.org/10.1002/lary.25431

Friedman, A. D., Burns, J. A., Heaton, J. T., & Zeitels, S. M. (2010). Early versus late injection medialization for unilateral vocal cord paralysis. *The Laryngoscope*, *120*(10), 2042–2046. https://doi.org/10.1002/lary.21097

Gaidulis, G., & Padala, M. (2023). Computational Modeling of the Subject-Specific Effects of Annuloplasty Ring Sizing on the Mitral Valve to Repair Functional Mitral Regurgitation. *Annals of Biomedical Engineering*, *51*(9), 1984–2000. https://doi.org/10.1007/s10439-023-03219-9

Galgano, J. F., Peck, K. K., Branski, R. C., Bogomolny, D., Mener, D., Ho, M., Holodny, A. I., & Kraus, D. H. (2009). Correlation between Functional MRI And Voice Improvement Following Type I Thyroplasty in Unilateral Vocal Fold Paralysis—A Case Study. *Journal of Voice*, *23*(5), 639–645. https://doi.org/10.1016/j.jvoice.2008.01.016

Garrett, C. G., Coleman, J. R., & Reinisch, L. (2000). Comparative Histology and Vibration of the Vocal Folds: Implications for Experimental Studies in Microlaryngeal Surgery. *The Laryngoscope*, *110*(5), Article 5. https://doi.org/10.1097/00005537-200005000-00011

Gaston, J., Quinchia Rios, B., Bartlett, R., Berchtold, C., & Thibeault, S. L. (2012). The Response of Vocal Fold Fibroblasts and Mesenchymal Stromal Cells to Vibration. *PLoS ONE*, *7*(2), e30965. https://doi.org/10.1371/journal.pone.0030965

Gayrard, C., & Borghi, N. (2016). FRET-based Molecular Tension Microscopy. *Methods*, *94*, 33–42. https://doi.org/10.1016/j.ymeth.2015.07.010

Geng, B., Movahhedi, M., Xue, Q., & Zheng, X. (2021). Vocal fold vibration mode changes due to cricothyroid and thyroarytenoid muscle interaction in a three-dimensional model of the canine larynx. *The Journal of the Acoustical Society of America*, *150*(2), 1176–1187. https://doi.org/10.1121/10.0005883

Gignac, P. M., & Kley, N. J. (2014). Iodine-enhanced micro-CT imaging: Methodological refinements for the study of the soft-tissue anatomy of post-embryonic vertebrates. *Journal of Experimental Zoology Part B: Molecular and Developmental Evolution*, *322*(3), 166–176. https://doi.org/10.1002/jez.b.22561

Gracioso Martins, A. M., Biehl, A., Sze, D., & Freytes, D. O. (2022). Bioreactors for Vocal Fold Tissue Engineering. *Tissue Engineering Part B: Reviews*, *28*(1), 182–205. https://doi.org/10.1089/ten.teb.2020.0285

Granato, F., Martelli, F., Comini, L. V., Luparello, P., Coscarelli, S., Le Seac, O., Carucci, S., Graziani, P., Santoro, R., Alderotti, G., Barillari, M. R., & Mannelli, G. (2019). The surgical treatment of unilateral vocal cord paralysis (UVCP): Qualitative review analysis and meta-analysis

study. *European Archives of Oto-Rhino-Laryngology*, *276*(10), 2649–2659. https://doi.org/10.1007/s00405-019-05587-2

Grundler, S., & Stacey, M. R. W. (1999). Thyroplasty under general anesthesia using a laryngeal mask airway and fibreoptic bronchoscope. *Canadian Journal of Anesthesia/Journal Canadien d'anesthésie*, *46*(5), 460–463. https://doi.org/10.1007/BF03012945

Guide for the Care and Use of Laboratory Animals: Eighth Edition (p. 12910). (2011). National Academies Press. https://doi.org/10.17226/12910

Hahn, M. S., Kobler, J. B., Starcher, B. C., Zeitels, S. M., & Langer, R. (2006). *Quantitative and Comparative Studies of the Vocal Fold Extracellular Matrix I : Elastic Eibers and Hyaluronic Acid* (2). *30*(2), Article 2.

Hassan, M. M., Yumoto, E., Sanuki, T., Kumai, Y., Kodama, N., Baraka, M. A., Wahba, H., Hafez, N. G., & El-Adawy, A. A. N. (2014). Arytenoid Adduction With Nerve-Muscle Pedicle Transfer vs Arytenoid Adduction With and Without Type I Thyroplasty in Paralytic Dysphonia. *JAMA Otolaryngology–Head & Neck Surgery*, *140*(9), 833. https://doi.org/10.1001/jamaoto.2014.1444

Havas, T., Lowinger, D., & Priestley, J. (1999). UNILATERAL VOCAL FOLD PARALYSIS: CAUSES, OPTIONS AND OUTCOMES. *Australian and New Zealand Journal of Surgery*, *69*(7), 509–513. https://doi.org/10.1046/j.1440-1622.1999.01613.x

Henak, C. R., Anderson, A. E., & Weiss, J. A. (2013). Subject-Specific Analysis of Joint Contact Mechanics: Application to the Study of Osteoarthritis and Surgical Planning. *Journal of Biomechanical Engineering*, *135*(2), 021003. https://doi.org/10.1115/1.4023386

Henrich, N., Sundin, G., Ambroise, D., d'Alessandro, C., Castellengo, M., & Doval, B. (2003). Just noticeable differences of open quotient and asymmetry coefficient in singing voice. *Journal of Voice*, *17*(4), 481–494. https://doi.org/10.1067/S0892-1997(03)00005-5

Hirano, M. (1974). Morfological structure of the vocal fold as a vibrator and its variations. *Folia Phoniatr (Basel).*, *26*, 89–4.

Hizal, E., Buyuklu, F., Ozdemir, B. H., & Erbek, S. S. (2014). Long-term inflammatory response to liquid injectable silicone, cartilage, and silicone sheet. *The Laryngoscope*, *124*(11). https://doi.org/10.1002/lary.24800

Hsia, T.-Y., Conover, T., Figliola, R., & Modeling of Congenital Hearts Alliance (MOCHA) Investigators. (2020). Computational Modeling to Support Surgical Decision Making in Single Ventricle Physiology. *Seminars in Thoracic and Cardiovascular Surgery. Pediatric Cardiac Surgery Annual*, *23*, 2–10. https://doi.org/10.1053/j.pcsu.2020.01.001

Huang, J. Y., Kerns, J. R., Nute, J. L., Liu, X., Balter, P. A., Stingo, F. C., Followill, D. S., Mirkovic, D., Howell, R. M., & Kry, S. F. (2015). An evaluation of three commercially available metal artifact reduction methods for CT imaging. *Physics in Medicine and Biology*, *60*(3), 1047–1067. https://doi.org/10.1088/0031-9155/60/3/1047

Isshiki, N., Okamura, H., & Ishikawa, T. (1975). Thyroplasty Type I (Lateral Compression) For Dysphonia Due To Vocal Cord Paralysis Or Atrophy. *Acta Oto-Laryngologica*, *80*(1–6), 465–473. https://doi.org/10.3109/00016487509121353

Iwahashi, T., Ogawa, M., Hosokawa, K., Mochizuki, R., & Inohara, H. (2015). Computed tomographic assessment of the causal factors of unsuccessful medialization thyroplasty. *Acta Oto-Laryngologica*, *135*(3), 283–289. https://doi.org/10.3109/00016489.2014.950325

Jamal, N., Mundi, J., & Chhetri, D. K. (2014). Higher risk of superficial injection during injection laryngoplasty in women. *American Journal of Otolaryngology*, *35*(2), 159–163. https://doi.org/10.1016/j.amjoto.2013.09.002

Johns, M. M., Arviso, L. C., & Ramadan, F. (2011). Challenges and Opportunities in the Management of the Aging Voice. *Otolaryngology–Head and Neck Surgery*, *145*(1), 1–6. https://doi.org/10.1177/0194599811404640

Kanazawa, T., Watanabe, Y., Komazawa, D., Indo, K., Misawa, K., Nagatomo, T., Shimada, M., Iino, Y., & Ichimura, K. (2014). Phonological outcome of laryngeal framework surgery by different anesthesia protocols: A single-surgeon experience. *Acta Oto-Laryngologica*, *134*(2), 193–200. https://doi.org/10.3109/00016489.2013.847283

Kelchner, L. N., Stemple, J. C., Gerdeman, E., Le Borgne, W., & Adam, S. (1999). Etiology, pathophysiology, treatment choices, and voice results for unilateral adductor vocal fold paralysis: A 3-year retrospective. *Journal of Voice: Official Journal of the Voice Foundation*, *13*(4), 592–601. https://doi.org/10.1016/s0892-1997(99)80013-7

Kim, D., Lim, J.-Y., & Kwon, S. (2016). Development of Vibrational Culture Model Mimicking Vocal Fold Tissues. *Annals of Biomedical Engineering*, *44*(10), 3136–3143. https://doi.org/10.1007/s10439-016-1587-5

Kim, J., Chung, S. E., Choi, S.-E., Lee, H., Kim, J., & Kwon, S. (2011). Programming magnetic anisotropy in polymeric microactuators. *Nature Materials*, *10*(10), 747–752. https://doi.org/10.1038/nmat3090

Kim, Y. S., Choi, J. W., Park, J.-K., Kim, Y. S., Kim, H. J., Shin, Y. S., & Kim, C.-H. (2015). Efficiency and durability of hyaluronic acid of different particle sizes as an injectable

material for VF augmentation. *Acta Oto-Laryngologica*, *135*(12), 1311–1318. https://doi.org/10.3109/00016489.2015.1070966

Kim, Y.-M., Yi, T., Choi, J.-S., Lee, S., Jang, Y. H., Kim, C.-H., Song, S. U., & Lim, J.-Y. (2013). Bone Marrow-Derived Clonal Mesenchymal Stem Cells as a Source of Cell Therapy for Promoting Vocal Fold Wound Healing. *Annals of Otology, Rhinology & Laryngology*, *122*(2), 121–130. https://doi.org/10.1177/000348941312200208

Kimball, E. E., Sayce, L., Powell, M., Gartling, G. J., Brandley, J., & Rousseau, B. (2021). Different Vibratory Conditions Elicit Different Structural and Biological Vocal Fold Changes in an In-Vivo Rabbit Model of Phonation. *Journal of Voice*, *35*(2), 216–225. https://doi.org/10.1016/j.jvoice.2019.08.023

Kimball, E. E., Sayce, L., Xu, X. C., Kruszka, C. M., & Rousseau, B. (2021). Protein Substrate Alters Cell Physiology in Primary Culture of Vocal Fold Epithelial Cells. *Cells Tissues Organs*, *210*(1), 10–23. https://doi.org/10.1159/000514200

Kirsch, A., Hortobagyi, D., Stachl, T., Karbiener, M., Grossmann, T., Gerstenberger, C., & Gugatschka, M. (2019). Development and validation of a novel phonomimetic bioreactor. *PLOS ONE*, *14*(3), e0213788. https://doi.org/10.1371/journal.pone.0213788

Klemuk, S. A., Jaiswal, S., & Titze, I. R. (2008). Cell viability viscoelastic measurement in a rheometer used to stress and engineer tissues at low sonic frequencies. *The Journal of the Acoustical Society of America*, *124*(4), 2330–2339. https://doi.org/10.1121/1.2973183

Klepacek, I., Jirak, D., Duskova Smrckova, M., Janouskova, O., & Vampola, T. (2016). The Human Vocal Fold Layers. Their Delineation Inside Vocal Fold as a Background to Create 3D Digital and Synthetic Glottal Model. *Journal of Voice*, *30*(5), 529–537. https://doi.org/10.1016/j.jvoice.2015.08.004

Koçdor, P. (2014). Injection laryngoplasty outcomes in vocal fold paralysis using calcium hydroxylapatite. *The Turkish Journal of Ear Nose and Throat*, *24*(5), 271–275. https://doi.org/10.5606/kbbihtisas.2014.65807

Kodama, N., Kumai, Y., Sanuki, T., & Yumoto, E. (2017). Arytenoid adduction combined with nerve-muscle pedicle flap implantation or type I thyroplasty. *The Laryngoscope*, *127*(1), 159–166. https://doi.org/10.1002/lary.26032

Kolosova, K., Gao, Q., Tuznik, M., Bouhabel, S., Kost, K. M., Wang, H., Li-Jessen, N. Y. K., Mongeau, L., & Wiseman, P. W. (2021). Characterizing Vocal Fold Injury Recovery in a Rabbit Model With THREE-DIMENSIONAL Virtual Histology. *The Laryngoscope*, *131*(7), 1578–1587. https://doi.org/10.1002/lary.29028

Kumai, Y. (2019). Pathophysiology of Fibrosis in the Vocal Fold: Current Research, Future Treatment Strategies, and Obstacles to Restoring Vocal Fold Pliability. *International Journal of Molecular Sciences*, *20*(10), 2551. https://doi.org/10.3390/ijms20102551

Kumai, Y., Kobler, J. B., Park, H., Galindo, M., Herrera, V. L. M., & Zeitels, S. M. (2010). Modulation of vocal fold scar fibroblasts by adipose-derived stem/stromal cells. *The Laryngoscope*, *120*(2), 330–337. https://doi.org/10.1002/lary.20753

Kupfer, R. A., Merati, A. L., & Sulica, L. (2015). Medialization Laryngoplasty for Odynophonia. *JAMA Otolaryngology–Head & Neck Surgery*, *141*(6), 556. https://doi.org/10.1001/jamaoto.2015.0333

Kurata, K., Sumida, K., & Takamatsu, H. (2019). Open-source cell extension system assembled from laser-cut plates. *HardwareX*, *5*, e00065. https://doi.org/10.1016/j.ohx.2019.e00065

Kwak, P. E., Tritter, A. G., Donovan, D. T., & Ongkasuwan, J. (2016). Long-term Voice Outcomes of Early Thyroplasty for Unilateral Vocal Fold Paralysis Following Aortic Arch Surgery. *Annals of Otology, Rhinology & Laryngology*, *125*(7), 559–563. https://doi.org/10.1177/0003489416636127

Kwon, T., An, S., Ahn, J., Kim, K. H., & Sung, M. (2010). Calcium hydroxylapatite injection laryngoplasty for the treatment of presbylaryngis: Long-term results. *The Laryngoscope*, *120*(2), 326–329. https://doi.org/10.1002/lary.20749

Kwon, T.-K., Rosen, C. A., & Gartner-Schmidt, J. (2005). Preliminary Results of a New Temporary Vocal Fold Injection Material. *Journal of Voice*, *19*(4), 668–673. https://doi.org/10.1016/j.jvoice.2005.01.009

Latifi, N., Heris, H. K., Thomson, S. L., Taher, R., Kazemirad, S., Sheibani, S., Li-Jessen, N. Y. K., Vali, H., & Mongeau, L. (2016). A Flow Perfusion Bioreactor System for Vocal Fold Tissue Engineering Applications. *Tissue Engineering Part C: Methods*, *22*(9), 823–838. https://doi.org/10.1089/ten.tec.2016.0053

Leder, S. B., Suiter, D. M., Duffey, D., & Judson, B. L. (2012). Vocal Fold Immobility and Aspiration Status: A Direct Replication Study. *Dysphagia*, *27*(2), 265–270. https://doi.org/10.1007/s00455-011-9362-0

Lee, M., Ang, C., Andreadis, K., Shin, J., & Rameau, A. (2021). An Open-Source Three-Dimensionally Printed Laryngeal Model for Injection Laryngoplasty Training. *The Laryngoscope*, *131*(3). https://doi.org/10.1002/lary.28952

Li, Z., Chen, Y., Chang, S., & Luo, H. (2020). A Reduced-Order Flow Model for Fluid–Structure Interaction Simulation of Vocal Fold Vibration. *Journal of Biomechanical Engineering*, *142*(2), 021005. https://doi.org/10.1115/1.4044033

Li, Z., Wilson, A., Sayce, L., Avhad, A., Rousseau, B., & Luo, H. (2021). Numerical and Experimental Investigations on Vocal Fold Approximation in Healthy and Simulated Unilateral Vocal Fold Paralysis. *Applied Sciences*, *11*(4), 1817. https://doi.org/10.3390/app11041817

Lin, W.-Y., Chang, W.-D., Ko, L.-W., Tsou, Y.-A., & Chen, S.-H. (2020). Impact of patient-related factors on successful autologous fat injection laryngoplasty in thyroid surgical treated related unilateral vocal fold paralysis- observational study. *Medicine*, *99*(1), e18579. https://doi.org/10.1097/MD.0000000000018579

Loewen, M., & Walner, D. (2001). Dimensions of rabbit subglottis and trachea. *Laboratory Animals*, *35*, 253–256. https://doi.org/10.1258/0023677011911714

Luo, H., Mittal, R., & Bielamowicz, S. A. (2009). Analysis of flow-structure interaction in the larynx during phonation using an immersed-boundary method. *The Journal of the Acoustical Society of America*, *126*(2), 816–824. https://doi.org/10.1121/1.3158942

M. Dominguez, L., Villarreal, R., & Simpson, C. B. (2019). Voice Outcomes of Lipoinjection Versus Medialization Laryngoplasty for Nonparalytic Glottic Insufficiency. *The Laryngoscope*, *129*(5), 1164–1168. https://doi.org/10.1002/lary.27573

Malik, A., Ramalingam, W. V. B. S., Nilakantan, A., Nair, S., Ramesh, A. V., & Raj, P. (2014). Comparison of the use of silastic with titanium prefabricated implant in type I thyroplasty☆☆Please cite this article as: Malik A, Ramalingam WVBS, Nilakantan A, Nair S, Ramesh AV, Raj P. Comparison of the use of silastic with titanium prefabricated implant in type I thyroplasty. Braz J Otorhinolaryngol. 2014;80:156-60. *Brazilian Journal of Otorhinolaryngology*, *80*(2), 156–160. https://doi.org/10.5935/1808-8694.20140032

Mallur, P. S., Morrison, M. P., Postma, G. N., Amin, M. R., & Rosen, C. A. (2012). Safety and efficacy of carboxymethylcellulose in the treatment of glottic insufficiency: CMC Treatment for Glottic Insufficiency. *The Laryngoscope*, *122*(2), 322–326. https://doi.org/10.1002/lary.21930

Maragos, N. E. (2001). Revision Thyroplasty. *Annals of Otology, Rhinology & Laryngology*, *110*(12), 1087–1092. https://doi.org/10.1177/000348940111001201

Mastronikolis, N. S., Remacle, M., Kiagiadaki, D., Lawson, G., Bachy, V., & Van Der Vorst, S. (2013). Medialization thyroplasty for voice restoration after transoral cordectomy. *European Archives of Oto-Rhino-Laryngology*, *270*(7), 2071–2078. https://doi.org/10.1007/s00405-013-2462-8

Mathison, C. C., Villari, C. R., Klein, A. M., & Johns, M. M. (2009). Comparison of outcomes and complications between awake and asleep injection laryngoplasty: A Case-Control Study. *The Laryngoscope*, *119*(7), 1417–1423. https://doi.org/10.1002/lary.20485

McCulloch, T. M., & Hoffman, H. T. (1998). Medialization Laryngoplasty with Expanded Polytetrafluoroethylene: Surgical Technique and Preliminary Results. *Annals of Otology, Rhinology & Laryngology*, *107*(5), 427–432. https://doi.org/10.1177/000348949810700512

McLaughlin, J. K., Lipworth, L., Murphy, D. K., & Walker, P. S. (2007). The Safety of Silicone Gel-Filled Breast Implants: A Review of the Epidemiologic Evidence. *Annals of Plastic Surgery*, *59*(5), 569–580. https://doi.org/10.1097/SAP.0b013e318066f0bd

Millon-Frémillon, A., Aureille, J., & Guilluy, C. (2017). Analyzing Cell Surface Adhesion Remodeling in Response to Mechanical Tension Using Magnetic Beads. *JoVE (Journal of Visualized Experiments)*, *121*, e55330. https://doi.org/10.3791/55330

Mizuta, M., Kurita, T., Kimball, E. E., & Rousseau, B. (2017). Structurally and Functionally Characterized In Vitro Model of Rabbit Vocal Fold Epithelium. *Tissue Cell*, *49*(3), Article 3. https://doi.org/10.1016/j.tice.2017.03.006

Mohammed, H., Masterson, L., Gendy, S., & Nassif, R. (2016). Outpatient-based injection laryngoplasty for the management of unilateral vocal fold paralysis – clinical outcomes from a UK centre. *Clinical Otolaryngology*, *41*(4), 341–346. https://doi.org/10.1111/coa.12516

Montgomery, W. W., Bunting, G., McLean-Muse, A., Hillman, R. E., Doyle, P., Varvares, M., & Eng, J. (2000). Montgomery® Thyroplasty Implant for Vocal Fold Immobility: Phonatory Outcomes. *Annals of Otology, Rhinology & Laryngology*, *109*(4), 393–400. https://doi.org/10.1177/000348940010900410

Movahhedi, M., Geng, B., Xue, Q., & Zheng, X. (2021). A computational framework for patient-specific surgical planning of type 1 thyroplasty. *JASA Express Letters*, *1*(12), 125203. https://doi.org/10.1121/10.0009084

Munin, M. C., Rosen, C. A., & Zullo, T. (2003). Utility of laryngeal electromyography in predicting recovery after vocal fold paralysis11No commercial party having a direct financial interest in the results of the research supporting this article has or will confer a benefit upon the author(s) or upon any organization with which the author(s) is/are associated. *Archives of Physical Medicine and Rehabilitation*, *84*(8), 1150–1153. https://doi.org/10.1016/S0003-9993(03)00146-1

Netterville, J. L., Stone, R. E., Civantos, F. J., Luken, E. S., & Ossoff, R. H. (1993). Silastic Medialization and Arytenoid Adduction: The Vanderbilt Experience: A Review of 116 Phonosurgical Procedures. *Annals of Otology, Rhinology & Laryngology*, *102*(6), 413–424. https://doi.org/10.1177/000348949310200602

Novaleski, C. K., Kimball, E. E., Mizuta, M., & Rousseau, B. (2016). Acute exposure to vibration is an apoptosis-inducing stimulus in the vocal fold epithelium. *Tissue and Cell*. https://doi.org/10.1016/j.tice.2016.08.007

Orestes, M. I., Neubauer, J., Sofer, E., Salinas, J., & Chhetri, D. K. (2014). Phonatory effects of type I thyroplasty implant shape and depth of medialization in unilateral vocal fold paralysis: Phonatory Effects of Type 1 Thyroplasty. *The Laryngoscope*, *124*(12), 2791–2796. https://doi.org/10.1002/lary.24851

Owusu-Ayim, M., Majumdar, S., & Reid, L. (2020). Creating a dynamic cadaveric laryngeal model. *The Clinical Teacher*, *17*(6), 729–731. https://doi.org/10.1111/tct.13166

Parker, N. P., Barbu, A. M., Hillman, R. E., Zeitels, S. M., & Burns, J. A. (2015). Revision Transcervical Medialization Laryngoplasty for Unilateral Vocal Fold Paralysis. *Otolaryngology–Head and Neck Surgery*, *153*(4), 593–598. https://doi.org/10.1177/0194599815585091

Plaat, B. E. C., Van Der Laan, B. F. A. M., Wedman, J., Halmos, G. B., & Dikkers, F. G. (2014). Distal chip versus fiberoptic laryngoscopy using endoscopic sheaths: Diagnostic accuracy and image quality. *European Archives of Oto-Rhino-Laryngology*. https://doi.org/10.1007/s00405-014-2916-7

Prendes, B. L., Yung, K. C., Likhterov, I., Schneider, S. L., Al-Jurf, S. A., & Courey, M. S. (2012). Long-term effects of injection laryngoplasty with a temporary agent on voice quality and vocal fold position. *The Laryngoscope*, *122*(10), 2227–2233. https://doi.org/10.1002/lary.23473

Ricci Maccarini, A., Stacchini, M., Mozzanica, F., Schindler, A., Basile, E., De Rossi, G., Woo, P., Remacle, M., & Magnani, M. (2018). Efficacy of trans-nasal fiberendoscopic injection laryngoplasty with centrifuged autologous fat in the treatment of glottic insufficiency due to

unilateral vocal fold paralysis. *Acta Otorhinolaryngologica Italica*, *38*(3), 204–213. https://doi.org/10.14639/0392-100X-2012

Rosen, C. A., Amin, M. R., Sulica, L., Simpson, C. B., Merati, A. L., Courey, M. S., Johns, M. M., & Postma, G. N. (2009). Advances in office-based diagnosis and treatment in laryngology. *The Laryngoscope*, *119*(S2). https://doi.org/10.1002/lary.20712

Rosenthal, L. H. S., Benninger, M. S., & Deeb, R. H. (2007). Vocal Fold Immobility: A Longitudinal Analysis of Etiology Over 20 Years: *The Laryngoscope*, *117*(10), 1864–1870. https://doi.org/10.1097/MLG.0b013e3180de4d49

Rosow, D. E., & Sulica, L. (2010). Laryngoscopy of vocal fold paralysis: Evaluation of consistency of clinical findings. *The Laryngoscope*, *120*(7), 1376–1382. https://doi.org/10.1002/lary.20945

Rousseau, B., Kojima, T., Novaleski, C. K., Kimball, E. E., Valenzuela, C. V., Mizuta, M., Daniero, J. J., Garrett, C. G., & Sivasankar, M. P. (2017). Recovery of vocal fold epithelium after acute phonotrauma. *Cells, Tissues, Organs*, *204*(2), Article 2. https://doi.org/10.1159/000472251

Saadeh, C. K., Rosero, E. B., Joshi, G. P., Ozayar, E., & Mau, T. (2017). Reducing sedation time for thyroplasty with arytenoid adduction with sequential anesthetic technique. *The Laryngoscope*, *127*(12), 2813–2817. https://doi.org/10.1002/lary.26743

Sadeghi, H., Kniesburges, S., Falk, S., Kaltenbacher, M., Schützenberger, A., & Döllinger, M. (2019). Towards a Clinically Applicable Computational Larynx Model. *Applied Sciences*, *9*(11), 2288. https://doi.org/10.3390/app9112288

Salmerón-González, E., García-Vilariño, E., Llópez-Carratalá, I., Collado-Martin, D., María Perolada-Valmaña, J., & Armengot-Carceller, M. (2020). Augmentation of Scarred Vocal

Folds With Centrifuged and Emulsified Autologous Fat Grafts. *Otolaryngology–Head and Neck Surgery*, *163*(6), 1226–1231. https://doi.org/10.1177/0194599820932836

Sanuki, T., Yumoto, E., Nishimoto, K., & Minoda, R. (2014). Laryngeal Muscle Activity in Unilateral Vocal Fold Paralysis Patients Using Electromyography and Coronal Reconstructed Images. *Otolaryngology–Head and Neck Surgery*, *150*(4), 625–630. https://doi.org/10.1177/0194599814520999

Sayce, L. J., Powell, M. E., Kimball, E. E., Chen, P., Gartling, G. J., & Rousseau, B. (2020). Continuous Rate Infusion of Ketamine Hydrochloride and Dexmedetomidine for Maintenance of Anesthesia during Laryngotracheal Surgery in New Zealand White Rabbits (*Oryctolagus cuniculus*). *Journal of the American Association for Laboratory Animal Science*, *59*(2), 176–185. https://doi.org/10.30802/AALAS-JAALAS-19-000076

Shen, T., Damrose, E. J., & Morzaria, S. (2013). A Meta-analysis of Voice Outcome Comparing Calcium Hydroxylapatite Injection Laryngoplasty to Silicone Thyroplasty. *Otolaryngology–Head and Neck Surgery*, *148*(2), 197–208. https://doi.org/10.1177/0194599812464193

Shiba, T., Hardy, J., & Long, J. (2015). Laryngeal Tissue Engineering Using Rabbit Adipose Derived Stem Cells In Fibrin: A Pre-Clinical Model. *Journal of Otolaryngology Advances*, *1*(1), 27–39. https://doi.org/10.14302/issn.2379-8572.joa-14-611

Sivasankar, M., & Ivanisevic, A. (2007). Atomic Force Microscopy Investigation of Vocal Fold Collagen. *The Laryngoscope*, *117*(10), 1876–1881. https://doi.org/10.1097/MLG.0b013e3180caa1df

Sniadecki, N. J., Anguelouch, A., Yang, M. T., Lamb, C. M., Liu, Z., Kirschner, S. B., Liu, Y., Reich, D. H., & Chen, C. S. (2007). Magnetic microposts as an approach to apply forces to

living cells. *Proceedings of the National Academy of Sciences*, *104*(37), 14553–14558. https://doi.org/10.1073/pnas.0611613104

Sproson, E., Nightingale, J., & Puxeddu, R. (2010). Thyroplasty type I under general anaesthesia with the use of the laryngeal mask and a waking period to assess voice. *Auris Nasus Larynx*, *37*(3), 357–360. https://doi.org/10.1016/j.anl.2009.07.009

Stanisz, I., Leonhard, M., Denk-Linnert, D.-M., & Schneider-Stickler, B. (2021). Diagnostic limitation of laryngostroboscopy in comparison to laryngeal electromyography in synkinesis in unilateral vocal fold paralysis. *European Archives of Oto-Rhino-Laryngology*, *278*(7), 2387–2395. https://doi.org/10.1007/s00405-021-06714-8

Subramaniam, D. R., Arens, R., Wagshul, M. E., Sin, S., Wootton, D. M., & Gutmark, E. J. (2018). Biomechanics of the soft-palate in sleep apnea patients with polycystic ovarian syndrome. *Journal of Biomechanics*, *76*, 8–15. https://doi.org/10.1016/j.jbiomech.2018.05.013

Suehiro, A., Hirano, S., Kishimoto, Y., Tanaka, S., & Ford, C. N. (2009). Comparative Study of Vocal Outcomes with Silicone versus Gore-Tex Thyroplasty. *Annals of Otology, Rhinology & Laryngology*, *118*(6), 405–408. https://doi.org/10.1177/000348940911800602

Sulica, L. (2008). The Natural History of Idiopathic Unilateral Vocal Fold Paralysis: Evidence and Problems: *The Laryngoscope*, *118*(7), 1303–1307. https://doi.org/10.1097/MLG.0b013e31816f27ee

Svensson, B., Nagubothu, S. R., Cedervall, J., Chan, R. W., Le Blanc, K., Kimura, M., Ährlund-Richter, L., Tolf, A., & Herteg\aard, S. (2011). Injection of human mesenchymal stem cells improves healing of vocal folds after scar excision—A xenograft analysis. *Laryngoscope*, *121*(10), Article 10. https://doi.org/10.1002/lary.22143

Thibeault, S. L., Gray, S. D., Bless, D. M., Chan, R. W., & Ford, C. N. (2002). Histologic and rheologic characterization of vocal fold scarring. *Journal of Voice*, *16*(1), Article 1. https://doi.org/10.1016/S0892-1997(02)00078-4

Titze, I. R., Hitchcock, R. W., Broadhead, K., Webb, K., Li, W., Gray, S. D., & Tresco, P. A. (2004). Design and validation of a bioreactor for engineering vocal fold tissues under combined tensile and vibrational stresses. *Journal of Biomechanics*, *37*(10), Article 10. https://doi.org/10.1016/J.JBIOMECH.2004.01.007

Titze, I. R., Jiang, J., & Drucker, D. G. (1988). Preliminaries to the body-cover theory of pitch control. *Journal of Voice*, *1*(4), 314–319. https://doi.org/10.1016/S0892-1997(88)80004-3

Titze, I. R., Klemuk, S. A., & Lu, X. (2012). Adhesion of a Monolayer of Fibroblast Cells to Fibronectin under Sonic Vibrations in a Bioreactor. *Annals of Otology, Rhinology & Laryngology*, *121*(6), 364–374. https://doi.org/10.1177/000348941212100602

Tomás, A. R., Gonçalves, A. I., Paz, E., Freitas, P., Domingues, R. M. A., & Gomes, M. E. (2019). Magneto-mechanical actuation of magnetic responsive fibrous scaffolds boosts tenogenesis of human adipose stem cells. *Nanoscale*, *11*(39), 18255–18271. https://doi.org/10.1039/C9NR04355A

Tong, Z., Duncan, R. L., & Jia, X. (2013). Modulating the Behaviors of Mesenchymal Stem Cells Via the Combination of High-Frequency Vibratory Stimulations and Fibrous Scaffolds. *Tissue Engineering Part A*, *19*(15–16), 1862–1878. https://doi.org/10.1089/ten.tea.2012.0694

Tong, Z., Zerdoum, A. B., Duncan, R. L., & Jia, X. (2014). Dynamic Vibration Cooperates with Connective Tissue Growth Factor to Modulate Stem Cell Behaviors. *Tissue Engineering Part A*, *20*(13–14), 1922–1934. https://doi.org/10.1089/ten.tea.2013.0496

Tsai, M.-S., Yang, M.-Y., Chang, G.-H., Tsai, Y.-T., Lin, M.-H., & Hsu, C.-M. (2017). Autologous thyroid cartilage graft implantation in medialization laryngoplasty: A modified approach for treating unilateral vocal fold paralysis. *Scientific Reports*, *7*(1), 4790. https://doi.org/10.1038/s41598-017-05024-6

United States Department of Agriculture, A. and P. H. I. S. (2019). *Animal welfare act and regulations*. https://www.aphis.usda.gov/aphis/ourfocus/animalwelfare/sa_publications/ct_publications_and_guidance_documents

Ustundag, E., Boyaci, Z., Keskin, G., Kaur, A., & Ozkarakas, H. (2005). Soft Tissue Response of the Larynx to Silicone, Gore-Tex, and Irradiated Cartilage Implants: *The Laryngoscope*, *115*(6), 1009–1014. https://doi.org/10.1097/01.MLG.0000162644.63752.BC

Van Ardenne, N., Vanderwegen, J., Van Nuffelen, G., De Bodt, M., & Van De Heyning, P. (2011). Medialization thyroplasty: Vocal outcome of silicone and titanium implant. *European Archives of Oto-Rhino-Laryngology*, *268*(1), 101–107. https://doi.org/10.1007/s00405-010-1327-7

Van Den Broek, E. M. J. M., Vokes, D. E., & Dorman, E. B. (2016). Bilateral In-Office Injection Laryngoplasty as an Adjunctive Treatment for Recalcitrant Puberphonia: A Case Report and Review of the Literature. *Journal of Voice*, *30*(2), 221–223. https://doi.org/10.1016/j.jvoice.2015.03.019

Verdolini, K., & Ramig, L. O. (2001). Review: Occupational risks for voice problems. *Logopedics, Phoniatrics, Vocology*, *26*(1), 37–46.

Verma, S. P., & Dailey, S. H. (2014). Office-Based Injection Laryngoplasty for the Management of Unilateral Vocal Fold Paralysis. *Journal of Voice*, *28*(3), 382–386. https://doi.org/10.1016/j.jvoice.2013.10.006

Wang, C.-C., Chang, M.-H., Wang, C.-P., & Liu, S.-A. (2008). Prognostic Indicators of Unilateral Vocal Fold Paralysis. *Archives of Otolaryngology–Head & Neck Surgery*, *134*(4), 380. https://doi.org/10.1001/archotol.134.4.380

Wang, J. H.-C., & Thampatty, B. P. (2006). An Introductory Review of Cell Mechanobiology. *Biomechanics and Modeling in Mechanobiology*, *5*(1), 1–16. https://doi.org/10.1007/s10237-005-0012-z

Waring, J. P., Baron, T. H., Hirota, W. K., Goldstein, J. L., Jacobson, B. C., Leighton, J. A., Mallery, J. S., & Faigel, D. O. (2003). Guidelines for Conscious Sedation and Monitoring During Gastrointestinal Endoscopy. *Gastrointestinal Endoscopy*, *58*(3), 317–322. https://doi.org/10.1067/S0016-5107(03)00001-4

Wilson, A., Kimball, E. E., Sayce, L., Luo, H., Khosla, S. M., & Rousseau, B. (2021). Medialization Laryngoplasty: A Review for Speech-Language Pathologists. *Journal of Speech, Language, and Hearing Research*, *64*(2), 481–490. https://doi.org/10.1044/2020_JSLHR-20-00344

Wilson, A., Sayce, L., Li, Z., Gartling, G., Luo, H., & Rousseau, B. (2023). Custom Laser-Cut Silastic® Implants for Type I Thyroplasty in a Preclinical Model. *ORL*, *85*(5), 294–298. https://doi.org/10.1159/000530419

Wolchok, J. C., Brokopp, C., Underwood, C. J., & Tresco, P. A. (2009). The effect of bioreactor induced vibrational stimulation on extracellular matrix production from human derived fibroblasts. *Biomaterials*, *30*(3), 327–335. https://doi.org/10.1016/j.biomaterials.2008.08.035

Wong, E., Smith, M., Stone, D. B., Palme, C. E., Smith, M. C., & Riffat, F. (2020). Arytenoid vertical height discrepancy in predicting outcomes after unilateral vocal cord medialization. *The Laryngoscope*, *130*(2), 418–422. https://doi.org/10.1002/lary.27900

Wong, V. W., Sorkin, M., Glotzbach, J. P., Longaker, M. T., & Gurtner, G. C. (2011). Surgical Approaches to Create Murine Models of Human Wound Healing. *Journal of Biomedicine and Biotechnology*, *2011*, 1–8. https://doi.org/10.1155/2011/969618

Woo, P., Pearl, A. W., Hsiung, M., & Som, P. (2001). Failed Medialization Laryngoplasty: Management by Revision Surgery. *Otolaryngology–Head and Neck Surgery*, *124*(6), 615–621. https://doi.org/10.1177/019459980112400603

Xue, Q., Zheng, X., Mittal, R., & Bielamowicz, S. (2014). Subject-specific computational modeling of human phonation. *The Journal of the Acoustical Society of America*, *135*(3), 1445–1456. https://doi.org/10.1121/1.4864479

Yamashita, M., Bless, D. M., & Welham, N. V. (2010). Morphological and Extracellular Matrix Changes following Vocal Fold Injury in Mice. *Cells Tissues Organs*, *192*, 262–271. https://doi.org/10.1159/000315476

Yang, J., Wang, X., Krane, M., & Zhang, L. T. (2017). Fully-coupled aeroelastic simulation with fluid compressibility—For application to vocal fold vibration. *Computer Methods in Applied Mechanics and Engineering*, *315*, 584–606. https://doi.org/10.1016/j.cma.2016.11.010

Yılmaz, T. (2012). Sulcus vocalis: Excision, primary suture and medialization laryngoplasty: personal experience with 44 cases. *European Archives of Oto-Rhino-Laryngology*, *269*(11), 2381–2389. https://doi.org/10.1007/s00405-012-2058-8

Young, V. N., Zullo, T. G., & Rosen, C. A. (2010). Analysis of laryngeal framework surgery: 10-year follow-up to a national survey. *The Laryngoscope*, *120*(8), 1602–1608. https://doi.org/10.1002/lary.21004

Yuan, Z., Memarzadeh, K., Stephen, A. S., Allaker, R. P., Brown, R. A., & Huang, J. (2018). Development of a 3D Collagen Model for the In Vitro Evaluation of Magnetic-assisted Osteogenesis. *Scientific Reports*, *8*(1), 16270. https://doi.org/10.1038/s41598-018-33455-2

Zdrahala, R. J. (1996). Small Caliber Vascular Grafts. Part I: State of the Art. *Journal of Biomaterials Applications*, *10*(4), 309–329. https://doi.org/10.1177/088532829601000402

Zeitels, S. M., Lombardo, P. J., Chaves, J. L., Faquin, W. C., Hillman, R. E., Heaton, J. T., & Kobler, J. B. (2019). Vocal Fold Injection of Absorbable Materials: A Histologic Analysis With Clinical Ramifications. *Annals of Otology, Rhinology & Laryngology*, *128*(3_suppl), 71S-81S. https://doi.org/10.1177/0003489418805503

Zeitels, S. M., Mauri, M., & Dailey, S. H. (2003). Medialization Laryngoplasty with Gore-Tex for Voice Restoration Secondary to Glottal Incompetence: Indications and Observations. *Annals of Otology, Rhinology & Laryngology*, *112*(2), 180–184. https://doi.org/10.1177/000348940311200213

Zeleník, K., Walderová, R., Kučová, H., Jančatová, D., & Komínek, P. (2017). Comparison of long-term voice outcomes after vocal fold augmentation using autologous fat injection by direct microlaryngoscopy versus office-based calcium hydroxylapatite injection. *European Archives of Oto-Rhino-Laryngology*, *274*(8), 3147–3151. https://doi.org/10.1007/s00405-017-4600-1

Zhang, Z., Kreiman, J., Gerratt, B. R., & Garellek, M. (2013). Acoustic and perceptual effects of changes in body layer stiffness in symmetric and asymmetric vocal fold models. *The Journal of the Acoustical Society of America*, *133*(1), 453–462. https://doi.org/10.1121/1.4770235

Zhang, Z., Wu, L., Gray, R., & Chhetri, D. K. (2020). Three-dimensional vocal fold structural change due to implant insertion in medialization laryngoplasty. *PLOS ONE*, *15*(1), e0228464. https://doi.org/10.1371/journal.pone.0228464

Zhao, X., Kim, J., Cezar, C. A., Huebsch, N., Lee, K., Bouhadir, K., & Mooney, D. J. (2011). Active scaffolds for on-demand drug and cell delivery. *Proceedings of the National Academy of Sciences*, *108*(1), 67–72. https://doi.org/10.1073/pnas.1007862108

Zimmermann, T. M., Orbelo, D. M., Pittelko, R. L., Youssef, S. J., Lohse, C. M., & Ekbom, D. C. (2019). Voice outcomes following medialization laryngoplasty with and without arytenoid adduction. *The Laryngoscope*, *129*(8), 1876–1881. https://doi.org/10.1002/lary.27684

[i] The author would like to acknowledge the Craniofacial Regeneration Microcomputed Tomography Core Shared Instrumentation Grant: S10OD021533 for supporting this work.